MODELING OF FLOCCULATION SYSTEMS USING

PARTICLE SIZE DISTRIBUTION

By

BYUNG-HYUN MOON

B.S. in Chemical Engineering
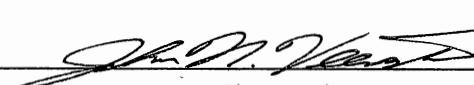Sung Kyun Kwan University
Seoul, Korea
1984

M.S. in Chemical Engineering
Oklahoma State University
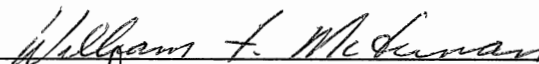Stillwater, Oklahoma
1988

Submitted to the Faculty of the
Graduate College of the
Oklahoma State University
in partial fulfillment of
the requirements for
the Degree of
DOCTOR OF PHILOSOPHY
May, 1992
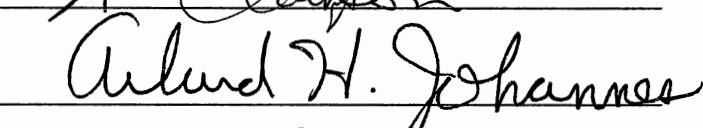
MODELING OF FLOCCULATION SYSTEMS USING

PARTICLE SIZE DISTRIBUTION

Thesis Approved:

_____
Thesis Advisor

_____

_____

_____

_____

_____
Dean of the Graduate College

ii

ACKNOWLEDGMENTS

TABLE OF CONTENTS

LIST OF TABLES

LIST OF FIGURES

viii

Figure   page

CHAPTER I

INTRODUCTION

One of the primary purposes of a water treatment plant is the removal of solids. The main processes used to achieve this end are rapid mixing, flocculation, sedimentation, and filtration. The proper operation of a treatment plant depends on the effectiveness of these processes in removing particles. Many contaminants in water such as bacteria, viruses, metals, and other pollutants are either particles themselves or are adsorbed on particles. Therefore, the removal of these pollutants depends on the removal of particles. Traditionally, turbidity has been the indicator of the effectiveness of particle removal during water treatment. This indicator does not provide enough useful information to characterize the removal of the pollutant they carry; because this information comes from the indirect measurement of particulate material based on the light scattered by particles. To some extent, the emphasis on measurement of turbidity alone biases the investigator toward improvement of the physical parameters of the system. In addition, large changes in the particle size distribution during flocculation or sedimentation do not produce corresponding changes in turbidity, but do influence relative size of the particles (Lawler and

Wilkes, 1984). Various researchers have mentioned that particle size distribution is reliable for evaluating a flocculation process (Treweek and Morgan, 1977; Tate and Trussell, 1978; Akers, 1987; Lawler and Wilkes, 1984; Kuo et al., 1988). An efficient and effective water treatment plant design method based on removal of particles is needed. This study will investigate and model the changes in the number and size distribution of particles as they occur in the flocculation basin of a water treatment plant.

Flocculation is one of the primary unit processes used in a water treatment plant. In flocculation, particles in water are subjected to a combined physical/chemical system. Flocculation changes the size distribution of particles from a large number of small particles to a small number of large particles for removal in later processes. Little work concerning the joint physical and chemical nature of this system as it relates to particle size distribution has been published. In addition, only a few studies comparing predicted changes in particle size distribution against actual treatment plant performance have been reported. Lawler and Wilkes (1984) tested a model considering the physical system, which was based on the fundamental work of Smoluchowski (1917), against results from an actual water treatment plant. Under different operational conditions, the model predicted changes in either the small or large particles, but not both. The authors concluded that the model was too simple to reflect reality from a microscopic

viewpoint and not accurate enough to use routinely in design. The overall objective of this study is to make an attempt to develop a model that shows more realistically what happens to particles during flocculation by incorporating the mechanisms which underlie the process. A more realistic model might alleviate problems of design (over-design or insufficient capability) and operation (poor or inefficient performance). Verification of the model by testing it against data obtained from actual water treatment facilities will be made. Uncertainty analysis, sensitivity analysis and Monte Carlo simulation, will be applied to the model to assess the relative contributions of input parameters to uncertainty in the model and to determine the safety factor to be used with the model prediction in design. It is hoped the model will provide a tool to improve understanding of the process as well as the efficiency of the overall water treatment process.

The following list sets out the specific objectives of this modeling study:

1. Incorporating of interparticle forces (chemical system) to transport mechanisms (physical system) between particles.

    Interparticle forces : Hydrodynamic Forces

                                  Electrostatic Forces

                                  Van der Waals' Forces.

    Transport mechanisms : Brownian Motion

                                  Fluid Shear

Differential Sedimentation.

2. Consideration of floc (particle aggregates) break-up

3. Consideration of the density and shape effects of floc which are varied by the flocculation process.

4. Consideration of velocity gradients in the actual flocculation basin.

5. Verification of the model by different particle count techniques such as an electronic particle counter and an optical technique.

6. Uncertainty analysis of the model.

CHAPTER II

LITERATURE REVIEW

Introduction

Flocculation is an important step for the removal of finely divided particulate matter which, due to its small size, is difficult to remove in an economical time frame by sedimentation and filtration. If the particles to be removed are too small for effective separation, their size can be increased by causing them to form aggregates. An understanding of flocculation theory and previous related work is important in order to accomplish the objectives of this research.

Terminology

There are different terms used to describe the process of particle destabilization, transport and aggregation in water treatment. Commonly, two steps describe the forming of aggregates. The first step is to effect destabilization of particles. The second step is to transport particles for inter-particle contact.

O'Melia (1978) has used the term coagulation to describe both the destabilization and transport steps, whereas Gregory (1989) has used flocculation as a term

covering all steps involved. The two terms are often used interchangeably. Others use coagulation to describe aggregation due to electrolytes and flocculation to describe aggregation due to polymers (Stumm & Morgan, 1981). Montgomery (1985) used coagulation to describe destabilization and flocculation to represent transport steps. In this work, the term flocculation will be used to cover the overall process of aggregation.

Destabilization Mechanisms

The destabilization of contaminants, which usually occurs by means of chemicals that are added in the rapid mix reactor, is followed by provisions for particle contacts. Particle contacts are achieved in the rapid mixing, flocculation, sedimentation, and filtration portions of conventional water treatment. Destabilization mechanisms include compression of the electrical double layer, charge neutralization, formation of sweep floc and inter-particle bridging. The following short discussion of the destabilization mechanisms is taken from Montgomery (1985) and Gregory (1989).

Double layer compression occurs when ions of opposite charge to the particles are concentrated in the solution layer that is immediately adjacent to the particle. As a result, the electric potential that is projected into the bulk solution is mitigated. A schematic of the double layer is shown in Figure 1. As depicted in Figure 1, increasing
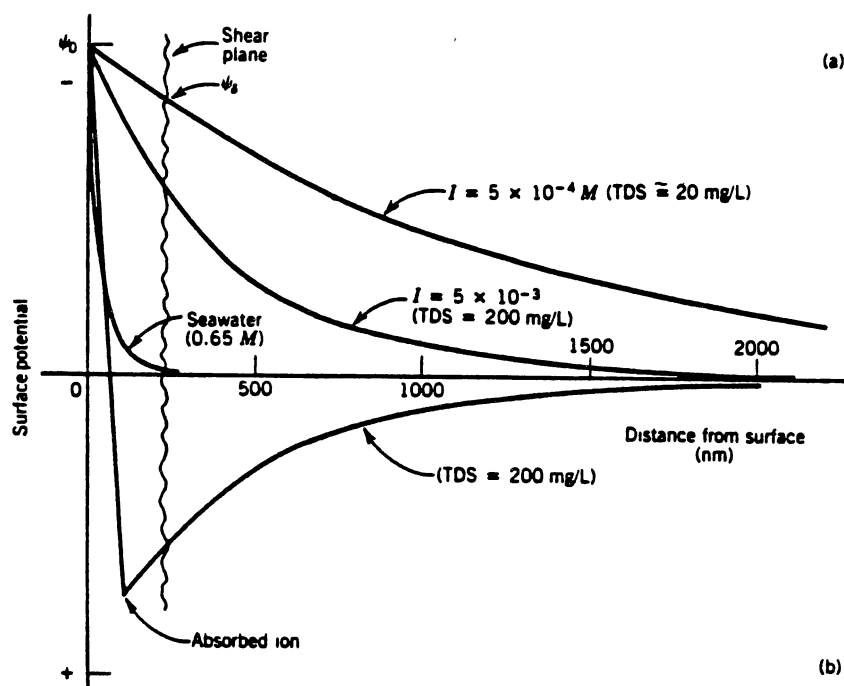
Figure 1. Schematic of double layer. (a) Effect of increasing concentration of indifferent electrolyte. (b) Reversal of potential by specific adsorption (Montgomery, 1985).

the ionic strength compresses the double layer, causing a decrease in its thickness. The potential is determined by an experimental method, particle electrophoresis. Particle electrophoresis can be used to calculate the zeta potential. Reduction of the zeta potential (below $\pm$ 20 mv) permits close approach of particulates such that short range attractive forces (London Van der Waals forces) can act to produce collisions. In addition to double layer compression, particulates can be destabilized by electrostatic attraction, which occurs when surfaces are oppositely charged. Quite often the reaction between a coagulant and particulates is strong enough that the bulk concentration of coagulant is extremely low. This can be promoted by the adsorption of specific ions on the surface of the particulates. This is shown in Figure 1. If charge neutralization is responsible for destabilization, then a stoichiometry exists between the coagulant and contaminant, and restabilization of the complex can occur upon overdosing. If excessive coagulant is added, the system is restabilized.

Particulates can be removed by means of association with coagulant solids that are intentionally formed during water treatment processes. For example, aluminum in alum hydrolyzes and forms an insoluble precipitate. The hydrolysis products are strongly adsorbed by many particles and, because of their positive charge, can cause charge neutralization and reversal. This can explain some observed

flocculation behavior, but it is not the whole story. In many practical applications, the precipitation of aluminum hydroxide plays a very important role. When alum is added to water, the hydroxide forms fairly rapidly, initially as a colloidal precipitate, with subsequent growth to form quite large flocs. During this precipitation and growth, many of the particles originally present in the water become coated with hydrolyzed species or colloidal hydroxide particles and enmeshed in the growing flocs. The original particles are said to be swept out of suspension by the hydroxide precipitate. Such a mode of action is referred to as sweep flocculation.

Particle Counting

Particle counting is a relatively new analytical tool used in water treatment plants. To gain a better understanding of this technique, it is appropriate to compare it to the traditional method of turbidimetry. Traditional flocculation research has been based on indirect measures of flocculation efficiency, such as settled water turbidity and filtered water turbidity (Lawler, 1987). Direct measurement of the particle size distribution allows the investigator to study directly the destabilization and aggregation of the particles, rather than measuring the end result of flocculation's effect on sedimentation and filtration. The direct measurement of changes in the particle size distribution (PSD) by

flocculation allows a better focus on the effect of changing variables related to the flocculation process. The motivation for monitoring changes in PSD is to optimize the growth of particles into a size range that can be efficiently removed by the sedimentation and filtration processes. The desired final particle size could be controlled by a knowledge of the effect of changing variables related to flocculation. In this section, turbidity and several particle counting methods are discussed. One of the hindrances concerning the use of particle counting for application in flocculation is the different particle size measurements yielded by different particle counting methods.

Turbidity

The turbidity of a sample may be measured either by its effect on the transmission of light, which is termed turbidimetry, or by its effects on the scattering of light, which is termed nephelometry (Sawyer & McCarty, 1978). A schematic diagram of both a turbidimeter and a nephelometer are shown in Figure 2. Both turbidity methods are based on a total particle effect. In Standard Mothods (APHA, 1985), turbidity is defined as "an expression of the optical property that causes light to be scattered and absorbed rather than transmitted in straight lines through the sample". Standard Methods (APHA, 1985) also mentions that correlation of turbidity with the weight concentration of
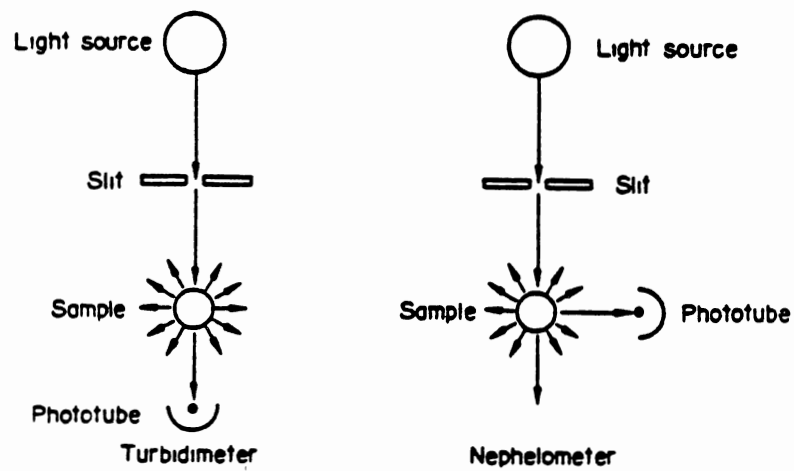
Figure 2. Schematic of a turbidimeter and a nephelometer

suspended matter is difficult because the size, shape, and refractive index of the particulates also affect the light scattering properties of the suspension. As mentioned earlier, turbidity measurements are determined by the total light scattered by particles. Hutchinson (1985) mentioned that this gives no information about the PSD present in the sample. Due to the complexities of light scattering by particles, there is not necessarily a correlation between the particle distribution and the total number of particles in two samples with the same turbidity. Turbidity indicates what happened but the additional information provided by particle counting is most useful in understanding the operation of flocculation.

Particle Counting Method

Several researchers (Lawler, 1984; Hutchinson, 1985; Kuo et al., 1988) recommended the use of PSD information in process design, process selection, and operation decisions. In order to obtain more accurate PSD, selection of an appropriate particle counting method is important. It is essential to realize the practical limitations which are inherent in any method of analysis which is available. Three particle counting methods will be discussed here.

Coulter Type Counter. The Coulter counter works on the principle that floc volume is correlated to the electrical resistance generated when the flocs pass through an

electric field (Li and Ganczarczyk, 1986). There are, however, a number of concerns when using the instrument with floc. The followings are major considerations:

- ○ Floc breakage.
- ○ Coincident counts causing larger particle measurement.
- ○ Measuring only a fraction of the flocs.

HIAC Particle Counter. The HIAC is a light blockage particle counter. The particles to be counted are suspended in a fluid which has a different refractive index than the particles. The HIAC also has the limitation of floc breakage. Gibbs (1981) mentioned that "extensive floc breakage was indicated for all samples after they passed through the HIAC sensor". His work on flocs of kaolinite and natural suspended sediment noted floc breakage in the upper two thirds of the recommended size range for the HIAC sensing cell. This severely limits the use of the particle counter for measuring floc size distribution. The breakage observed by other researchers is shown in Figures 3 and 4. Figure 3 illustrates the breakup observed by Gibbs (1981) and Figure 4 shows the comparison between HIAC PSD and PSD generated using a photographic technique by Reed and Mery (1986). Employing a large size of sensing cell to reduce breakup might cause coincident counts of relatively small particles. Reviewing the literature concerning the Coulter and HIAC counters, the following aspects were noticed:
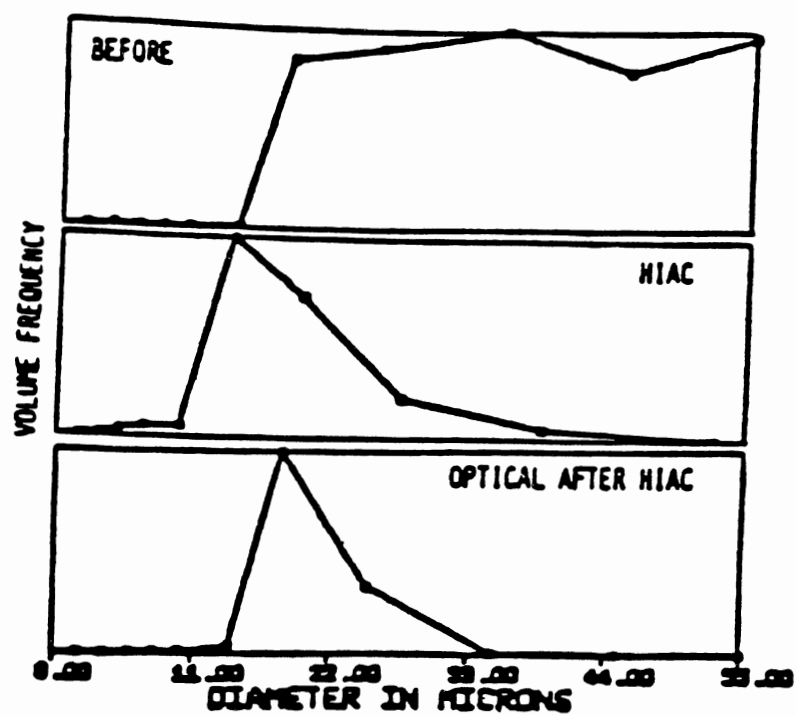
Figure 3. Size distribution for kaolinite flocs measured by
using a microscope before HIAC analysis (top), by HIAC
(middle), and by using a microscope after the floc had
passed through the HIAC sensor (bottom) (Gibbs, 1972).
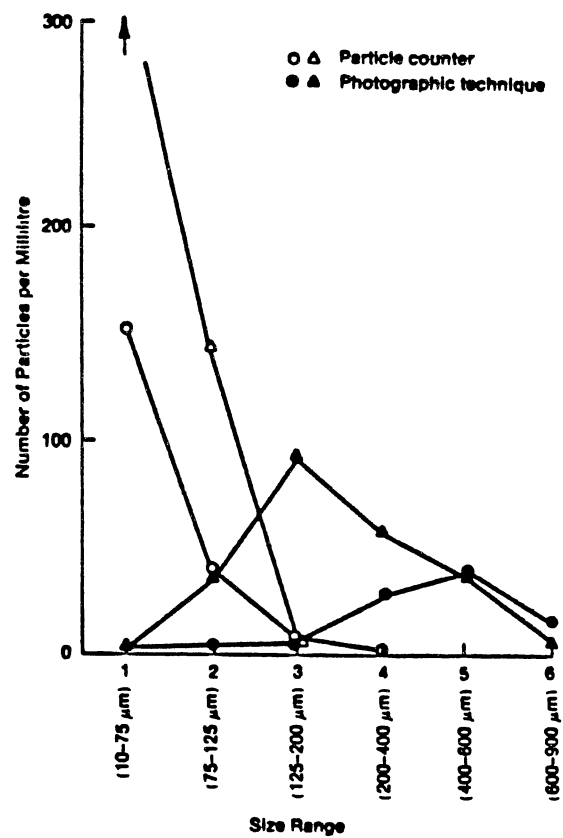
Figure 4. Comparison of floc size distribution as measured by an electronic particle counter and by a photographic technique; raw water (△ and ▲) and after flocculation (□ and ■) (Reed and Mery, 1986).

∘ No electrolyte is needed for the HIAC so there are no electrolyte effects.

∘ Porosity is considered in the HIAC.

∘ Floc breakage occurs in both counters.

∘ Sample dilution is needed in both counters.

∘ Coincident counts of small particles are possible in both counters.

A conclusion can be drawn from these aspects that HIAC is a more accurate particle counter than the Coulter counter.

Optical Particle Counter. A serious concern when using an electronic particle counter is floc breakup. It is important that the electronic particle counters which are commonly used to count and size flocculated material should be evaluated for floc breakup. For reducing breakup, the optical particle counting method is very useful. However, using an optical microscope also has limitations such as time requirements and bias caused by operator involvement. Recently, an automated image analysis system coupled with an optical instrument has been developed. The method works in the following manner: An optical video signal created by the blocking of the light path by the flocs is converted to a two-level electrical binary signal which is then processed in the preselected measurement module (Li and Ganczarczyk, 1986).

Two potentially limiting aspects of this method have to be discussed. The first potential limitation is the

optical system itself. In order to measure the wide range
of flocs, the image analyzer must be connected to the
correct type of optical system. The most important part is
to select the magnification of the system microscope. A 16x
objective was used for a study of activated sludge flocs
(Li and Ganczarczyk, 1986). A 20x objective (system
magnification of 474.6x) was used for alum treated floc by
Hanson (1989). If a wide range of floc sizes exists in the
sample, a single microscopic lens may not cover the whole
size range.

The second potential limitation is image processing
itself. There are several commercially available image
processing systems. Li and Ganczarczyk (1986) used an
OMNICON 3000 image processing system for studying activated
sludge flocs. Hanson used a Lemont OASYS image processing
for studying alum flocs. The resolution of the image is
limited by the magnification of the digitized object and
image processing. Another concern is the number of features
which must be counted by the image processing to give a
statistically sound sample. Hanson (1989) reported the
following guidelines to accomplish his flocculation
research goal:
- a goal of a minimum of 1000 features measured, if they
  can be measured in less than 20 frames,
- a goal of a minimum of 500 features measured, if they
  can be measured in 30 frames,
- an absolute minimum of 250 particles measured,

- a minimum of 100 particles in the particle class which represents the mode of the distribution,
- a minimum of 10 particles in any particle class important to the shape of the distribution curve.

Hanson's (1989) image system took 30 minutes to count 1000 particles, but the HIAC he also used would count 60,000 particles in the same time. According to Baba et al.(1988), PSD was calculated at a statistically reliable level in 5 to 20 minutes based on 2000-10,000 particles in 10 -15 images by using a high speed image processor.

PSD Application in Full Scale Water Treatment Plants

A few applications of PSD information for monitoring and controlling flocculation have been reported. Interestingly, two case studies in the open literature report the reduction of chemical cost (coagulant dosage) by about 30% by applying PSD information to their solids/liquid separation systems. The Southern Nevada Water System (SNWS) has used HIAC for obtaining PSD and applying the PSD to operate their direct filtration facilities (Hutchinson, 1985; Monscvitz and Rexing, 1983). Baba et al. (1988) reported a particle size monitoring system with image processing for a conventional water treatment system in Japan. This section will discuss how PSD has been used for water treatment applications.

The conventional water system operating in Japan was

equipped with underwater television cameras (Baba et al.,
1988). The system used the geometric mean diameters (GMD)
calculated from the PSD data to evaluate the degree of floc
formation. If the monitored GMD was between 0.55-0.60 mm in
the first basin, they considered this to confirm floc
formation. They mentioned that conserving coagulant is
possible when floc image monitoring offers an assurance of
floc formation in the first basin. The value of GMD
increased with increased coagulant doses. However, the
average effective density of the floc decreased at
increased coagulant dosages. The expected increase in the
magnitude of the settling velocity resulting from an
increase in floc size is not always observed because of the
reduction in floc density, which tends to reduce the
settling velocity. These results showed that turbidity in
the sedimentation basin outlet increased when more
coagulant than aN optimum dosage was injected.

The Southern Nevada Water System uses on-line particle
counting using HIAC as a means of controlling solid/liquid
separation. This system is one of the world's largest
direct filtration facilities (slightly over 600 cfs, 1500
ML/d). The on-line particle counting monitors the
effectiveness of the treatment process (chemical dosage
control) and initiates the automatic backwashing of
filters. The system is designed so that particle size
number can be observed. The system measures the PSD by
on-line particle counters in the raw water after

predisinfection, after flocculation, after filtration, and at the effluent of the treatment plant. By means of the above observations of the PSD through the plant, they try to produce an optimum size particle for optimum filtration with deep filter media penetration. Excess coagulation results in visible sweep flocs of such size that most of the particles remain on the surface of the media. As a general rule, surface straining becomes important when the ratio of particle size to filter media size is larger than 0.2 (Kuo, 1988). Therefore, assuming an average media size of 0.5 mm, flocs which are larger than 100 μm should not be applied to a filter. SNWS developed a mathematical evaluation of the filter's performance, termed the filter performance index equation. The equation is expressed as follows (Monscvitz and Rexing, 1983):

$$FPI = \frac{\dfrac{20}{XPC} \times \dfrac{XRF}{75.7} \times 3.4HR}{WW \times \dfrac{2.44}{HL}}$$

Where:

   FPI = Filter performance index

   XRF = Average rate of flow in ML/day throughout filter
          run

   XPC = Average effluent particle count throughout
          filter run

   HR = Total hours of filter run

   HL = Head loss in meters at backwash

WW = Total wash water in ML

According to Monscvitz and Rexing (1983) if a filter
performance index falls below 0.5 standard deviations of
the mean (mean value in the SNWS was 194.25), there is a
fair chance that something is wrong with the filter
(mudballs, defective loss of head meters, inadequate
backwashing, and breakthrough).

A second index developed by Monscvitz and Rexing
(1983) is the dosage optimization index.

$$k=\frac{p}{kg/ML}$$

Where:

k = the dosage optimization index

p = percent particle removal between raw and finished
    water

kg/ML = coagulant dosage/water treated

This index evaluates percent particle removal between raw
and finished water in relation to solids removal chemicals
(coagulants, filter aids). The index varied from 0.27 to
0.33 in the SNWS.

Representation of PSD Data

In this section, some graphical and mathematical
presentations of PSD are discussed. The simplest type of
graphical representation is to plot the particle number or
particle volume vs particle size. Number of particles (ΔN,
in #/cm^3) in increments of particle size (Δd) can be

plotted. The plotting of ΔN vs Δd takes the form of a histogram. In a histogram, the width of rectangles represents the size interval (increment) and the height the number of particles in each size interval. But the histogram may show a distorted picture of the particle size distribution because the height of any interval is dependent on the width of that interval. The same sample (particle size distribution) measured with another instrument with different particle increments would yield a different histogram. To overcome this, other representations of particle size distribution have to be made. Part B and D in Figure 5 illustrate cumulative number distributions. A cumulative number distribution plot can be prepared to see how the flocculation process affects the total number of particles. But the cumulative number distribution plot might not clearly show what size range of particles are affected by flocculation. Several researchers (Lawler et al., 1980; Stumm & Morgan, 1981; Lawler, 1987) discussed manipulating the PSD data to characterize PSD in a given environment by using a PSD function. The slope of the cumulative number distribution curve (Part D of Figure 5), $\Delta N/\Delta d$, is known as a particle size distribution function, n(d), i.e.,

$$\frac{\Delta N}{\Delta d} = n(d) \qquad (number/cm^3 \mu m)$$

Each value of ΔN is divided by the increment of particle size (Δd) corresponding to the value log d. This division

23
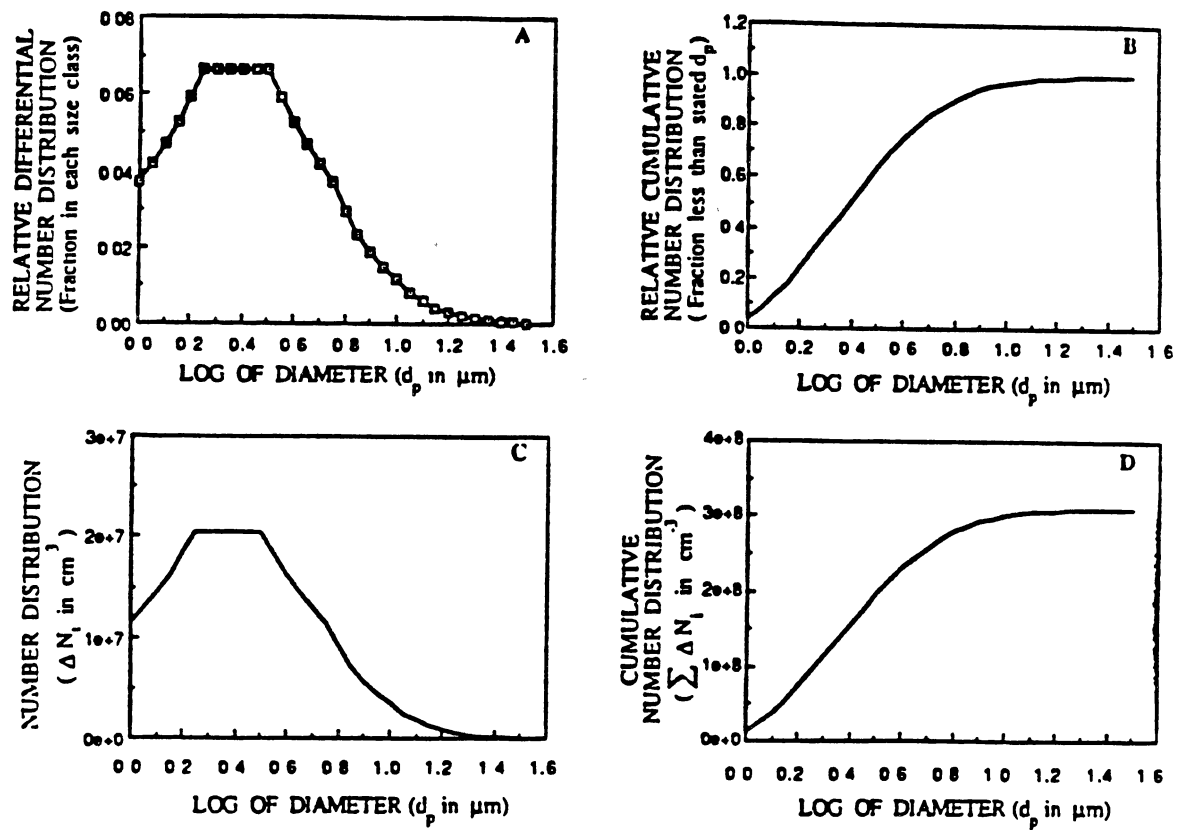
Figure 5. Methods for plotting particle size distribution:
relative vs. absolute and differential vs. cumulative
(Lawler, 1987).

accomplishes normalization, so that the same sample (particle size distribution) measured by different instruments (with different increments of log diameter) would show the same distribution on this graph. The differential curves illustrate what size range contains most of the particles more clearly. The size distribution of particles in water can often be characterized by the power law shown below (Montgomery, 1985):

$$n(d) = Ad^{-b}$$

Where A is a constant and b is the power law coefficient. A plot of $\log(\Delta N/\Delta d)$ versus log d yields a straight line with slope b, if the size distribution of the particles follows the power law. Several examples of power law size characteristics for suspensions are shown in Figure 6. The slope of the power law function is a useful parameter to characterize the type of suspensions being treated. A decrease in the slope (smaller b value) with time or each successive basin indicates the reduction of particle number due to flocculation.

The absolute differential distribution of the above particle size distribution ($\Delta N/\Delta d$) can be improved by dividing each cumulative particle number value by the logarithmic interval of particle size associated with each size, i.e. $\Delta N/\log d$. This division again accomplishes normalization, so that the same suspension measured by different instruments (with different values of $\Delta \log d$) would yield the same distribution on this graph. This
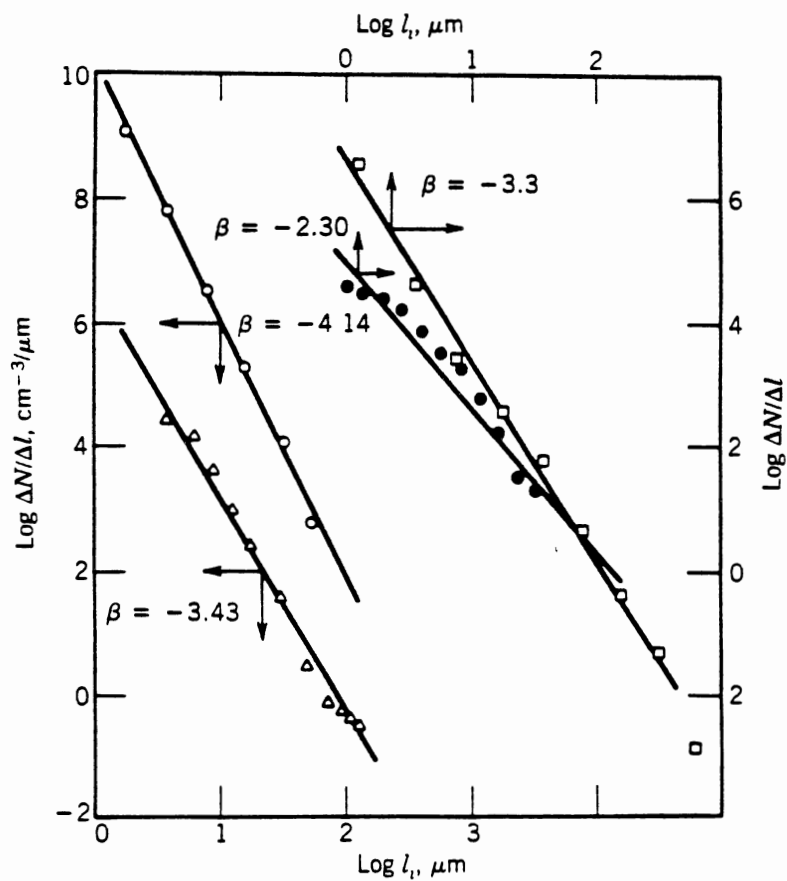
Figure 6. Example of particle size distribution: (△)
effluent, sedimentation basin, pilot-activated sludge
plant; (•) Lake Zurich, 40 m; (□) Deer Creek Reservoir,
Utah, 20 m; (○) digested primary and secondary sludge
(Montgomery, 1985).

division also means that the area under the graph between two values of log d equals the particle number concentration between those two sizes. The total particle number concentration equals the area under the graph between the smallest and the largest size. Assuming that the particles are spherical, volume distribution and surface distribution also can be expressed as the following equations:

For the surface distribution,

$$(\Delta S/\Delta \log d) = (\Delta N/\Delta \log d)(\pi d^2)$$

For the volume distribution,

$$(\Delta V/\Delta \log d) = (\Delta N/\Delta \log d)(\pi d^3/6)$$

If this assumption is not true, the area is proportional to surface or volume concentration. Four type of PSD graphs are shown in Figure 7. These methods of presenting data are all used in the subsequent sections. Although these representations are mathematically related and contain the same information, each one can provide specific insight into certain phenomena more easily than others.
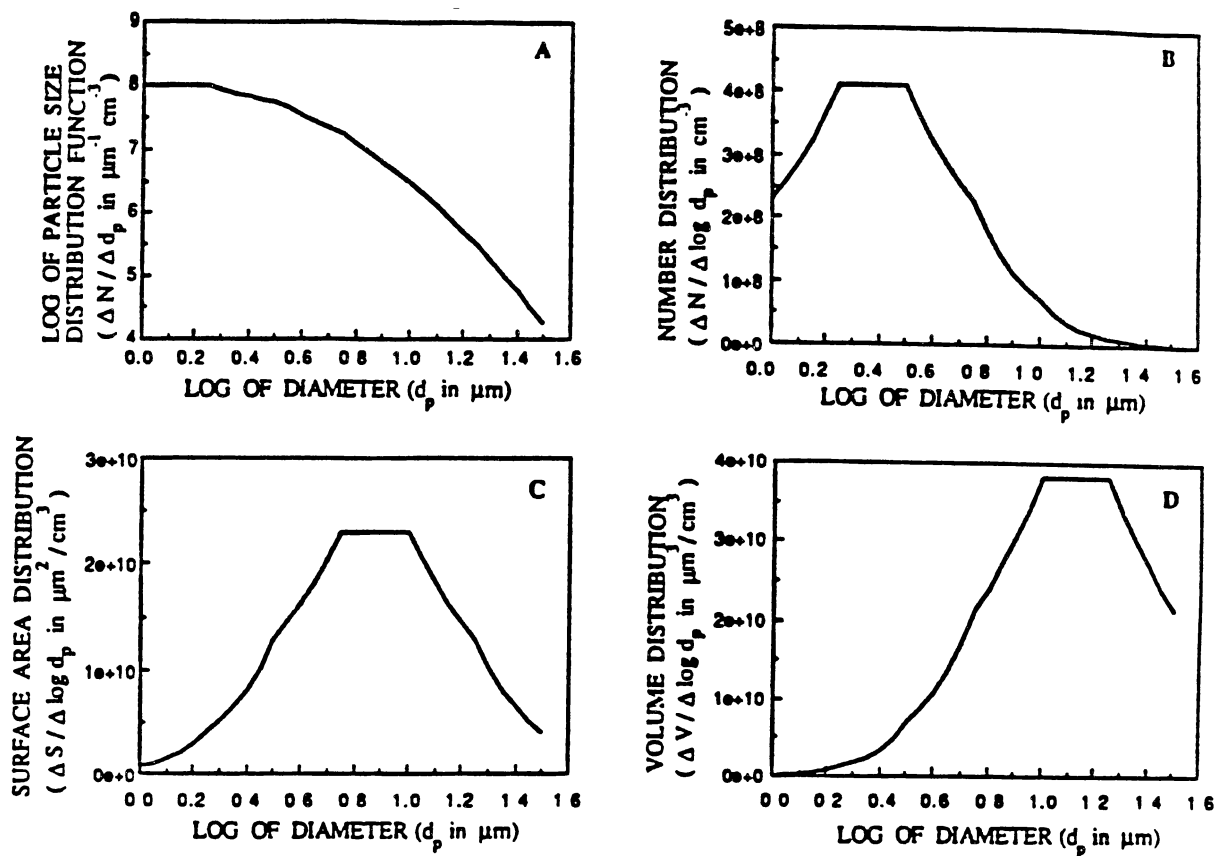
Figure 7. Methods for plotting particle size distribution:
particle size distribution function, number distribution,
surface area distribution, volume distribution (Lawler,
1987).

CHAPTER III

MODEL DEVELOPMENT

The mathematical analysis of changes in particle
numbers (flocculation) was developed by Smoluchowski
(1917). He calculated the number of collisions between
particles in a given time due to Brownian motion and fluid
shear. Lawler et al. (1980) used the discrete form of the
Smoluchowski equation as the basis of their model. The
discrete form of the equation is as follows:

$$\frac{dn_k}{dt} = \frac{1}{2}\alpha \sum_{i+j=k} \beta(i,j)\, n_i n_j - \alpha n_k \sum_{i=1}^{r} \beta(i,k)\, n_i \tag{1}$$

Where:

i,j,k = subscripts denoting particle size i, j,
and k,

r = the maximum allowable value of i,j,or k in the
model,

n = particle number concentration (cm^{-3}),

t = time (s),

β(i,j) = the sum of collision frequency functions for
particles size i and j, and

α = collision efficiency factor, which is the
fraction of predicted collisions that result in
attachment.

28

The notation i+j=k in the first summation on the right hand side of equation 1 indicates that the summation is taken over those collisions for which the particles of size i and size j are involved. This also represents the generation of particles of size k by the collision of any two particles of size i and j. The factor 1/2 is introduced because each collision is counted twice (i.e. i+j=k and j+i=k) in the summation. The second term represents the loss of particles of size k due to their collision with any size i particles. Separate collision frequency functions, $\beta(i,j)$, for interparticle contacts brought about by Brownian motion, fluid motion, and differential sedimentation have been developed and are expressed (Lawler and Wilkes, 1984), respectively, as:

for Brownian motion

$$\beta_b(i,j) = \left(\frac{2kT}{3\mu}\right)\left(\frac{1}{d_i} + \frac{1}{d_j}\right)(d_i + d_i) \tag{2}$$

for fluid motion

$$\beta_f(i,j) = \frac{1}{6}(d_i + d_j)^3 G \tag{3}$$

for differential sedimentation

$$\beta_d(i,j) = \frac{1}{4}(d_i + d_j)^2 |w_i + w_j| \tag{4}$$

Where:

d_i, d_j = diameters of particles of sizes i and j,

k = Boltzmann's constant,

T = absolute temperature,

μ = absolute fluid viscosity,

G = the root-mean-square velocity gradient,

g = the gravitational constant,

The settling velocity of a particle is calculated as

$$w_i = \left[\frac{4g}{3C_{di}}\left(\frac{\rho_p - \rho_w}{\rho_w}\right)d_i\right]^{1/2} \tag{5}$$

The drag coefficient (C_{di}) is estimated using the following relationship:

$$C_{di} = 24/Re \qquad\qquad \text{if } Re < 1 \tag{6a}$$

$$C_{di} = 24/Re + 3/Re + 0.34 \quad \text{if } Re > 1 \tag{6b}$$

Where:

Re = Reynolds number

$$= w_i\ d_i\ \rho_p/\mu \tag{7}$$

ρ_p, ρ_w = the densities of the particles and water,

w_i, w_j = the settling velocity of particle i and j.

When Re < 1, the settling velocity is the Stokes settling velocity, but when Re > 1, the settling velocity is found by the trial-and-error solution of the equations 6b and 7.

All of the collision frequency functions, $\beta(i,j)$, were developed with assumptions that: (1) there exists no interparticle force, but particles coagulate when they collide (2) there is no break-up of aggregates (3) the density of particles and aggregates are constant (4) the particles are spherical in shape. Thus, the new model has to improve the collision frequency functions to account for

the interparticle forces in nature such as the repulsive
hydrodynamic forces, the attractive van der Waals' forces
(interparticle attraction), and electrostatic repulsion.
Flocculation is accompanied by the break-up of aggregates
in most actual systems so that a consideration of break-up
should be incorporated. Particle (aggregates or flocs)
density and porosity effects need to be considered in the
modeling.

Consideration of Interparticle Forces

Collisions predicted by the model, equations 1 - 4,
with the previously mentioned assumptions were
overestimated due to the lack of consideration of the
interparticle forces between the approaching particles.
These effects have been studied mathematically using
trajectory analysis, a technique in which the forces acting
on two particles as they approach one another are
calculated and the resulting motions are determined.
Research in this area has been performed by several
investigators. For equal size spherical particles in a
shear flow, van de Ven and Mason (1976) calculated the
trajectories considering the effects of hydrodynamic
interaction, interparticle attraction, and electrostatic
repulsion. Higashitani et al.(1982) and Adler(1981)
calculated the collision efficiency for unequal size
particles in a shear flow using a method similar to that of
van de Ven and Mason (1976). Valioulis and List (1984)

reported the collision frequency efficiency considering van der Waals' forces and hydrodynamic interaction of particles for shear flow by doing a regression on Adler's data. Also, they reported interparticle forces effects for Brownian motion. Melik and Fogler (1984) investigated interparticle forces effects for differential sedimentation.

In this study, Valioulis and List's (1984) modified collision frequency functions for Brownian diffusion and fluid shear will be employed. They incorporated the influence of interparticle forces by multiplying collision frequency functions by a collision frequency efficiency term, $\gamma(i,j)$. Collision frequency efficiency is a function of the sizes of the interacting particles and is unique for each transport mechanism. For differential sedimentation, Melik and Fogler's (1984) results will be employed in this study by regression of their data. All of the following expressions only account for hydrodynamic and van der Waals forces so that electric double layer repulsion was not considered. Although electric double layer repulsion can be included in trajectory analysis, it is still not possible to account for all chemical interactions.

Approximations for the collision frequency efficiencies in Brownian diffusion accounting for hydrodynamic and van der Waals forces were reported by Valioulis and List (1984). These collision frequency efficiency factors depend on the Hamaker groups ($H/(KT)$) and the ratio of the particle diameters. In the calculation

of Hamaker group values, H is the Hamaker constant, K
Boltzmann's constant and t the absolute temperature. The
collision frequency efficiency factors are estimated by the
following equation:

$$\gamma_b = a + b\lambda + c\lambda^2 + d\lambda^3 \qquad (8)$$

Where:

$$\lambda = d_i/d_j, \quad d_i > d_j$$

In this equation, a, b, c, and d are determined on the
basis of the values of H/(KT) and shown in Table I
(Valioulis and List, 1984). Approximations for collision
frequency efficiencies of fluid motion are estimated by the
following equation where a, b, c, and d are determined on
the basis of the value of $H/(18\pi\mu d^3 G_i)$ and shown in Table II
(Valioulis and List, 1984):

$$\gamma_f(i,j) = \left[\frac{a+b\lambda}{1+c\lambda+d\lambda^2}\right]\left[\frac{8}{(1+1/\lambda)^2}\right] \qquad (9)$$

The value of Hamaker constant depends on the density
and polarizability of the material (Stumm and Morgan,
1981). Values of the Hamaker constant for materials in
water were reported by Visser (1977). In his paper, values
of the Hamaker constant for polystyrene and kaolinite in
water were 3.5×20^{-20} and 2×10^{-19} J, respectively.
Recently, Gregory (1989) mentioned that dense mineral
particles have values toward the upper end of this range,
whereas low density, especially biological, materials have
quite low values. A value of 2×10^{-19} J will be used in

TABLE I

APPROXIMATION FOR COLLISION FREQUENCY
EFFICIENCIES IN BROWNIAN DIFFUSION

$H/(KT)$	a	$b \times 10^{-2}$	$c \times 10^{-4}$	$d \times 10^{-6}$
10^{-4}	0.21811	2.9593	-4.9962	2.6953
10^{-3}	0.25878	3.0338	-5.3031	2.9043
10^{-2}	0.31151	3.0339	-5.4760	3.0409
10^{-1}	0.37254	2.9251	-5.4055	3.0318
1	0.44285	2.6954	-4.3310	2.4569
10	0.53814	2.2834	-4.3310	2.4569
10^{2}	0.70480	1.3481	-2.4753	1.3845

TABLE II

APPROXIMATIONS FOR COLLISION FREQUENCY
EFFICIENCIES OF FLUID MOTION

$H/(18\pi\mu d^3 G_1)$	a	b	c	d
10^{-2}	-1.189	0.118	-3.431	0.331
10^{-3}	0.766	0.007	-0.006	1.547
10^{-4}	0.145	-0.0006	-1.137	0.775
10^{-5}	0.017	-0.001	-1.442	0.557

the model because kaolinite in water is similar to dirt in water.

Corrections for collision frequency efficiencies of differential sedimentation were mentioned but not explicitly expressed by Melik and Fogler (1984). Therefore, regressions were conducted using their reported graphical results which showed the effect of particle ratio on the collision frequency factors for various values of the dimensionless parameter, N_G. The collision frequency efficiency factors are estimated using the following equation:

$$\gamma_d = a\lambda^2 + b\lambda + c \tag{10}$$

Where:

$$N_G = \frac{\pi g \Delta \rho d^4}{3H} (\lambda+1)^2 (\lambda-1)^2 \tag{11}$$

Where g is the local acceleration of gravity and $\Delta\rho$ is the density difference between the particles and the suspending medium.

Consideration of Floc Density

The density and shape of the floc are some of the most important factors of concern in flocculation because they are related to the settling velocity distribution. The volume of the flocculated particles is larger than the sum of the volumes of primary particles due to inclusion of water, so that the assumption of constant density should be changed. Tambo and Watanabe (1979) illuminated some

TABLE III

APPROXIMATIONS FOR COLLISION FREQUENCY
EFFICIENCIES OF DIFFERENTIAL
SEDIMENTATION

N_G	a	b	c
10^{-1}	-0.31818	0.26333	0.41267
10^2	-0.12386	0.11031	0.03282
10^6	-0.03106	0.02792	0.0027

characteristics of clay-aluminum flocs by experiments and model floc simulation. Recently, Li and Ganczarczyk (1989) investigated the relationship between floc density and size for inorganic and biological flocs. They concluded that the size-density relationship and the structure of the flocs depend on their physical and chemical characteristics. The relationship between floc density and size, the floc density function, was expressed as the following equation:

$$\rho_e = \rho_f - \rho_w = \frac{a}{d_f^k} \tag{12}$$

Where:

ρ_e = the floc effective density (g cm^{-3})

ρ_f = the floc density (g cm^{-3})

ρ_w = the water density (g cm^{-3})

a, k = constant

d_f = the floc diameter (cm)

This equation indicates that the effective density of a floc decreases as the floc size increases. There is a transition point in the floc density and size relationship. At a point smaller than this transition point, density varied slightly and flocs were formed by a process similar to particle addition and were more compact than the larger ones. This fact suggests that flocs smaller than the transition point can be assumed to have a constant density. Larger than this point, the floc density function is applied. As shown in equation 12, the floc density function

is characterized by two constants, k and a. Tambo and Watanabe (1979) reported values of the a (14×10^{-4} from 2×10^{-4}) and k (0.9 from 1.5) from experiments, and 13×10^{-4} and 0.9 from computer simulation, respectively. These constants of the floc density function for clay-aluminum floc are not greatly affected by pH, agitation intensity, raw water alkalinity and small dosages of coagulant aids but are significantly influenced by the ratio of aluminum ion concentration dosage to the suspended particle concentration (ALT ratio). The relationship between the ALT ratio and the constants, k and a at a neutral pH can be expressed as the following linear equations:

$$a = -0.00126 \log(ALT) - 0.00106 \tag{13}$$

$$k = 0.4854 \log(ALT) + 1.885 \tag{14}$$

Where ALT is the ratio of aluminum ion concentration dosed to suspended particle concentration. The above equation 14 shows that an increasing aluminum ion concentration dosage relative to suspended particle concentration considerably increases the absolute value of the exponential constant k. Thus, the floc density at a fixed size increases as ALT decreases.

The decreased floc density with increased floc size implies that the porosity of floc increases as the floc size increases. The porosity of the floc describes the open space in floc occupied by water. The space indicates that the flow streamlines could cross the floc. The following are expressions obtained by the regression of Adler's

(1981) tabulated numerical results for fluid motion. For differential sedimentation, expressions reported by Adler (1981) are used to account for the open space in porous floc:

For fluid motion

$$\psi_f = 1.6185 \; \exp(-0.4902\xi) \tag{15}$$

Where:

$$\xi = d_i/p^{1/2}$$

$$p = \frac{c^2}{18}\left[3 + \frac{4}{1-e} - 3\left(\frac{8}{1-e} - 3\right)^{1/2}\right]$$

$$c = \frac{1}{20}d_i$$

$$e = \frac{\rho_p - \rho_f}{\rho_p - \rho_w}$$

For differential sedimentation

$$\psi_d(i,j) = 1 - \frac{b}{\xi} - \frac{a}{\xi} \tag{16}$$

Where:

$$a = -\frac{1}{\zeta}\left(\xi^5 + 6\xi^3 - \frac{\tanh\xi}{\xi}\right)(3\xi^5 + 6\xi^3)$$

$$b = \frac{3\xi^3}{\zeta}\left(1 - \frac{\tanh\xi}{\xi}\right)$$

$$\zeta = 2\xi^2 + 3 - 3\frac{\tanh\xi}{\xi}$$

The above equations are used when the value of ξ is smaller

than 100. When the value of ξ is larger than 50 (when porosity, e, is less than 0.5), the collision efficiency, ψ, approaches 0 and when the value of ξ decreases to 0 (when porosity, e, is close to 1), the collision efficiency, ψ, approaches 1.

Consideration of Floc Shape

During flocculation, particle aggregates and flocs are generated. The generated aggregates have irregularly shaped forms. Because of the irregular shape, the collision frequency function needs to be modified to include the shape effects.

The total particle volume consists of the raw water particle, together with the dissolved organic carbon (DOC) and coagulant absorbed on the particle. Wiesner and Mazounie (1989) suggested that particle volume concentration and floc volume concentration could be related by using the following equation:

$$V_{floc} = a\phi_t^{3/D} \tag{17}$$

Where:

V_{floc} = floc volume concentration

a = constant

ϕ_t = floc volume

= $\phi_p + \phi_{Al} + \phi_{doc}$

ϕ_p = raw particle volume

ϕ_{Al} = coagulant added

ϕ_{doc} = DOC adsorbed

D = the fractal dimension

They reported a fractal dimension of 2.3 for ferric chloride floc and 1.4 to 1.7 for aluminum floc. Comparison of these values shows that the ferric chloride flocs have a much less open structure. The fractal dimension represents the shape of floc used in the simulation of floc growth. A solid, three-dimensional body has a mass which depends on the third power of some characteristic length (such as the diameter of a sphere), so that a log-log plot of mass against size would give a straight line with a slope of three. When such plots are made for aggregates, lower slopes with noninteger values are found. The slope of the line is known as the fractal dimension, D (Gregory, 1989). Li and Graczarczyk (1989) determined the fractal dimension of aggregates formed in water and wastewater treatment processes by computer simulation and compared the result with literature values. According to them, the settling velocity, density, and mass of aggregates can be expressed in terms of the fractal dimension.

$$v \propto d^{D-1}$$

$$\rho \propto d^{D-3}$$

$$M \propto d^{D}$$

The fractal dimension contains information on both the density and the shape of the floc in given physical and chemical environments and can be useful in comparing flocs of different origins and interpreting simulations of floc

growth.

The above discussion suggests that resulting floc
size, when two particles or flocs collide, is larger than
the sum of the colliding particles' diameters. Assume that
particles of diameter, d_i and d_j are colliding. The volumes
of these particles are ϕ_1 and ϕ_j, respectively. If we use
particle size distribution of raw water, we need to
consider the increased diameter caused by the adsorbed DOC
and coagulant amount added during rapid mixing. However,
data concerning the proportional constant (a) and the
fractal dimension (D) have not been fully reported. More
research or another approach is needed to obtain this type
of information. Coagulated floc consists of four
components, namely, suspended particles in the raw water
(ϕ_p), hydrolyzed aluminum (ϕ_{Al}), DOC adsorbed (ϕ_{doc}) and water
entrapped during floc growth. The hydrolyzed aluminum and
DOC are adsorbed on the surface of the suspended particles.
Therefore, the main components which make up floc size are
divided into two parts as the solid part and void
part(water part). The following relationships can be
obtained:

$$V_f = V_s + V_w \tag{18}$$

$$\rho_f V_f = \rho_s V_s + \rho_w V_w \tag{19}$$

Where:

$\quad\quad V_f$ = the volume of floc

$\quad\quad V_s$ = the volume of the solid part

$\quad\quad V_w$ = the volume of the water part

ρ_f = the density of floc

ρ_s = the density of solid part

ρ_w = the density of water

The volume of floc can be expressed by the following equation:

$$V_f = k_1 \, d_f^3 \tag{20}$$

Where k_1 is constant. The volume of solid part can be found from the floc size and density relation of equation 11.

$$(\rho_e + \rho_w)V_f = \rho_s k_2 d_s^3 + \rho_w(k_1 d_f^3 - k_2 d_s^3) \tag{21}$$

$$\rho_e = \frac{(\rho_s - \rho_w)d_s^3}{d_f^3} = a d_f^{-k} \tag{22}$$

$$d_f = \left(\frac{k_2}{k_1} \frac{\rho_s - \rho_w}{a} d_s^3 \right)^{\frac{1}{3-k}} \tag{23}$$

Where k_2 is constant and d_s is the volume equivalent diameter of the solid part. The above equation can be expressed using the fractal dimension, D, as follows:

$$d_f = \varphi^{1/D} \, d_s^{3/D} \tag{24}$$

Where:

$$\varphi = \frac{k_2}{k_1} \frac{\rho_s - \rho_w}{a}$$

When two flocs collide, the resulting floc size is larger than the sum of colliding floc diameters. However, the mass of flocs would be conserved. In this study, conservation of floc solids rather than volume will be incorporated using volume equivalent diameter of the solid

part of the floc. According to several researchers (Reed and Mery, 1986; Jiang and Logan, 1991), the collision frequency of irregular shape floc, fractal floc, is greater than that of spherical floc. The increased chance of collisions are accounted by using the floc diameter, d_f, in calculating the collision frequency function, $\beta(i,j)$. The collision frequency efficiency, $\gamma(i,j)$, is calculated by also using the volume equivalent diameter of the solid part. In this modeling study, the volume equivalent diameter is set equal to $(k_2/k_1)d_m$, where d_m is the size of particle measured by the particle counter.

Consideration of Floc Break-up

In existing models, aggregate size continues to grow infinitely as there is no upper size to limit the growth of the aggregates. Aggregation is accompanied by the break-up of some of the aggregates in all practical systems so that a consideration of break-up should be employed. Two floc break-up mechanisms (erosion and fragmentation) are believed to be occurring simultaneously in shear flow (Pandya and Spielman, 1982, Lu and Spielman, 1985. Akers et al.,1987). Several models for floc break-up mechanisms have been reported, such as the maximum stable aggregate size model, displacement model, number concentration model, and statistical model (Brown and Gratz,1987). Each model has advantages and disadvantages. In this study, the maximum stable aggregate size model will be used. Reasons behind

choosing this model are (1) its simple description and (2) the fairly large amount of information on this model in the literature. Above all, approximate possible maximum sizes of floc can be initially guessed during the particle size distribution process for initial input data and then easily changed after comparing simulated particle size distribution data and actual flocculated particle size distribution data. The model which depends on shear is as follows, (François, 1987):

$$d_{max} = r'G^{-r}$$

Where d_{max} is the maximum stable floc size, r' and r are characteristic constants, and G is velocity gradient. A literature survey of the experimentally and theoretically obtained values of the constant, r, were reported by François (1987). The values of r varied from 0.3 to 1 but values of r' were not reported. For an estimation of the maximum stable floc size, values as a function of velocity gradient recently reported by Glasgow and Kim (1989) can be used.

In the modeling conducted for this study, a procedure which has a maximum floc limit will be employed to prevent the permanent formation of oversized flocs. The procedure was introduced by Koh (1987). He called the procedure a zero collision efficiency approach. The approach is to make the collision efficiency function zero for all possible collisions resulting in an aggregate size greater than the limiting size. This approach is to view oversized flocs as

unstable, subjected to immediate break-up from the hydraulic stresses of the fluid motion. The zero collision efficiency factor, $\delta(i,j)$, is expressed as follows:

$$\delta(i,j) = \left(1 - \frac{d_i + d_j}{d_{max}}\right)^{\tau} \qquad 3 < \tau < 8 \qquad (25)$$

By obtaining the expressions of collision frequency efficiencies, $\gamma(i,j)$ for Brownian motion, $\gamma(i,j)$ and $\psi(i,j)$ for fluid motion and differential sedimentation, the modified collision frequency functions are represented as follows:

$$\beta_b'(i,j) = \beta_b(i,j)\gamma_b(i,j) \qquad (26)$$

$$\beta_f'(i,j) = \beta_f(i,j)\,[\gamma_f(i,j) + \psi_f(i,j)] \qquad (27)$$

$$\beta_d'(i,j) = \beta_d(i,j)\,[\gamma_d(i,j) + \psi_d(i,j)] \qquad (28)$$

The expression of $\gamma(i,j) + \psi(i,j)$ describes how the collision efficiency, $\gamma(i,j)$ decreases due to hydrodynamic effect, but $\psi(i,j)$ increases due to porosity effect. The value of $\gamma(i,j) + \psi(i,j)$ is not larger than 1 so that the modified collision frequency function, $\beta'(i,j)$, predicts less collision frequency than the original function, $\beta(i,j)$.

The zero collision efficiency factor, $\delta(i,j)$, is multiplied by the sum of collision frequency functions to account for the particle break-up process

$$\beta_{sum}'(i,j) = \delta(i,j)\,[\beta_b'(i,j) + \beta_f'(i,j) + \beta_d'(i,j)] \qquad (29)$$

Consideration of Velocity Gradient

The velocity gradient (or mean shear rate) G could be calculated from the power input P to a tank of volume V :

$$G = \sqrt{\frac{P}{\mu V}} \qquad (30)$$

Where μ is the fluid viscosity. The velocity gradient in flocculation could be calculated from the energy input or energy dissipation in the basin and the paddle configuration of the flocculator. The procedure for calculating the mean velocity gradient for mechanical stirring with paddle flocculators is described elsewhere (Reynolds, 1982). From the procedure set out in Reynolds, the following equation is obtained:

$$G = \left(\frac{C_d A \rho_w v_r^3}{2\mu V} \right)^{1/2} \qquad (31)$$

Where:

   A = paddle cross-sectional area in a plane

   perpendicular to its direction of motion

   C_d = coefficient of drag

   ρ_w = density of the water

   μ = absolute fluid viscosity

   V = volume of reactor

   v_r = relative velocity of the paddle with respect

   to the fluid

The relationship of velocity gradient to energy dissipation

rate, ε, has been given somewhat different terms. Dentel et al.(1985) summarized various relationships as part of a literature review. A notable difference between the relationship is the proportional constant, ω, shown below:

$$G = \sqrt{P/\mu V} = \omega\sqrt{\epsilon/\nu} \qquad (32)$$

Where ν is the kinematic viscosity. The value of ω ranges from 0.49 to 9.73. Koh (1984, 1987) proposed a compartmentalized model for batch flocculation in turbine stirred tanks under various flow conditions. He mentioned that the effective mean shear rate for flocculation was not the same as the mean value obtained from power input per unit mass; rather, it is equal to the volume average value obtained from the first moment of the shear rate distribution. He proposed the following expression:

$$G_1 = \sqrt{\epsilon_1 \nu} \qquad (33)$$

Where:

> G = the velocity gradient in a compartment 1
>
> ϵ_1 = the local mean rate of energy dissipation
>
> ν = the kinematic viscosity

According to Koh, the volume average shear rate of flocculation could be approximated by three velocity gradients as shown below:

$$s\overline{VG} = V_1 G_1 + V_2 G_2 + V_3 G_3 \qquad (34)$$

Where:

> s = dimensionless volume average shear rate

V_1, V_2, and V_3= The volume of impeller zone, bulk

zone, and dead zone respectively

A basin is approximated by three compartments, each perfectly mixed and of uniform shear rate (velocity gradient). After he studied various multi-compartment models, he concluded that a single-compartment stirred tank incorporating the effective shear rate, G_{eff}, was adequate for predicting flocculation rates when collision efficiencies were small. The effective shear rate, G_{eff}, is defined as follows:

$$G_{eff} = sG \tag{35}$$

The parameter s is highly dependent on geometry. Koh tabulated the value of s for various geometries of turbine stirred tanks. He also reported a comparison between the effective shear rates in stirred tanks and those in other systems normally used for flocculation. For paddle-blade mixed systems, the values of 0.32 and 0.45 for parameter s were reported. However, paddle dimensions were not reported. For incorporating s into the new model, the average value of 0.39 will be used.

Consideration of Flow Pattern

Hydraulic residence times of the actual flocculation basins affect the degree of flocculation considerably. Residence time characteristics of basins can be evaluated as plug flow, mixed flow, and dead space characteristics. Residence time can be expressed as follows (Hudson, 1981):

$$1-F(t) = e^{-\frac{1}{(1-P)(1-m)}\left[\frac{t}{T}-P(1-m)\right]}$$ (36)

Where:

F(t) = fraction of the fluid retained in the

flocculator for a duration less than time t

T = computed residence time

= Q/V

Q = rate of flow

V = flocculator basin volume

P = fraction of active flow volume acting as plug

flow

m = fraction of total basin volume that is dead

space

t = time

In order to get information about flow patterns, dead
space, and detention time, a tracer study is required. In
case there is no available information about flow pattern,
the flocculation basins are assumed to be ideal continuous
stirred tank reactors (CSTR). The flow patterns for a
series of equal size CSTR's in series can be described with
the following expression:

$$1-F(t) = [1 + t/T + (t/T)^2/2! + ... + (t/T)^{n-1}/(n-1)!] \exp(-t/T)$$ (37)

Time corresponding to the F(t) values can be determined for
each flocculator basin. To obtain the particle size
distribution of each flocculator, the particle size

distribution calculated at values of F(t) equal to 0.2, 0.4, 0.6, 0.8, and 0.975 are averaged.

Summary

The flocculation model was modified by incorporating terms for interparticle force, floc density, floc shape, floc break-up, and effective velocity gradient into the collision frequency functions. The flow pattern of the flocculation basins is incorporated using F(t). The effects of factors incorporated into the collision frequency functions on the collision frequency are summarized in Table IV. The interparticle force, floc break-up, and effective velocity gradient affect to decrease the collision frequency. Whereas, the floc density and floc shape causes an increase in the collision frequency. With the modified collision frequency functions, the flocculation model calculates particle size distribution at 0.2 increments of the F(t) value and averages the calculated particle size distributions.

TABLE IV

EFFECTS OF THE FACTORS INCORPORATED INTO
THE COLLISION FREQUENCY FUNCTIONS
ON COLLISION FREQUENCY

factor	expression	effect
interparticle forces	$\gamma(i,j)$	decrease
floc density	$\psi(i,j)$	increase
floc shape	d_f	increase
floc break-up	$\delta(i,j)$	decrease
effective velocity gradient	s	decrease

CHAPTER IV

MODEL SIMULATION

Comparison of Collision Frequency Functions

Comparisons between the original collision frequency function, $\beta(i,j)$, and the modified collision frequency function, $\beta'(i,j)$, have been conducted. For development of comparisons, one particle is held constant at 1 μm in case 1 and 10 μm in case 2 and the other particle size is varied. Reasons behind choosing the two particle constants are:

1) 1 μm size particle is in the size range that contains most of the clay minerals in raw water (Stumm and Morgan, 1981).

2) Brownian diffusion collision is the primary mechanism to flocculate particles with a size less 1 μm.

3) 10 μm size particle is in the intermediate range which can produce large settleable floc.

4) Fluid shear and differential sedimentation collision can be the predominant mechanisms of flocculation of the 10 μm size particle.

Simulations have been made with values of typical operating parameters:

$G = 22 \ \text{sec}^{-1}$

temperature = 20 °C

particle density = 2.65 g/cm^3

Hamaker constant (H) = 2.0 x 10^{-19} J

Case 1. Constant 1 μm Particle Size

The values of modified collision frequency functions
are shown in Figure 8. Figure 8 shows that fluid shear and
differential sedimentation are the predominant mechanisms
for flocculation. The ratio of the modified collision
frequency function, $\beta'(i,j)$, versus original collision
frequency function, $\beta(i,j)$, for Brownian, shear, and
differential sedimentation as a function of particle size
are calculated and plotted in Figures 9, 10, and 11. The
modified Brownian collision frequency function varied from
0.63 to 7.6 times of the original Brownian collision
frequency function. Until the particle size reaches log d =
0.9 (d = 7.94 μm), the modified Brownian collision
frequency function predicts less collision frequency than
the original Brownian collision frequency function due to
the hydrodynamic effects. However, above log d = 0.9, the
modified Brownian collision frequency function predicts
more collision frequency due to the increased floc diameter
and irregular shape or fractal dimension of the floc (see
equation 24). For shear, the modified collision frequency
function underpredicts the original collision frequency,
reaching a minimum value at log d = 1.0 (d = 10 μm), until
log d = 1.42 and then predicts collision frequency more
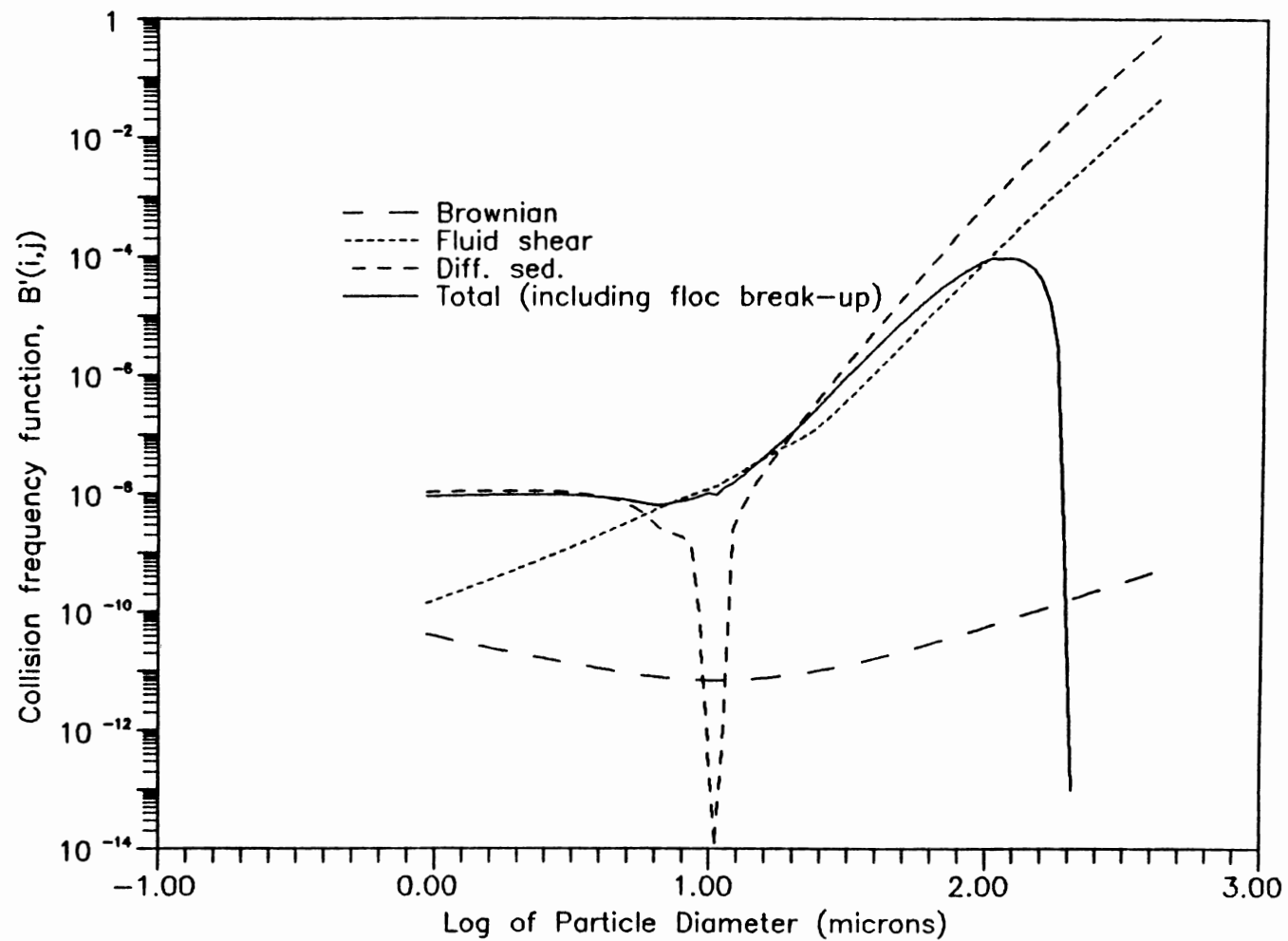
Figure 8 Influence of particle size on modified collision frequency
($d_1 = 1um$)
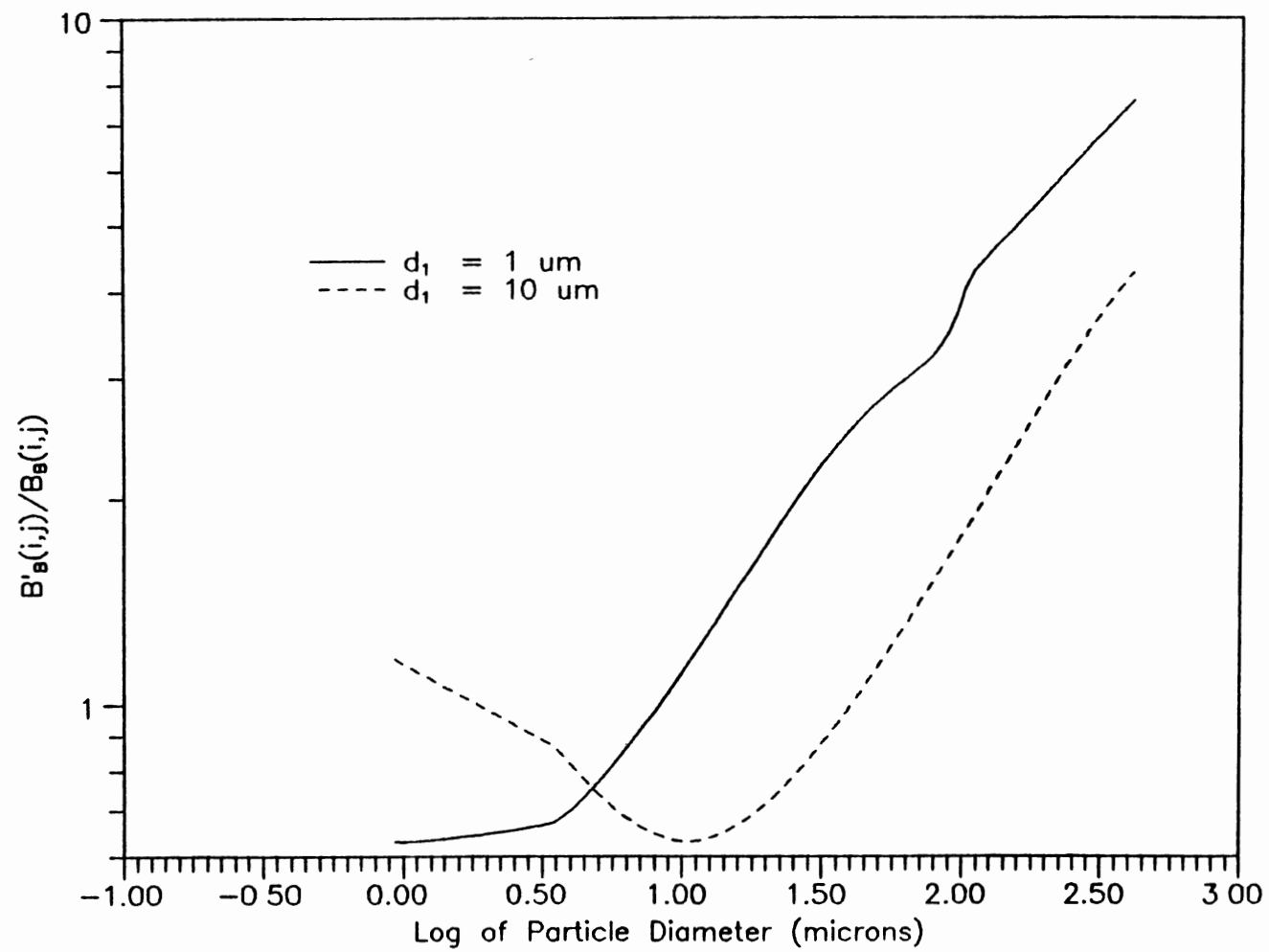
Figure 9. Ratio of modified and original collision frequencies for Brownian
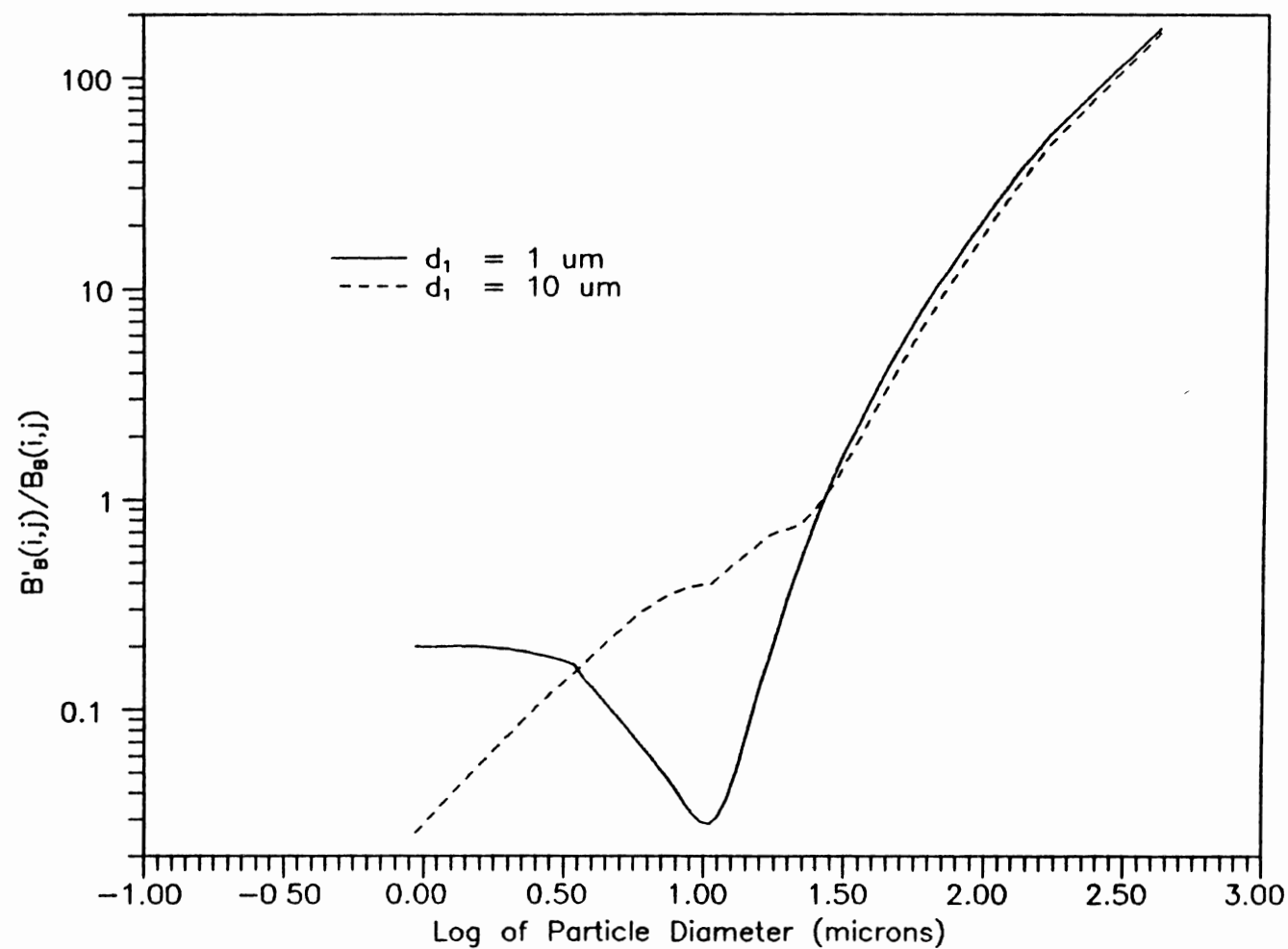
Figure 10. Ratio of modified and original collision frequencies for fluid
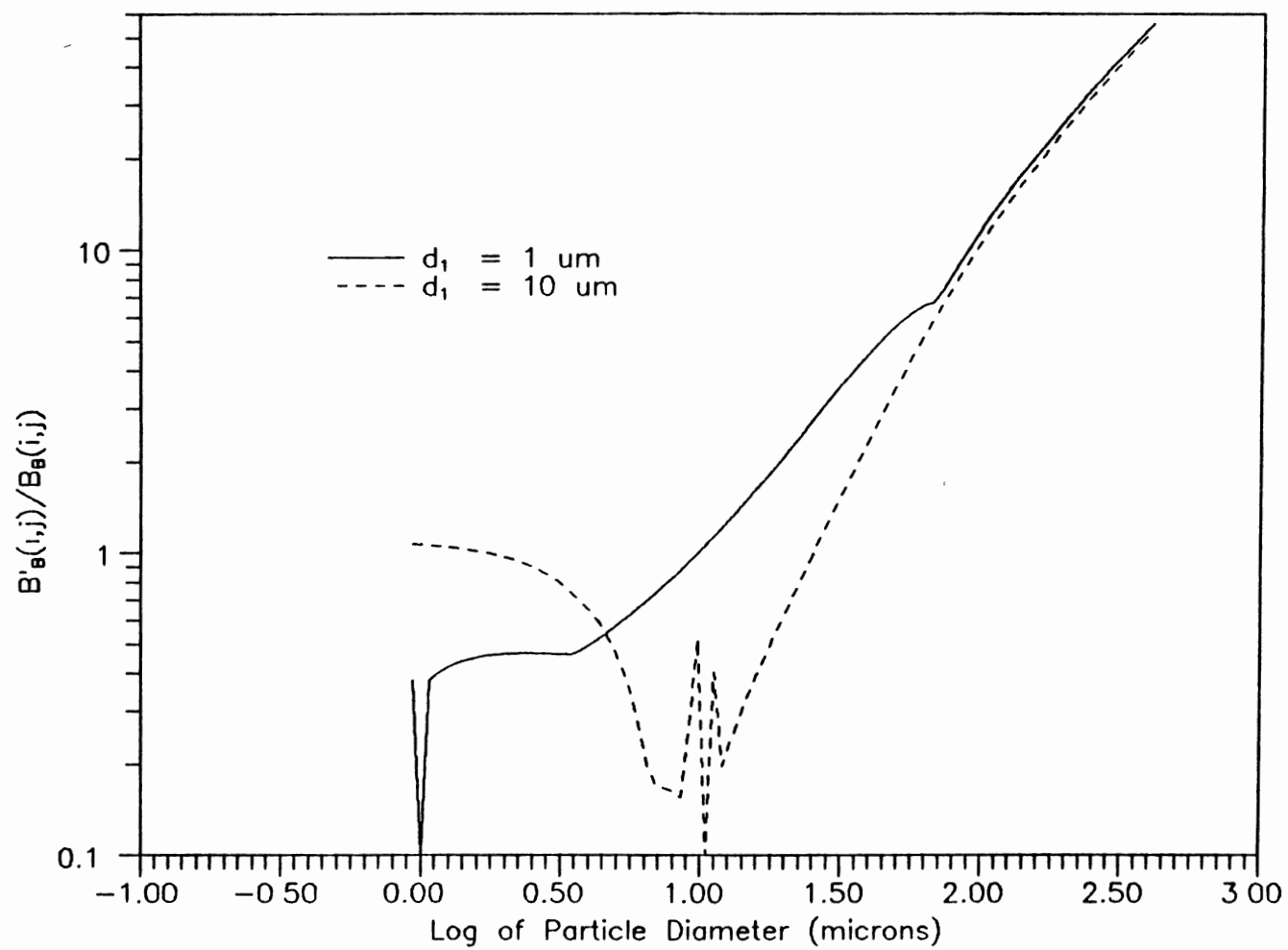
Figure 11. Ratio of modified and original collision frequencies for differ sed.

increased collision frequency is due to the increasing
porosity and floc diameter as the particle size grows. The
ratio of the modified shear collision frequency function
versus the original shear collision frequency function
varies from 0.03 to 170. The ratio of the modified
differential sedimentation collision frequency versus the
original differential sedimentation collision frequency
varies from 0.38 to 56. Figure 12 shows the ratio of the
modified total collision frequency function versus the sum
of the three original collision frequency functions. The
modified total collision frequency function represents the
sum of three modified collision frequency functions
multiplied by the zero collision efficiency term. As
mentioned earlier, the zero collision efficiency term
describes floc break-up. The value of maximum floc size was
set to 200 μm in the zero collision efficiency term. Figure
12 shows that the ratio is 0.31 at log d = -0.03 and 1 at
log d = 1.2. It reaches a maximum of 2.33 at log d = 1.71
and drops to 0 at log d = 2.3. The zero collision
efficiency reduces the sum of the three modified collision
frequency functions more as the particle size approaches
the maximum floc size.

Case 2. Constant 10 μm Particle Size

Figure 13 shows the values of the modified collision
frequency functions. As expected, differential
sedimentation and fluid shear are the more predominant
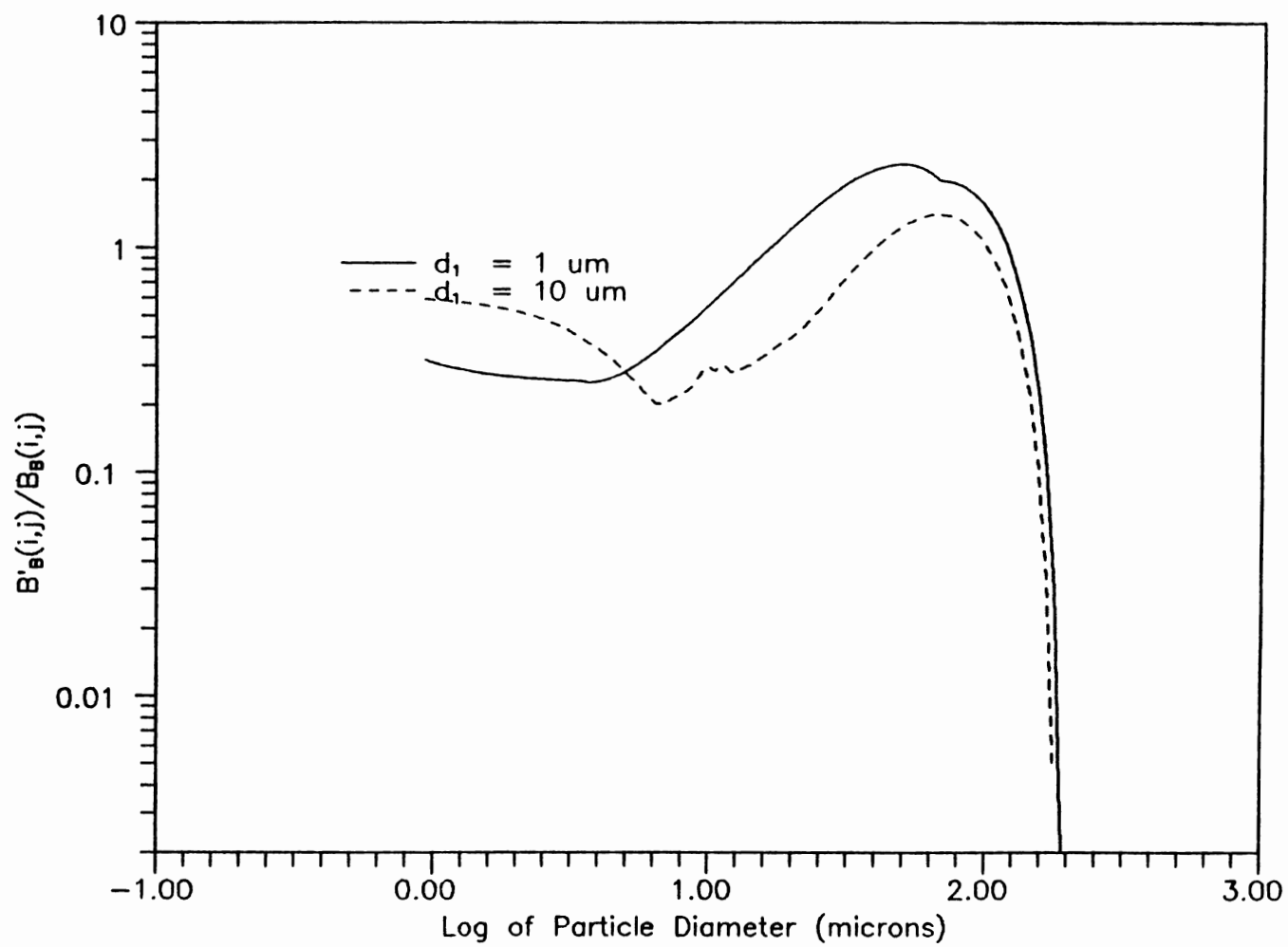
Figure 12. Ratio of modified and original collision frequencies for total
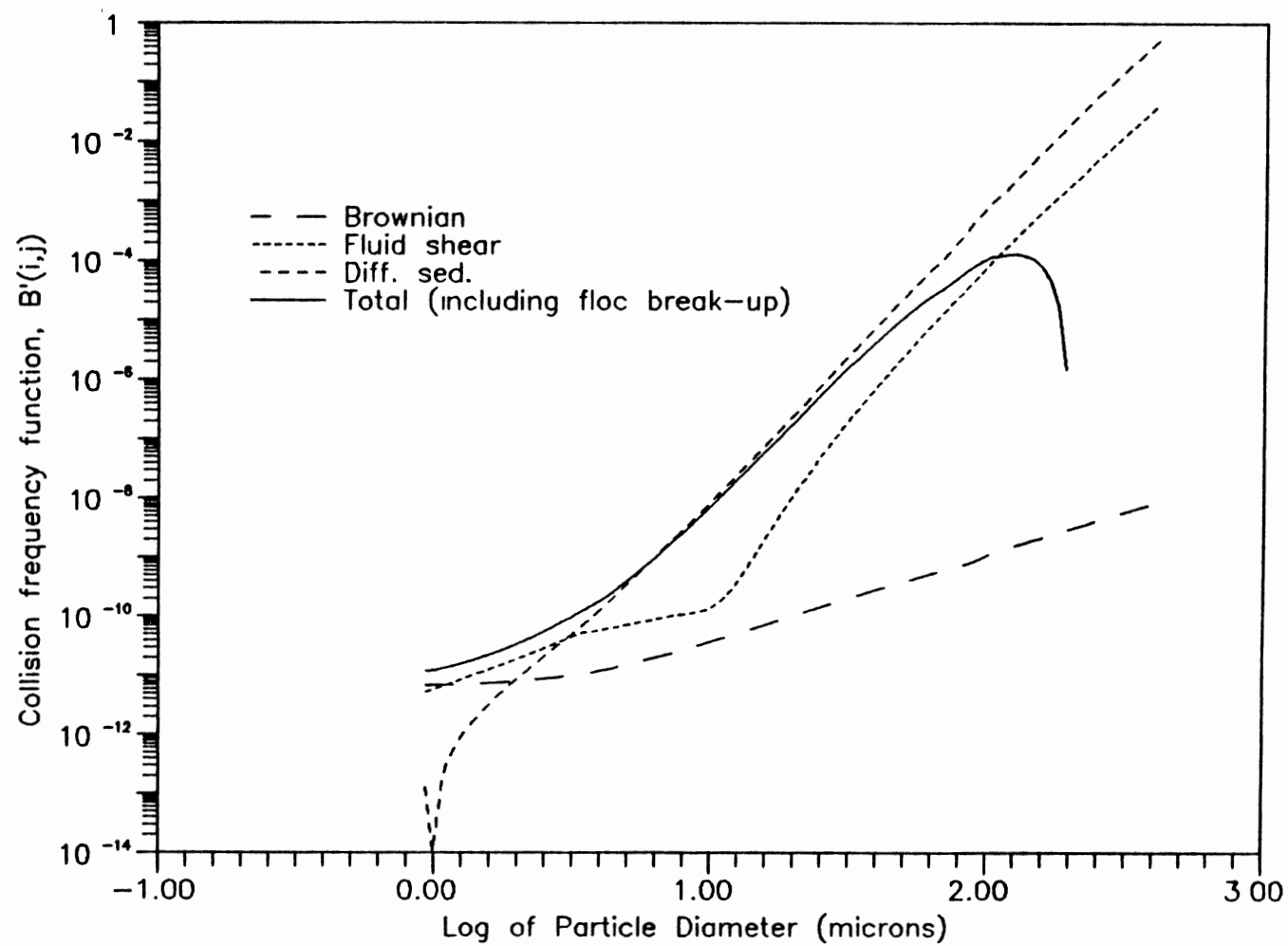
Figure 13. Influence of particle size on modified collision frequency $(d_1 = 10um)$

mechanisms for flocculation. The ratio varies from 0.63 to 4.3 for Brownian, 0.026 to 162 for shear and 0.15 to 54 for differential sedimentation, as shown in Figures 10, 11, and 12. The fluctuation observed at log d =1 in Figure 11 is caused by N_G. When the particle ratio (λ) approaches 1, N_G goes to zero. Therefore, the ratio of modified and original collision frequency approaches 1 because no hydrodynamic effect exists. When λ is equal to 1, however, the collision due to differential sedimentation does not exist since the particles are settling at the same rate. The modified collision frequency function predicts less collision frequency for small particle sizes but more for large particle sizes. The total ratio shown in Figure 12 varied from 0.59 at log d = -0.03, 1 at log d = 1.61, 1.4 at log d = 1.83 and 0 at log d = 2.3.

Comparisons between the original collision frequency function and the modified collision frequency function show that the modified collision frequency function predicts less collision frequency in the region of small particle sizes and more collision frequency in the region of large particle sizes. Lawler and Wilkes (1984) mentioned that their model based on the original collision frequency function overestimated the flocculation process. According to Lawler and Wilkes, the proposed collision frequency function had to predict less collision frequency than the original frequency function prediction. According to Jiang and Logan (1991), however, the original collision function

must be modified to predict more frequent collisions in order to account for the fractal geometry of the floc. The modified collision frequency function takes into account hydrodynamic effects to reduce collision frequency. The modified collision frequency function also represents the increasing collision frequency by considering the increased floc diameters and the porosity effects.

Description of the Computer Model

A computer model has been developed to predict the change over time of the particle size distribution during actual flocculation, using the equation for flocculation, equation 1, and the modified collision frequency functions. The program was written in FORTRAN 77 language, and consists of one main program and 8 subroutines. The order of the subroutines is set out below:

1. Start

2. Initialize variables and read input data

    Subroutine INITVA

    Subroutine EFLOW

3. Calculate collision functions

    Subroutine BETACA

4. Preliminary calculation of logarithmic divisions of particle size

    Subroutine FRACCA

5. Manipulate data for initial data output

    Subroutine MASSSU

Subroutine MASSSU

6. Print initial data

Subroutine OUTPUT

7. Execute numerical method until $T > T_{max}$

solve differential equations by Runge-Kutta method

Subroutine STIFDI

evaluate the terms in differential equation

Subroutine DIFFUN

8. Manipulate data for output

Subroutine MASSSU

9. Print output

Subroutine OUTPUT

10. End

Subroutine INITVA initializes values needed throughout the program and is the point at which input is given to the program. Inputs include information on the liquid (temperature, viscosity, density), the suspension (density and particle size relationship, Hamaker constant, maximum particle size, and particle size distribution), flow pattern (velocity gradient, detention time, number of flocculators, and F curve) and other control parameters such as print control, numerical step size, and maximum time etc.. Residence time distributions (F curve) of equal volume flocculators are calculated by Subroutine EFLOW. If available, an experimentally derived F curve also can be used in the program.

Subroutine BETACA evaluates the collision frequency

functions for the three modified collision mechanisms and sums them.

Logarithmic division of particle sizes are used to describe the PSD. All particles within one of the standard particle sizes that are equally spaced on the basis of the logarithm of their equivalent volume (density = 2.65 g/cm^3) are assumed to have the same size. The logarithmic division describes adequately the behavior of smaller particles in the suspension. If all possible particle numbers are assigned in equal divisions of particle volume, a large fraction of the total particle number size reside in the small standard size ranges because of the large number of small particles. Equal divisions of particle size would result in an inadequate description of the behavior of smaller particles. To save computer memory space, it is also convenient to use logarithmic size divisions. However, with standard particle sizes that are equally spaced on the basis of the logarithm of the volume, the arithmetic sum of any two standard volumes does not produce another standard volume. By using subroutine FRACCA developed by Lawler et al. (1980), weighted fractions of the new particle are assigned to standard particle sizes. A method to account for this is illustrated in Figure 14. When particles of size i and j aggregate, one new particle of equivalent volume, (V_i and V_j), is formed; and this new particle has an equivalent volume between standard sizes k and k+1. This is handled by assigning the fraction a/c of the new particle
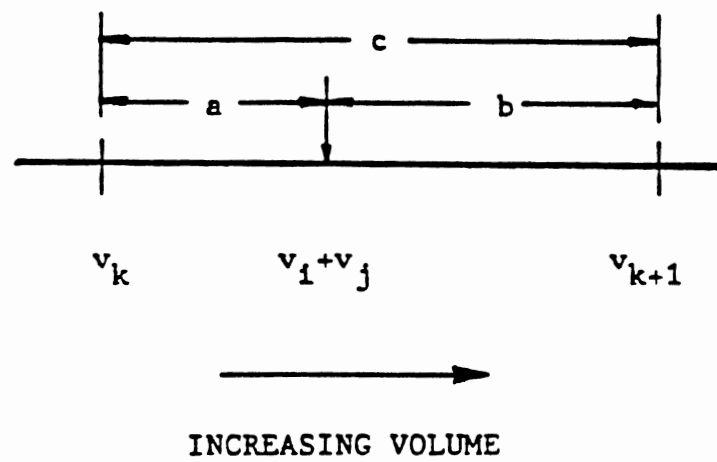
Figure 14. Assignment of aggregated particles to standard sizes

to standard size k and the fraction b/c to size k+1. This manipulation accomplishes the use of only standard size. This also allows the equivalent particle volume to be conserved. Finally, the equivalent particle volumes are converted to particle volume (floc volume) via the relationship of particle size and density.

This system is valid for all combinations of particles except when the resultant particle volume is greater than the largest standard size. The particle volume which is greater than the largest standard size is controlled by the zero collision efficiency factor (equation 25). The zero collision efficiency factor is described in the model development section. The largest size could be chosen from the available data for maximum stable particle size.

Subroutine DIFFUN evaluates each of the two terms on the right hand side of equation 1 for each standard size. The combinations which yield a total volume between size k and k+1 are dictated by the choice of the log increment between particle sizes. If the log of volume increments were not 0.09 (the log of diameter increments = 0.03), a different set of combinations would result in the formation of particles between size k and k+1 so that subroutine FRACCA would need revision to reflect this change.

Subroutine STIFDI is used for obtaining approximate solutions to a system of ordinary differential equations with the initial particle size distribution. A 4th order Runge-Kutta method is used.

Subroutine MASSSU evaluates several parameters, such as total particle number, total particle volume, total particle mass, particle size distribution, particle volume distribution, number fraction remaining, volume average diameter, surface average diameter, and number average diameter for desired output prints. Subroutine OUTPUT is used to print desired output.

Comparison of Reported Experimental Results
with Predictions of the Model

In order to use the model to compare predictions with reported experimental results, initial values for particle size distribution have to be supplied. The reported particle size distribution (PSD) was expressed in several ways. The new computer program is able to use particle size distribution function ($\Delta N/\Delta d$), and number of particles within logarithmic particle size interval ($\Delta \log V$, which, as mentioned earlier, is 0.09 or $\Delta \log d = 0.03$). In order to use PSD information in different particle size intervals for the model input, data manipulation has to be done. The number of particles within the preestablished model particle size intervals is calculated by obtaining the linear regression equation for reported experimental particle number and particle size range.

Several sources (Metcalf & Eddy, 1979, Peavy et al. 1985, Valioulis & List, 1984) defined suspended solids as all particles with diameters larger than 1 μm. The portion

of total solids retained by a glass-fiber filter is defined as suspended solids (APHA, 1985). A portion of the particles smaller than 1 μm could be retained according to the latter definition. In this work, suspended solids are defined as all particles with diameters larger than 0.89 μm, because the particle size of 0.89 μm was the smallest particle size for which particle size distribution information was obtained for the model verification.

Case 1. Davis Water Treatment Plant, Austin, Texas

Lawler and Wilkes (1984) reported a flocculation model. Their model was tested against actual treatment plant performance in terms of particle size distribution. Required particle size distribution data from the flocculation process in the operating water treatment plant was measured by a Coulter counter. The following is a brief description of the treatment plant. A more detailed description is given in their paper (Lawler and Wilkes, 1984). The plant is located adjacent to Lake Austin which is the source of water for the plant. This plant has a 100 MGD capacity. It has nine flocculation and sedimentation units and three filters for each unit. Each of the nine flocculation basins is divided into three sub-basins in series, with the volume of each sub-basin increasing from the first to the third basin. The lake has an average hardness of 170 mg/L, as calcium carbonate, so one of the primary treatment objectives is to reduce this hardness to

approximately 70 mg/L. The softening process uses 95 mg/L lime, as calcium oxide (CaO), to reduce the hardness. Small doses of ferrous sulfate (2.5 mg as $FeSO_4 \cdot 7H_2O$/L) are added as a coagulant.

Required input data for this modeling study was read from their Figures 10, 12, and 13 (Lawler and Wilkes, 1984). Their results were plotted as log of particle size distribution function $\Delta N/\Delta d$ (μm cm^{-3}) vs log of particle diameter (μm). The possibility exists that errors could be made while reading their data from the reported figures in order to obtain the data (influent) required to test the model. Model comparison and verification was also made by reading their effluent data from their Figures 10, 12, and 13.

Figure 15 shows the predictions of the two models using the measured influent (820 mg/L) and effluent particle size distribution of the Davis Water Treatment Plant. Lawler's model used $\alpha = 0.2$, and the model developed as part of this research used $\alpha = 1$. In Lawler's model, low collision efficiency factors ($\alpha < 1$) were necessary to compensate for an overprediction of particle growths by the model. Using the value of $\alpha = 1$ removes the need to compensate for an overprediction of particle growths by the model and essentially means no correction factor in the modified model. Input for the maximum particle size used was 100 μm. The predictions of both models agree well with the measured results in the size region log d < 0.1 (d <
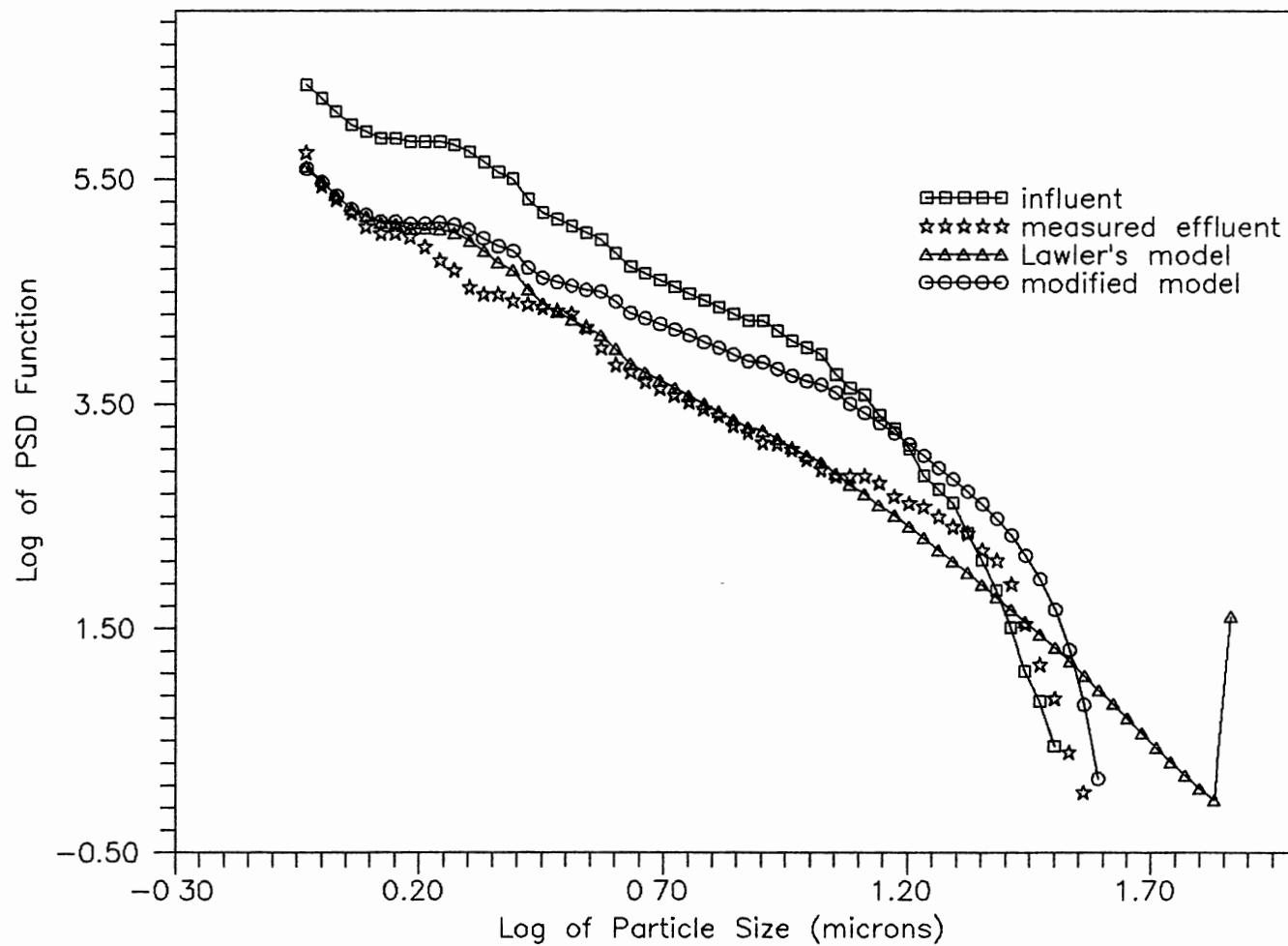
Figure 15. Comparison of measured results versus Lawler's and modified model predictions (820 mg/L)

1.6 μm). The modified model predicts a greater particle
number in the region log d > 0.1 than actual measured
particle number, while the comparison between Lawler's
model predictions and the measured results show good
agreement until log d < 1.4. A notable discrepancy appears
between Lawler's model predictions and the measured results
of particles larger than log d = 1.6. At the largest size
particle log d = 1.85, a sudden peak point can be noticed
using Lawler's model. According to Lawler et al. (1980),
his model used the largest size as a sink for the
flocculation process so that volume was not lost from the
upper end of the size spectrum. The modified model
predictions show better agreement with the measured results
in the region of large particle sizes.

Each model's predictions for the smaller concentration
case (417 mg/L) are shown in Figure 16. Both models'
predictions agree with the measured results in the range of
the large particles instead of the small ones. Actual
removal of small particles by flocculation was much greater
than the two models predict. The modified model predicts
sightly less flocculation than Lawler's model in the region
of log d < 0.7. The prediction of Lawler's model shows a
similar trend as before with a sudden peak point and
production of larger particles in the larger particle size
region. The modified model predictions show similar
distribution shape to the measured result in this region.
The modified model predictions fit the measured results in
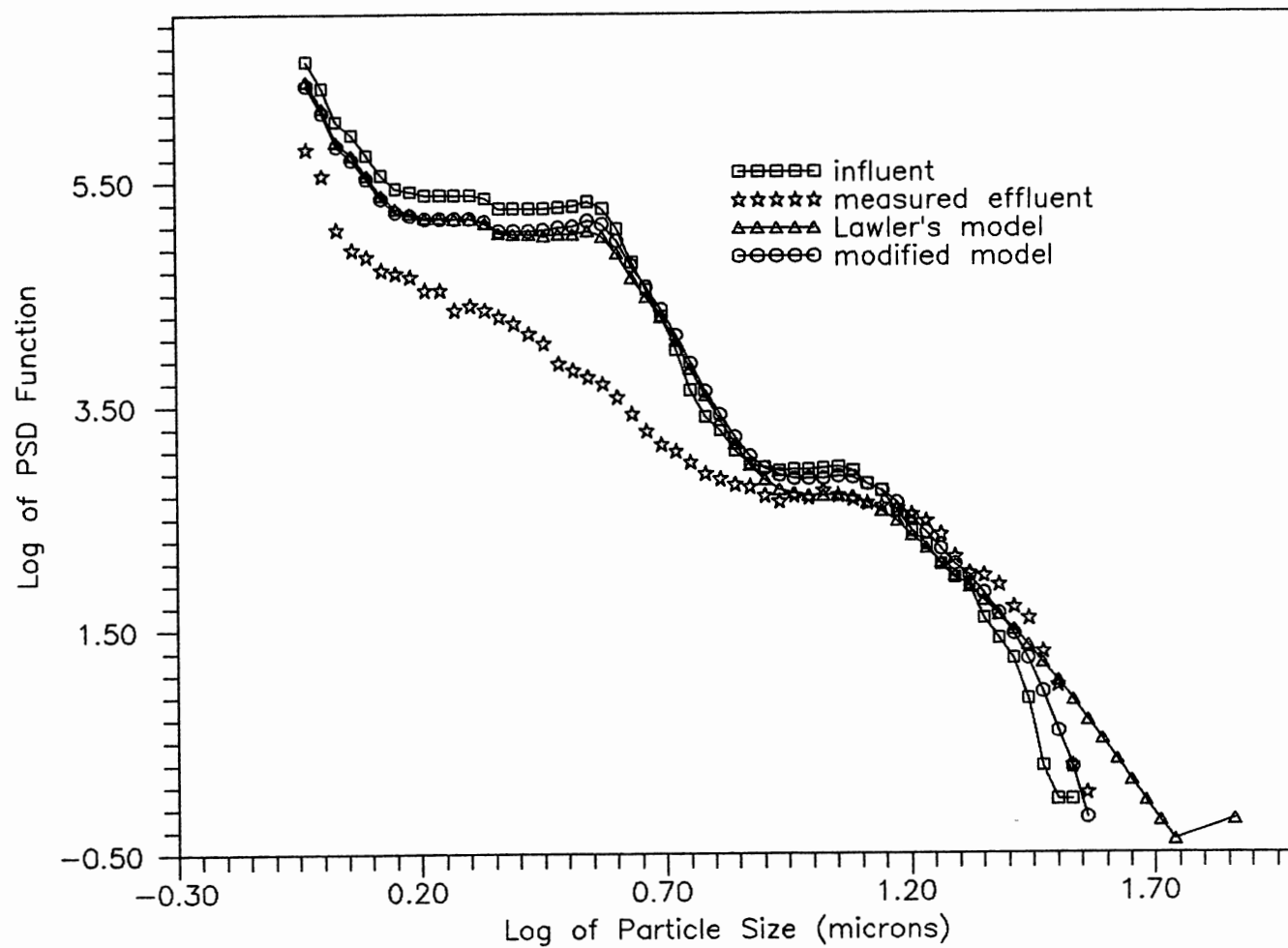
Figure 16. Comparison of measured results versus Lawler's
and modified model predictions (417 mg/L)

this region again.

A last comparison was made using another, greater, concentration case (915 mg/L). The predicted particle size distributions of Lawler's and the modified model are shown in Figure 17 along with the measured results. In the previous two cases Lawler's model used $\alpha = 0.2$, but a value of $\alpha = 0.1$ provided much better agreement with the measured results in this case. This change indicates that Lawler's model is sensitive to influent concentration. Using $\alpha = 0.1$, Lawler's model overestimates the particle number until log d = 0.95, then underestimates the particle number. However, the modified model consistently used $\alpha = 1$. Like the first case, the model predictions agreed with the measured result in the small particle size region, log d< 0.1. The modified model predictions are in reasonable agreement with the measured results in the small particle size region as well as in the large particle size region.

For a closer comparison between Lawler's model and the modified model predictions against the measured results, residual plots of the three previous cases (Figures 18, 19 and 20) were made. The y axis represents the difference between the measured and predicted values of the particle size distribution function. The x axis represents the value of particle size distribution. The symbol ∆ represents the difference between Lawler's model prediction and the measured result, the symbol ○ shows the difference between the modified and the measured results. The residual plots
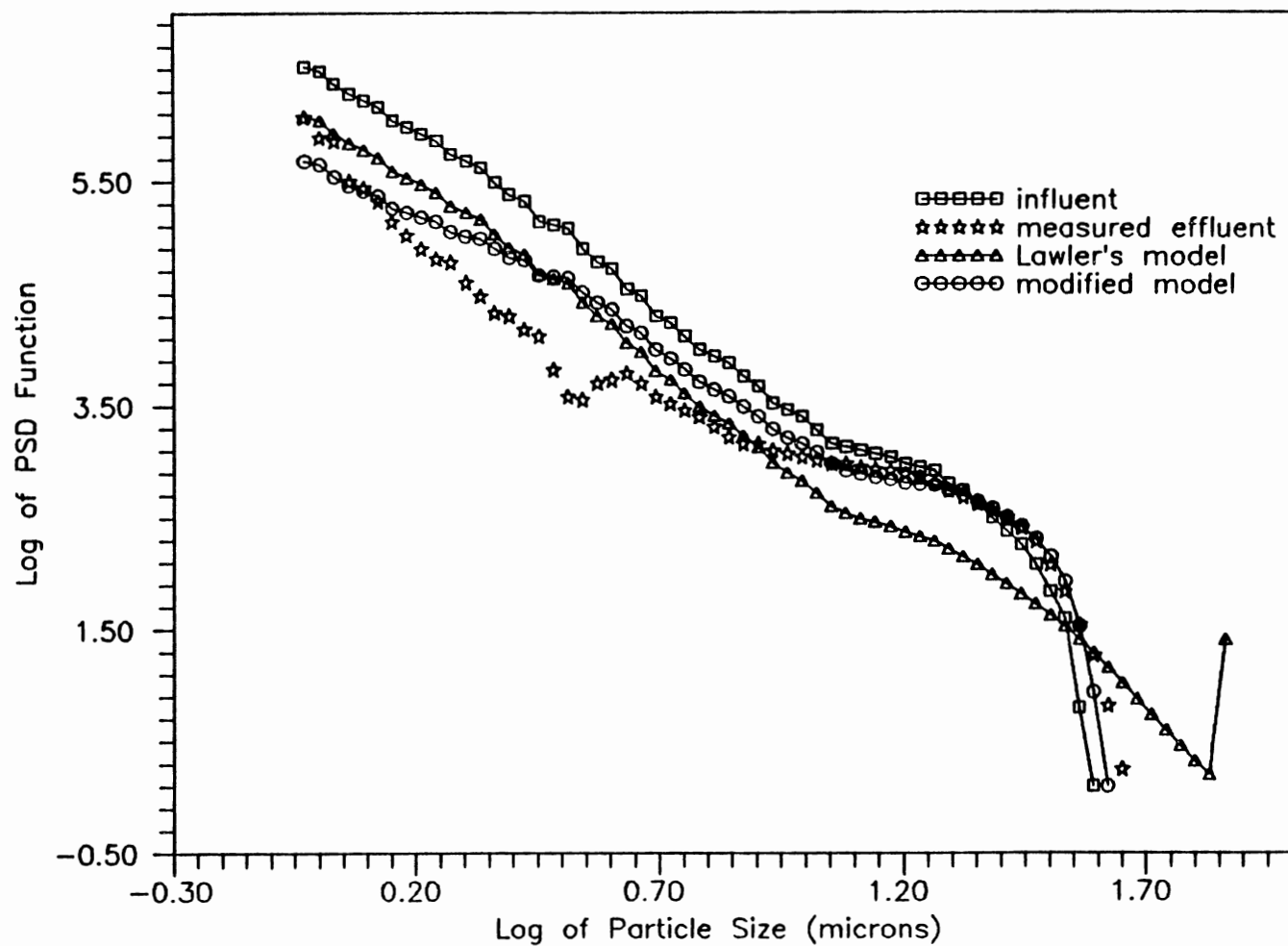
Figure 17.   Comparison of measured results versus Lawler's
and modified model predictions (915 mg/L)
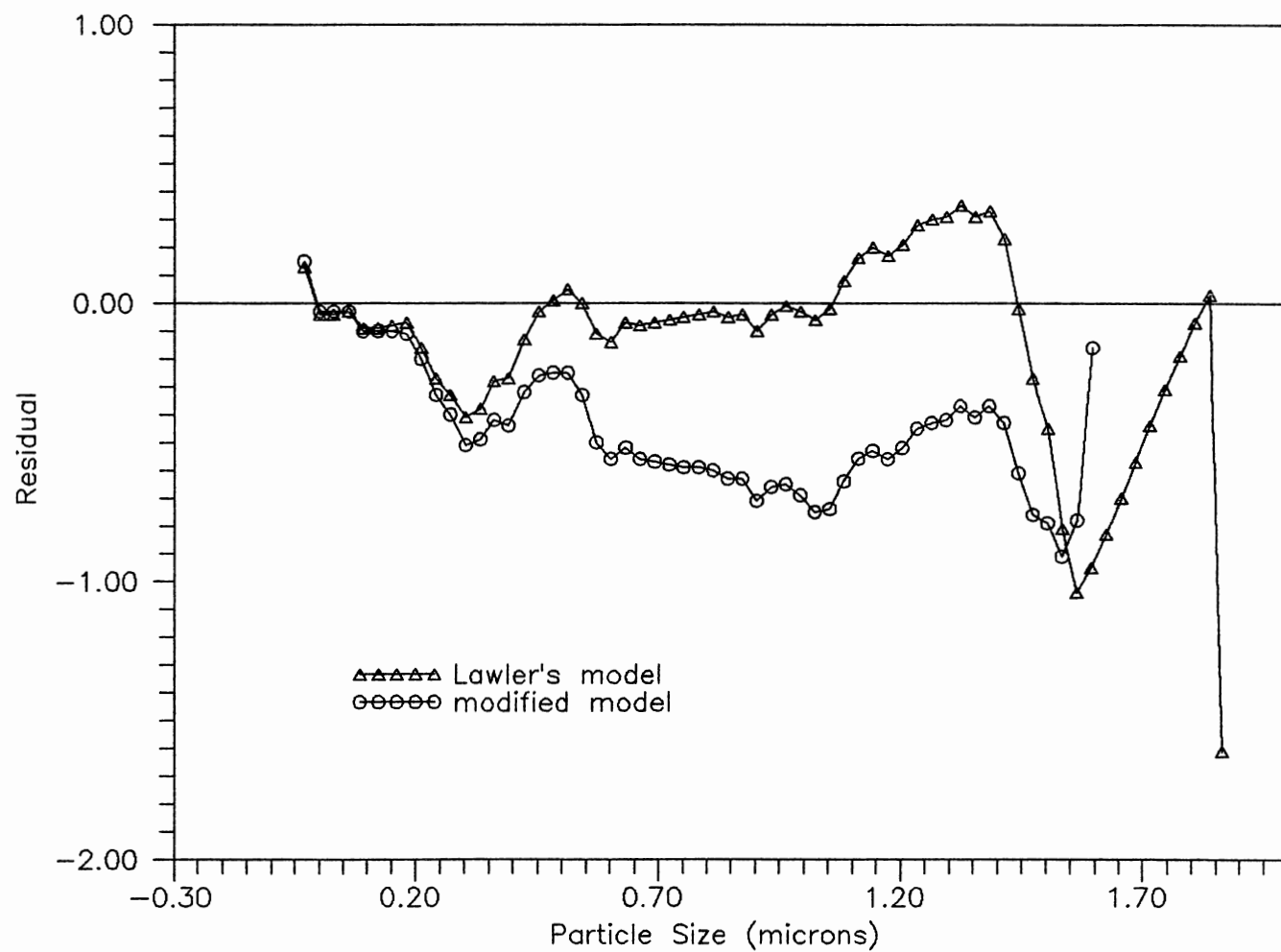
Figure 18. Residual (difference between the measured and predicted) plot (820 mg/L)

Figure 19. Residual (difference between the measured and predicted) plot (417 mg/L)

Figure 20. Residual (difference between the measured and predicted) plot
(915 mg/L)

are interpreted such that the more points cluster around y = 0 along the x axis, the more accurate the model predictions. The three residual plots show that Lawler's model's predictions are closer to the measured results in case of concentration of 820 mg/L because more residual points are located around 0 of the y axis. The two models' prediction for 417 mg/L reveal comparable results. However, the modified model better predicted the measured results for 915 mg/L. Also residuals of the modified model predictions in all three concentration show no residual in the region log d > 1.55. This means better prediction in this region.

Comparisons between the modified model predictions and the measured results show that the modified model underestimates the particle number within the intermediate particle size. The underestimation of particle number in this region requires investigation of the collision frequency function. The discussion of this fact will be undertaken in the discussion chapter.

Case 2. Southern Nevada Water System

This system (SNWS) supplies water to the cities of Las Vegas, North Las Vegas, Boulder City, Henderson, and to Nellis Air Force Base from the treatment plant at Lake Mead. The primary treatment process is directed at the separation of solids from the raw influent water. Chlorine or chlorine dioxide is added as a predisinfectant prior to

preparing particles for optimum coagulation. The primary
coagulant used is aluminum sulfate (alum). After the alum
is mixed with the plant influent, four stages of tapered
energy flocculation occur prior to direct filtration.
On-line particle counters measure the particle number and
size in the raw water immediately after predisinfection,
prior to flocculation, after flocculation (prior to
filtration), after filtration, and in the plant effluent.

For model simulation, the particle number and size
prior to flocculation were used as model input data while
the particle number and size after flocculation were used
as verification of model predictions. Flocculator influent
and effluent particle counts, collected every 15 minutes
for 5 consecutive days starting January 7, 1991 were
obtained (Rexing, 1991). The average operating conditions
of the flocculators during this 5 day period are as
follows:

- number of flocculation basins: 4
- detention time: 3.9 minutes per basin
- coagulant dosage: 0.6 mg/L of ferric chloride
- temperature: 12.4 °C
- velocity gradient of each basin: 36, 29, 21, 14.5 G

Particle number was obtained in six discrete particle
size ranges: 5-6, 6-10, 10-20, 20-40, 40-150 μm. In order
to use these data for model simulation, the data were
manipulated. The log of particle size distribution,
log($\Delta N/\Delta d$), vs log of particle size was prepared and a
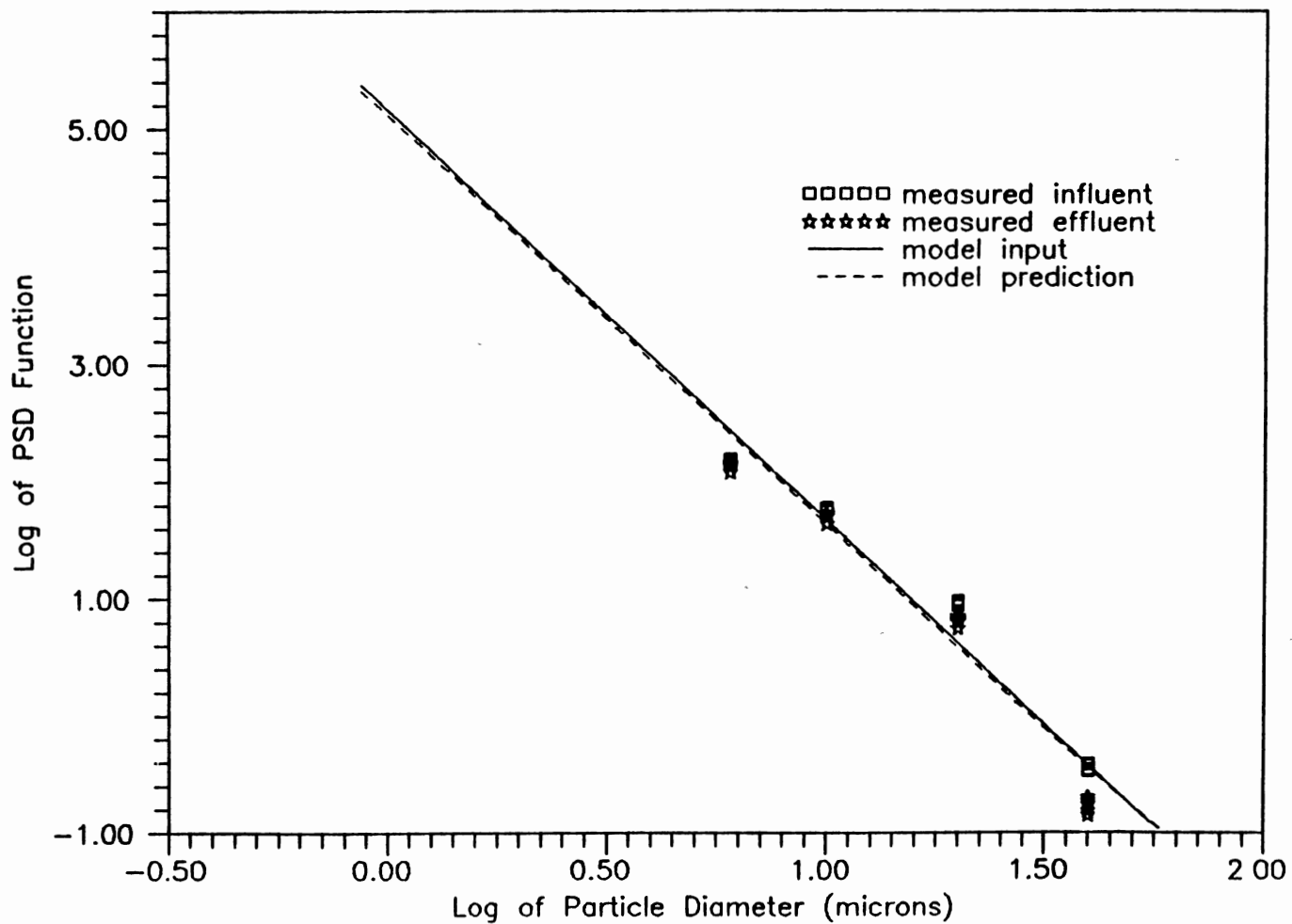
Figure 21. Comparison of measured results versus modified model predictions

linear regression was conducted (Figure 21) because the size distribution of particles in water is often characterized by the power law. No particles were reported in the range of 40-150 μm in the influent or effluent so this range was not used in the regression. The regression yielded the following power law equation with the correlation coefficient of 0.993:

$$\Delta N/\Delta d = 144543.977 \ d^{-3.49}$$

The input particle size distribution was prepared using the above equation. The predicted size distribution by the model is shown in Figure 21. The obtained effluent size distributions are also included for comparison. The measured total particle numbers in the influent and effluent were 471 and 404, respectively. The flocculation process in the SNWS resulted in 81.4% of the total particle number remaining. The model predicted 99.1% of the total particle number remaining. Comparison of the measured results and the model predictions show that the model predictions overestimate the total particle number remaining. The total particle number remaining of the measured results was calculated based on the particle size range from 5 μm to 40 μm whereas the total particle number remaining of the predicted was calculated based on the particle size range from 0.89 μm to 40 μm. Considering the narrow size range in the measured results, the model prediction greatly overestimated the total particle number remaining; in other words, the model prediction

underestimated the flocculation rate. The model here seems to underestimate the degree of flocculation at low concentration. However, close examination of the measured results show that the number of large particle sizes also decreases. This fact indicated the loss of particle number by sedimentation in the flocculation basin. This might be one explanation for the difference.

Case 3. Lab Data

The particle size distribution measured by an automatic image analysis system (AIA) was reported by Hanson and Cleasby (1990). The work was carried out in a bench-scale batch reactor. They conducted flocculation experiments using several different operating conditions. Three coagulants (alum, ferric sulfate and cationic polymer), two temperatures (5 and 20 °C) and several velocity gradients were used in their experiments. For the purpose of comparison between the results predicted by the modified model and the experimental particle size distribution measured by the AIA under different operating conditions, two of Hanson and Cleasby's (1990) data sets were used. The two data sets for the comparison of the model predictions were selected because these data sets were obtained by performing the experiment in triplicate and used for the baseline conditions for their study.

Experimental results were reported as the number of particles within discrete particle size ranges. The number

of particles was reported at the log diameter increment of 0.0765. The model developed here needed a number at the log diameter increments of 0.03. In order to obtain the required particle number at the increments of each log diameter of 0.03, a linear regression between each two particle numbers at log Δd in the cumulative number distribution plot was conducted. The total number of the particles measured was 0.3947E+7 and that obtained by the regression equation was 0.3949E+7.

The particle size distribution measured by the AIA after 0, 5, 15, 20, 25, 30 minutes of flocculation were reported. The experiments were conducted at an alum dosage of 5 mg/L, pH of 6.8, velocity gradient of 22 sec^{-1}, and temperature of 20 °C in a batch flocculator equipped with turbine impeller. Since the experiments were conducted in a batch reactor, the model did not consider the flow effects. The value of s, effective shear rate constant, used was 0.70. The value of 0.70 was used by Koh et al. (1987) for a turbine geometry batch reactor. The comparison between experimental results and the model predictions is shown in Figure 22. Figure 22 also shows Lawler's model predictions using α=1 and 0.2. The modified model prediction fit the experimental results well except for the large particle sizes (log d > 1.2). The number and volume distribution (Figures 23 and 24) show the comparison more clearly. The number distribution shows that the model predictions underestimate the flocculation process in the intermediate
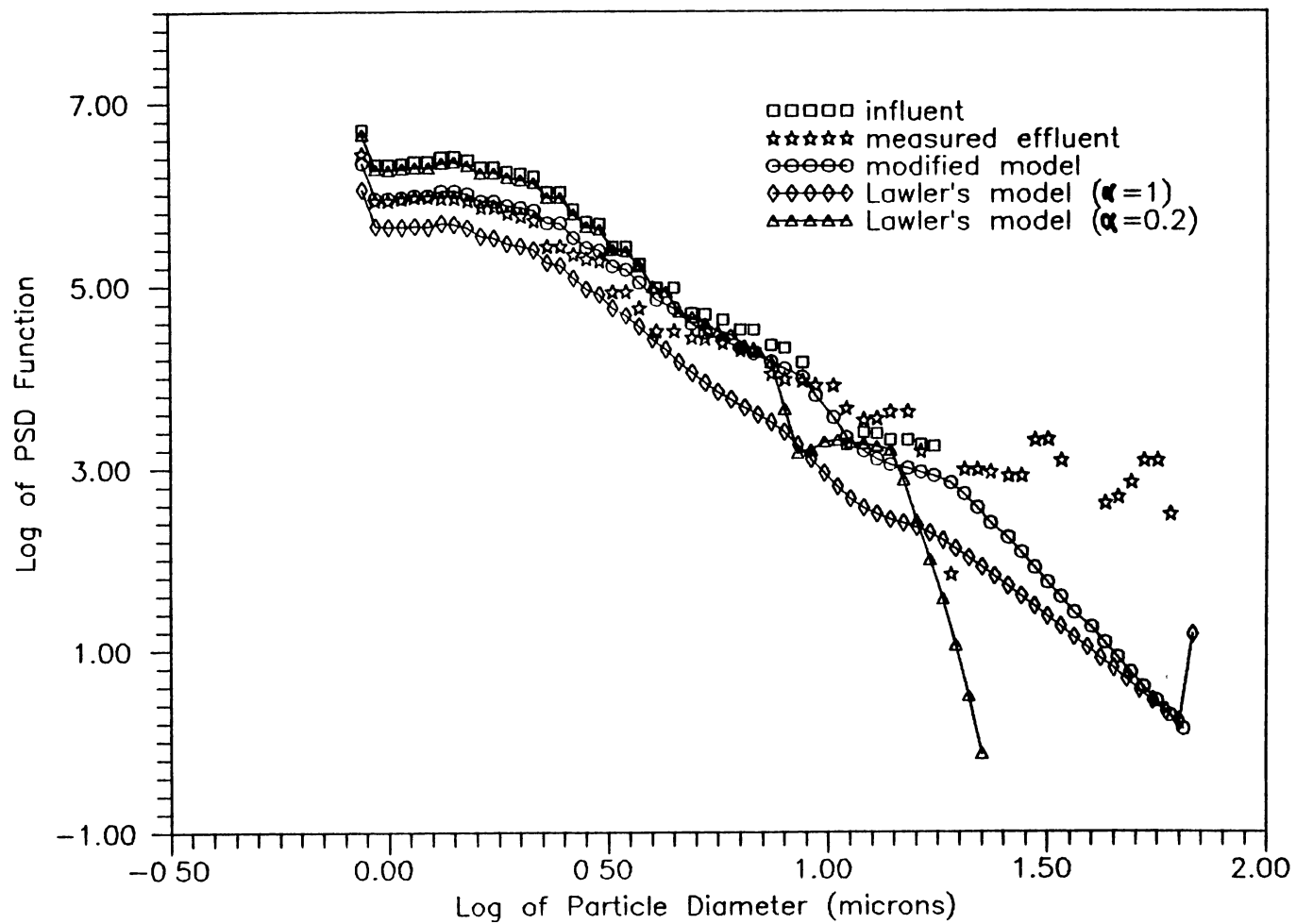
Figure 22. Comparison of measured results versus modified model predictions $(G = 22 \text{ sec}^{-1})$
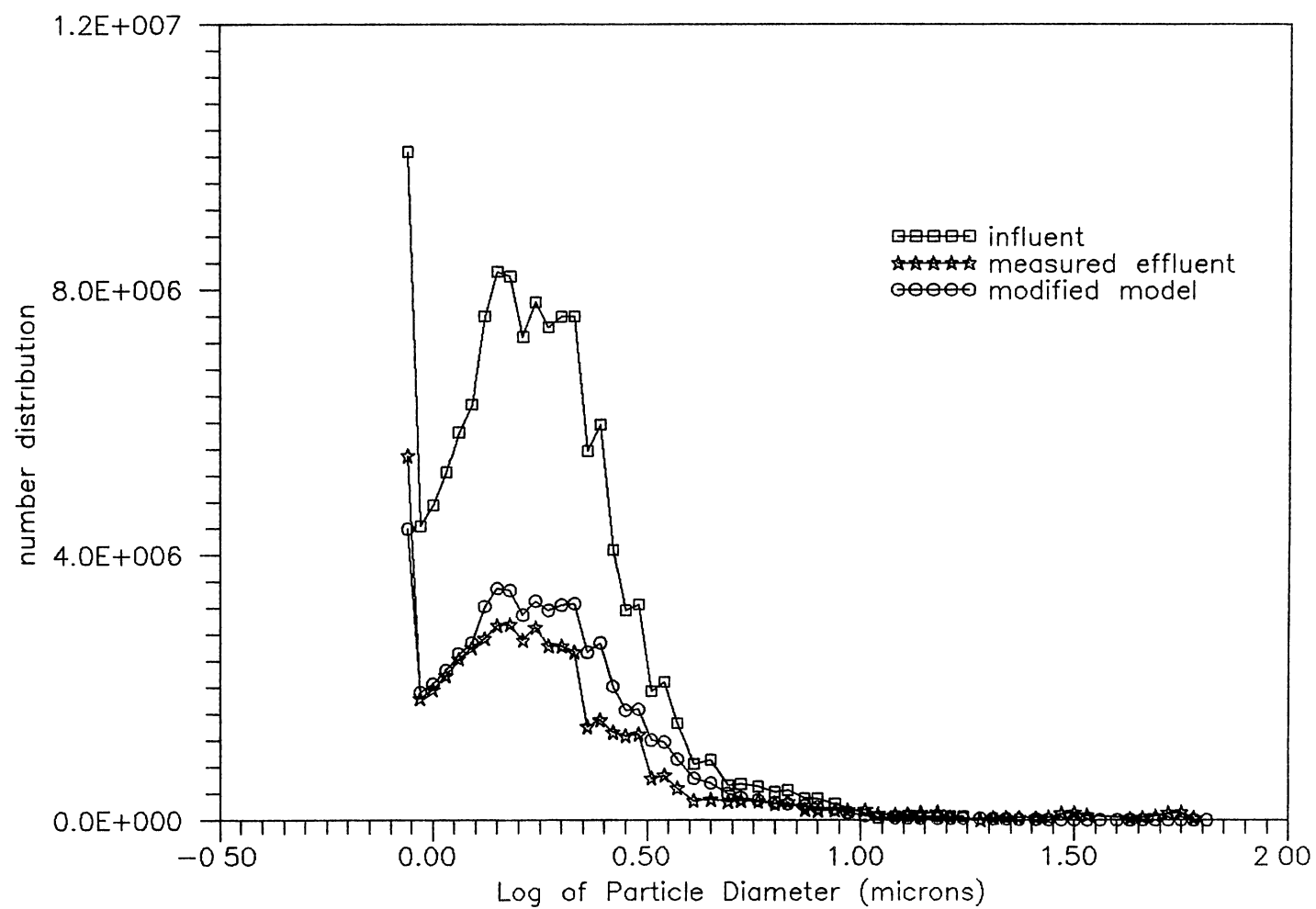
Figure 23. Comparison of measured results versus modified model predictions, Change in the number distribution
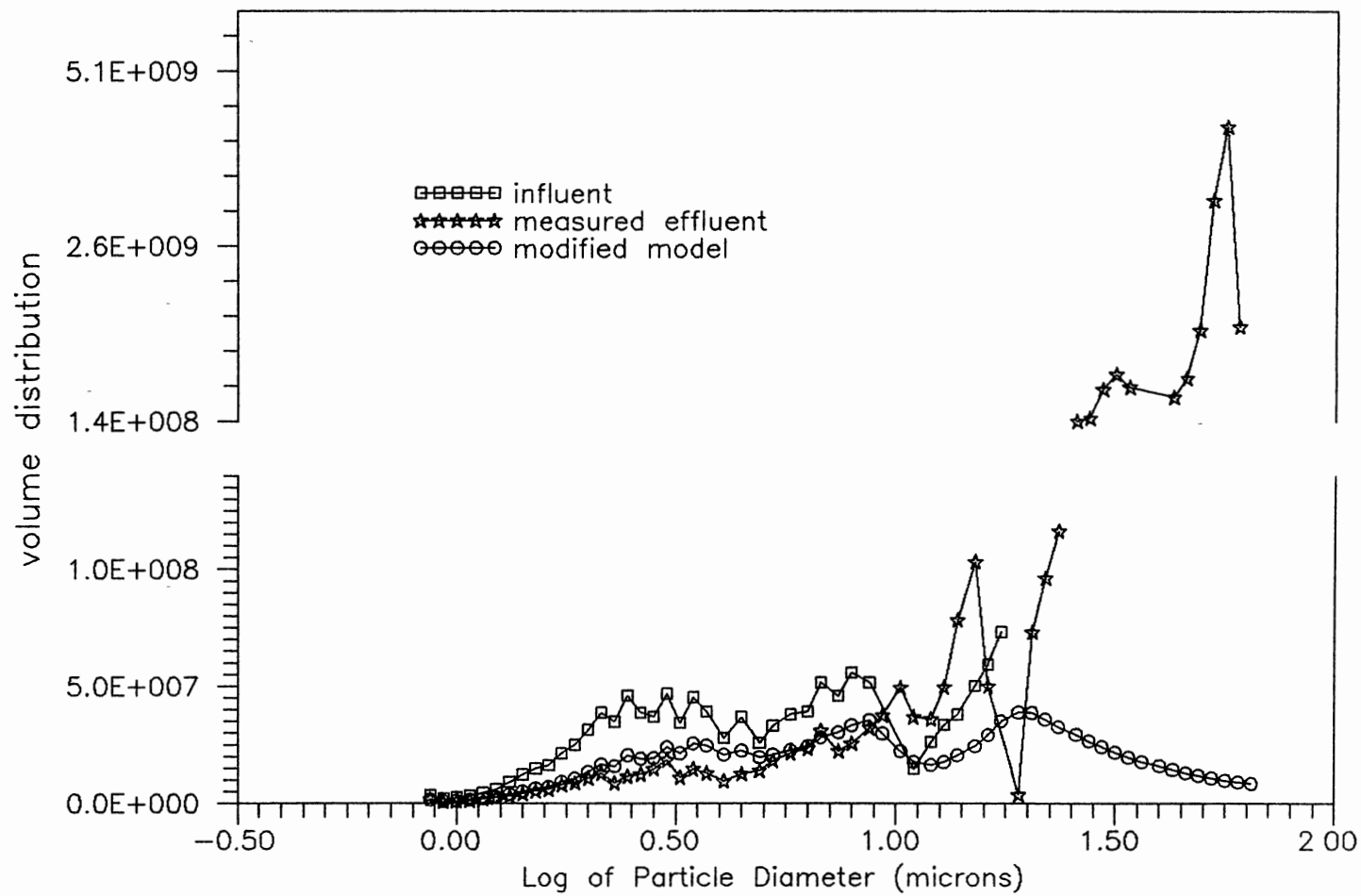
Figure 24. Comparison of measured results versus modified model predictions, Change in the volume distribution

particle size region. The volume distribution plot shows that the volume of the experimental results in the region of large particle sizes was much greater than the model predictions. The fact will be deliberated in the discussion chapter.

Figure 25 shows the comparison between the model prediction and the experimental results obtained under the same conditions as the previous case except G = 60 sec^{-1}. The number of particles in the model prediction is greater than the experimental result. The response of the model to increased G is less sensitive than that of the experiment. This might be caused by G itself. Several researchers (Cleasby, 1984; Glasgow & Kim, 1984; Clark, 1985; Amirtharajah & Trusler, 1986) have debated if G adequately reflects turbulence intensity.

The residual plots of two cases, G = 22 and 60 sec^{-1} were prepared for a comparison between Lawler's and the modified model predictions (Figures 26 and 27). The discontinuities shown in the plots were caused by either no particle number measured or a greater residual value than the y axis value. Figure 26 shows that the predictions of modified model fit better than the predictions of Lawler's model using α = 1 or 0.2 (α=1 means no correction factor). Either value for α is inadequate in this case. It seems that selecting an appropriate value between 1 and 0.2 for α would provide better agreement. The residual plot for G = 60 sec^{-1} is shown in Figure 27. Here, the predictions of
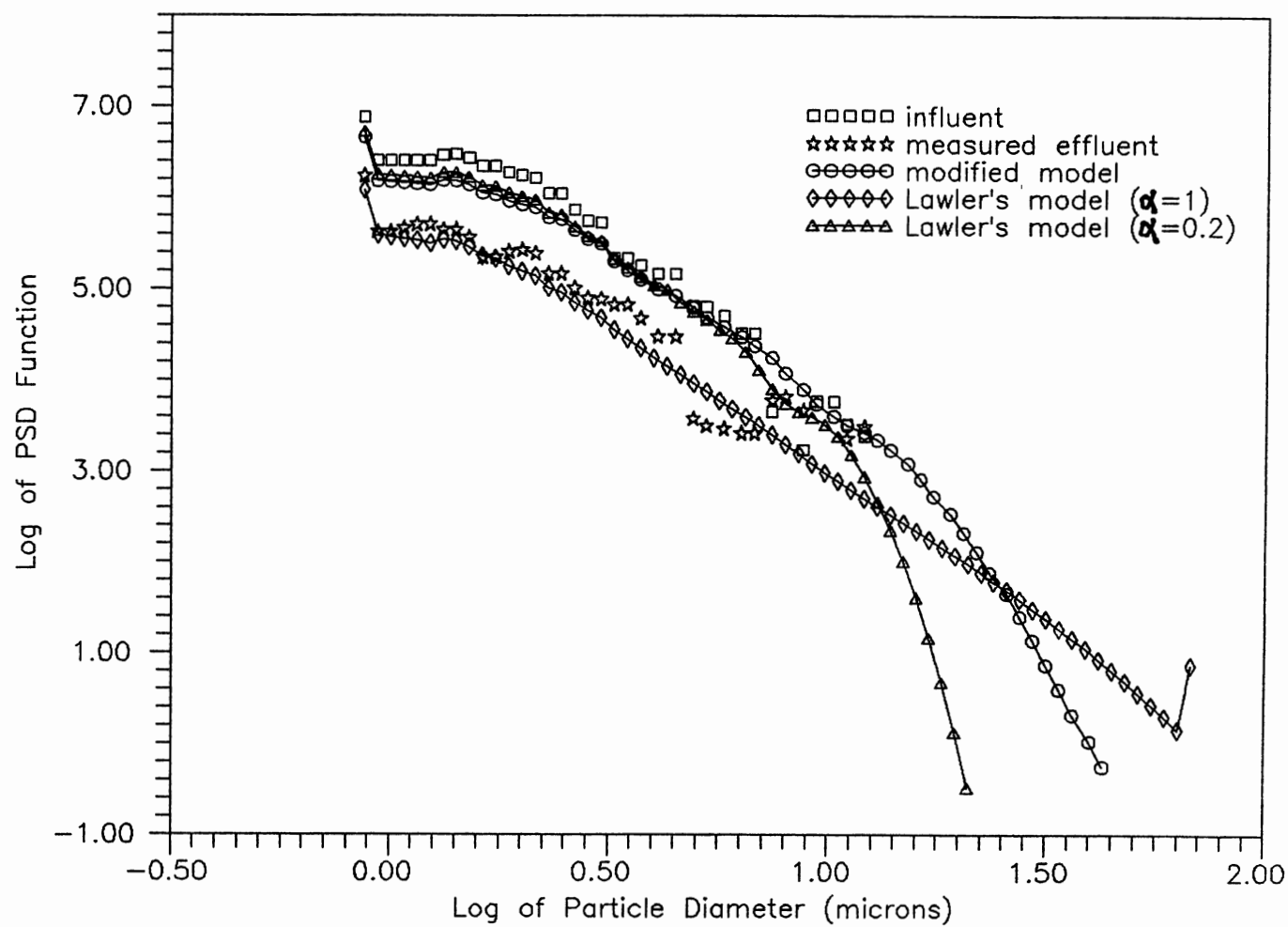
Figure 25. Comparison of measured results versus modified model predictions
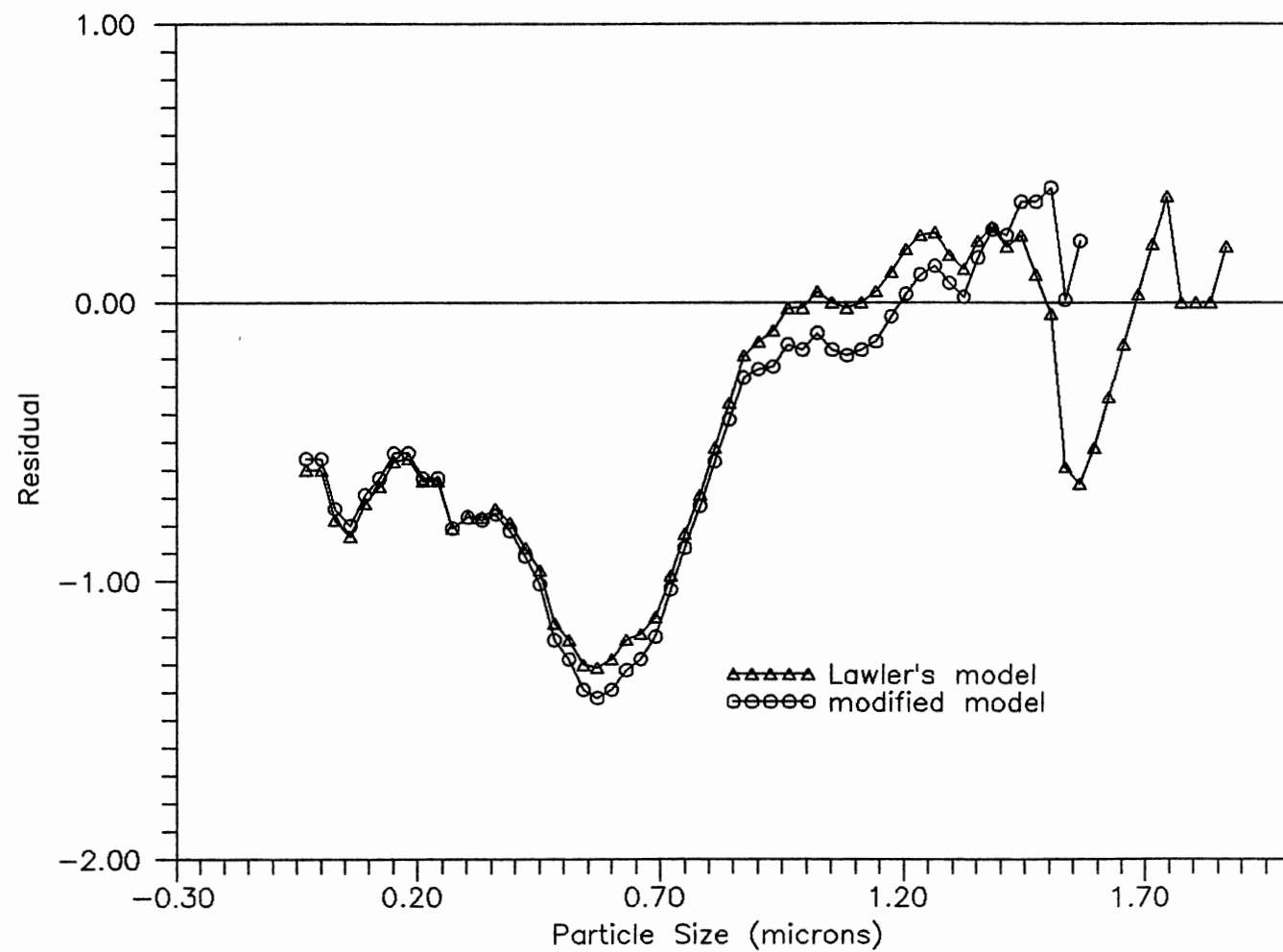(G = 60 sec^{-1})
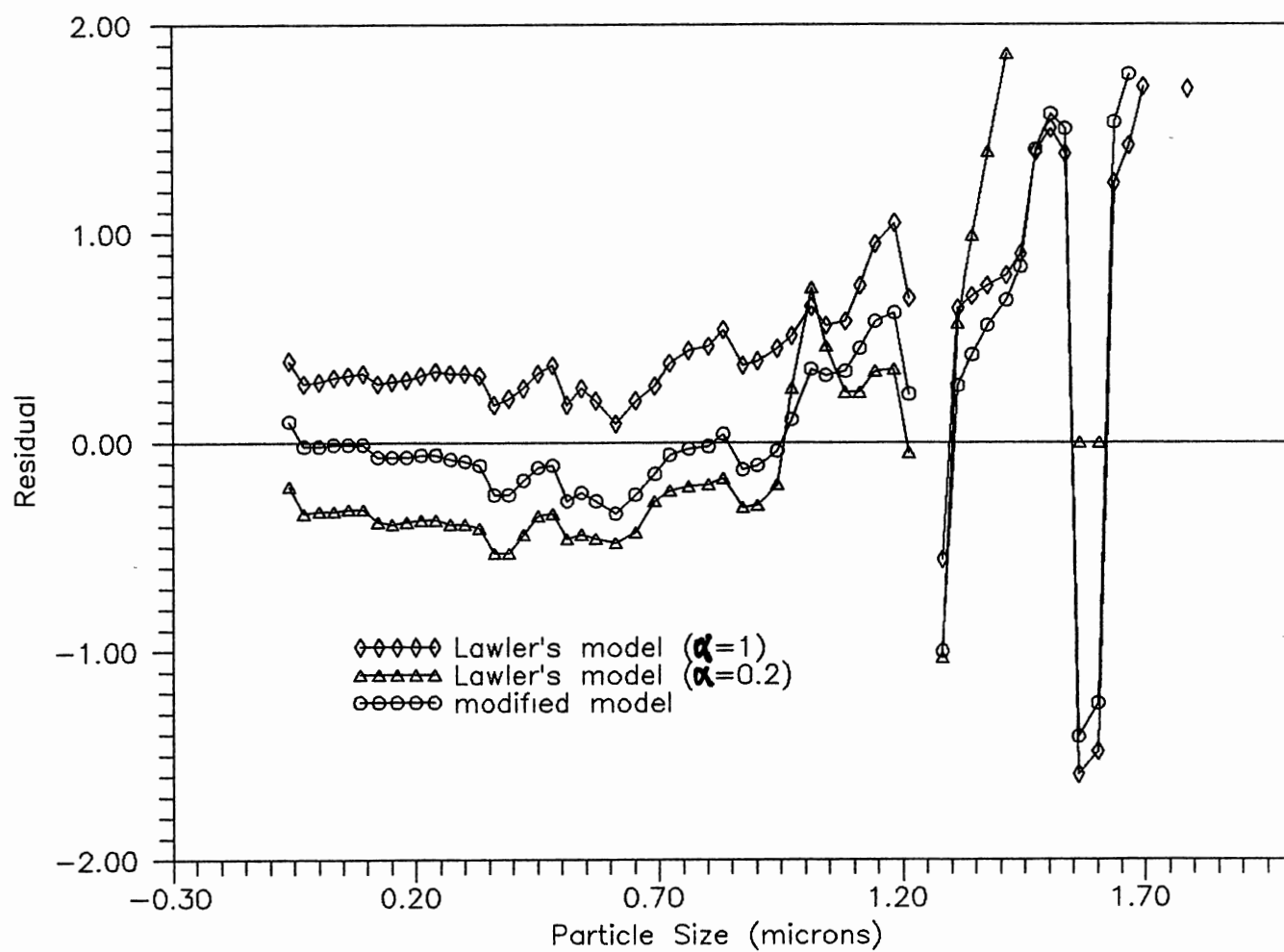
Figure 26. Residual (difference between the measure and predicted) plot
(22 sec^{-1})

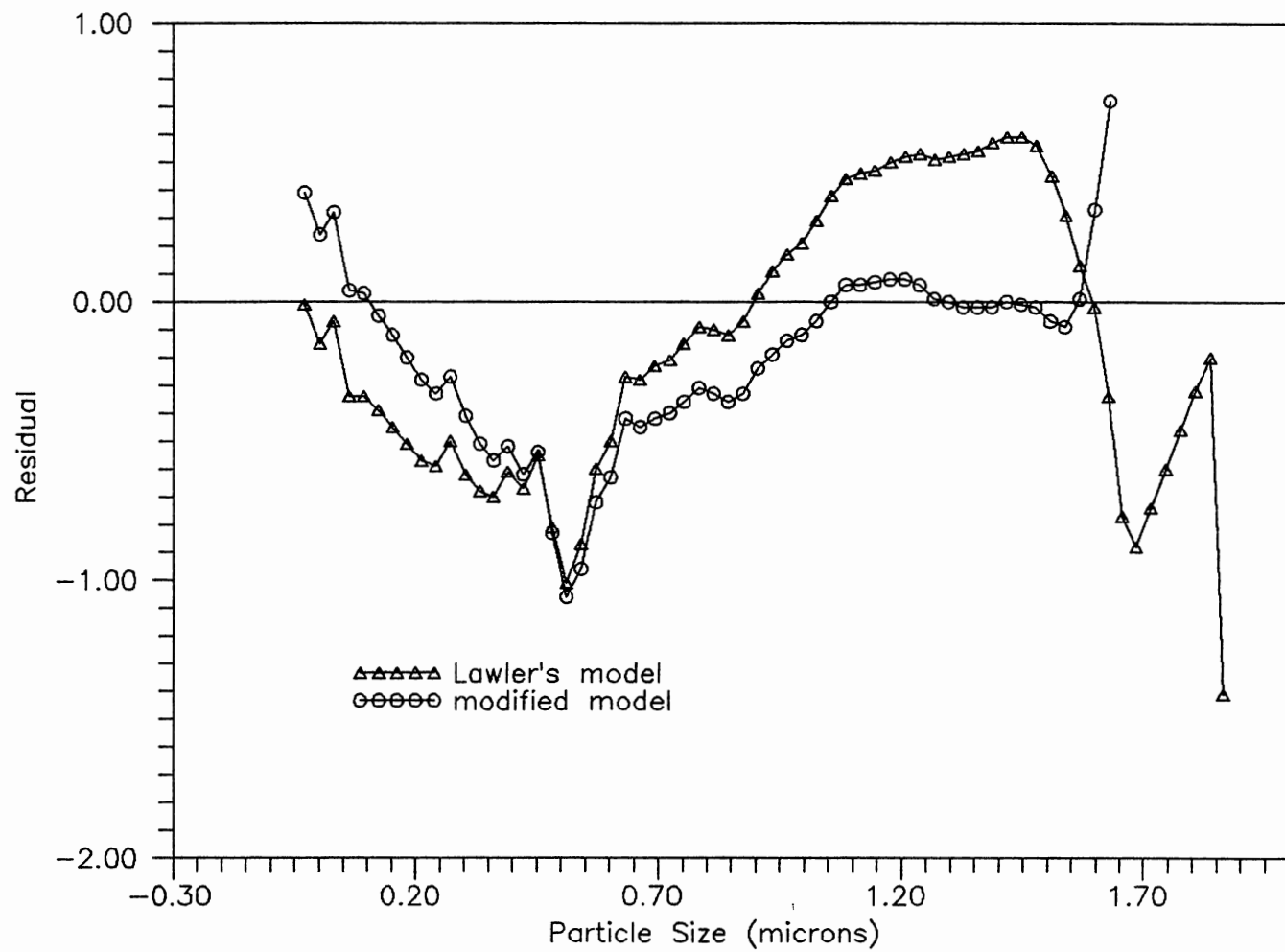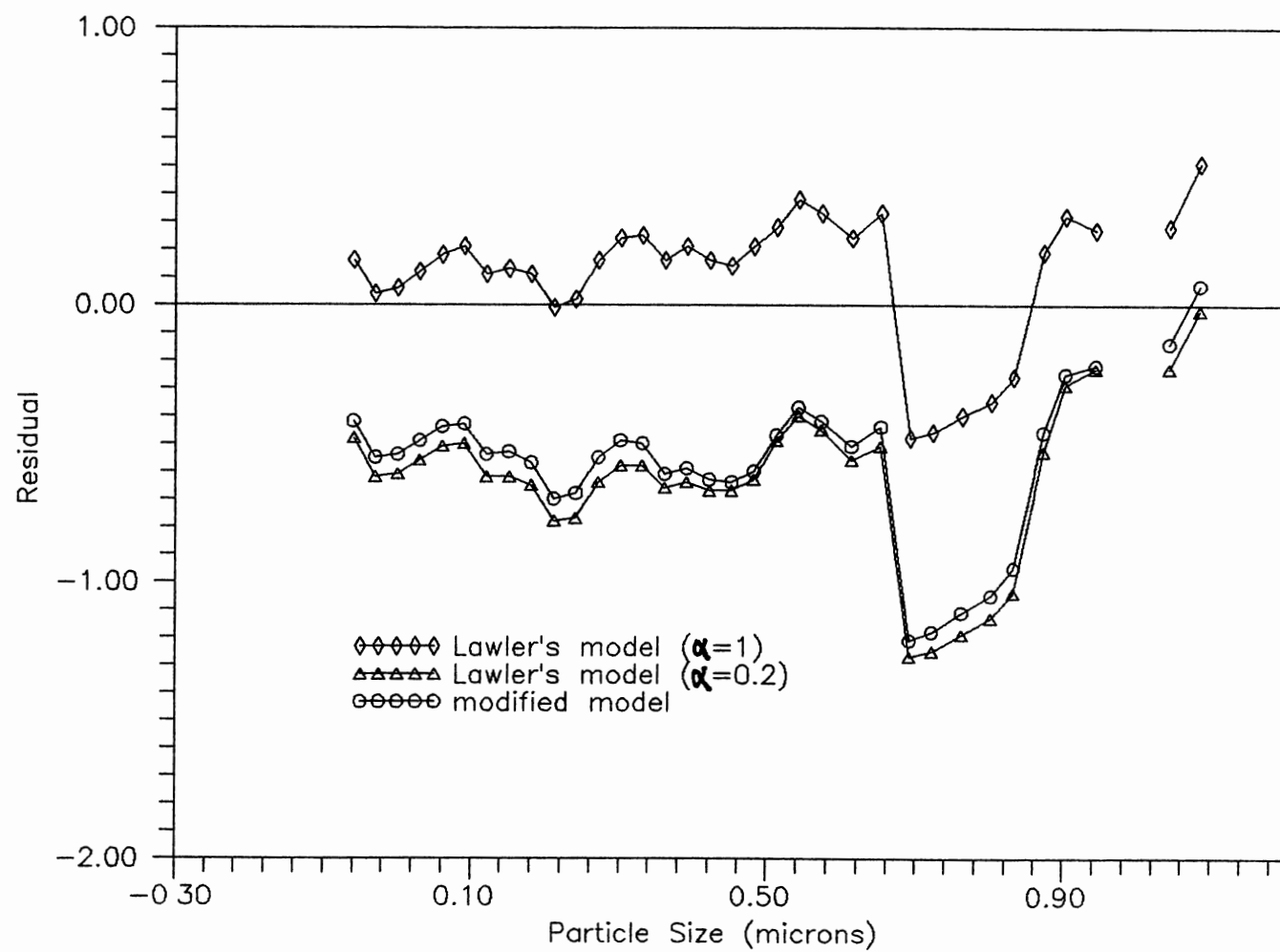Figure 27. Residual (difference between the measured and predicted) plot (60 sec^{-1})

Lawler's model using $\alpha = 1$ are better fit. But the predictions of Lawler's model using $\alpha = 0.2$ more underestimates to a greater extent the flocculation process in this case than the predictions of the modified model.

Uncertainty Analysis

The uncertainties associated with the model input parameters are not quantifiable since every aspect of particle growth and breakup are not understood. Sensitivity analysis can be used to determine the magnitude of the change in the value of model output (prediction) resulting from a change in the value of model input parameters. The sensitivity to an input parameter, p_k, is examined by perturbing one input at a time. The sensitivity of model prediction to a input parameter is called the sensitivity coefficient, S_i, and is defined as the ratio of the observed change in the predicted number of particles of size i (Δn_i) to Δp_k (Wolff, 1990):

$$S_i = (\Delta n_i / \Delta p_k) \tag{38}$$

S_i is a partial derivative of the i size particle number (ith dependent variable) with respect to the p_k. Normalized sensitivity coefficients can have the following form:

$$SN_i = (p_k / n_i)(\Delta n_i / \Delta p_k) \tag{39}$$

The components of variance for each output variable n are the percentage of output variance attributable to input p_k, computed in the following manner (Brown and Barnwell, 1987):

$$Var(n_i) = Var(p_k)(\Delta n_i / \Delta p_k)^2 \tag{40}$$

Where:

$Var(n_i)$ = variance of output variable n_i,

$Var(p_k)$ = variance of a input variable p_k,

The term $Var(p_k)$ can be transformed as follows:

$$Var(p_k) = (CV \times p_k)^2 \tag{41}$$

Where CV is the coefficient of variation for the input
parameter. Total number uncertainty associated with input
parameters can be expressed as follows:

$$Var_{tot}(n_{tot}) = \sum_{k=1}^{k} \sum_{i=1}^{N} Var(n_i) \tag{42}$$

Table I lists model parameters selected to illustrate
the sensitivity analysis. The coefficients of variation of
varied parameters were determined based on the information
reported by Cockerham and Himmelblau (1974). Obtaining the
information on the characteristics of input parameters
without effort is difficult, if not impossible. For this
study, the same value of the coefficients of variation used
by Cockerham and Himmelblau (1974), 0.0333, was applied to
the parameters of concern in the model. Values in Table V
are mean values of parameters used in this study. In this
study, the mean values of parameters were selected to
represent a typical case in the flocculation process and
assumed that all parameters were mutually independent.
Constants a and k in the equation of the effective particle
density (equation 12) are 0.0013 and 0.9, respectively.

TABLE V

MEAN VALUES OF VARIED PARAMETERS

Varied parameters

velocity gradient : $G = 25 \text{ sec}^{-1}$

effective shear rate constant : $s = 0.39$

Hamaker constant : $H = 2 \times 10^{-19}$ J

maximum particle size : $D_{max} = 200 \ \mu m$

effective particle density : $\rho_f = a/d^k$

particle size distribution : $n(d) = A \ d^{-B}$

detention time of each flocculator: $Dt = 15$ minute

Constant A from particle size distribution equation (power law) is found using the assumption of a total solid concentration of 100 mg/L. The constant A was calculated to be 2.0E+7. The power law coefficient B was set to 4 (Lawler et al. 1980). The influent particle size distribution in the size from 0.89 to 30 μm was prepared by the power law. For d < 3.5 μm, the particle density was fixed at 2.65 g/cm^3, otherwise the particle density relationship (effective particle density) was used. Seven varied parameters were selected, but the sensitivity study was conducted on nine input parameters, because two of the parameters have two characteristic constants. Three equal sized flocculation basins (15 minute detention time each) in series were assumed. The magnitude of the input perturbation, $\Delta p_k/p_k$ is specified to be 0.0333.

The values of variance for each varied input parameter were computed at the third flocculator. Table VI shows variances and percentage contributions to the total variance by the nine parameters. The percentage contribution to uncertainty can be expressed by the percentage contributions to total variance. The parameters of power law coefficient, B, and effective density constant, k, are shown to contribute most to uncertainty in the total particle number remaining in the flocculation model.

In another approach, a Monte Carlo simulation led to more precise statements about the effect of uncertainty.

TABLE VI

TOTAL VARIANCE AND PERCENTAGE
OF TOTAL VARIANCE

parameter	total variance	% of total variance
G	7.9E+8	0.52
s	7.9E+8	0.52
H	1.8E+6	0.00
D_{max}	1.1E+9	0.75
a	3.5E+9	2.33
k	4.9E+10	32.55
Dt	1.5E+9	0.98
A	9.6E+7	0.06
B	9.4E+10	62.28
Total	1.5E+11	100.00

The Monte Carlo simulation can be used to estimate various statistics of the model output, although the Monte Carlo simulation does not reduce the existing uncertainty. The general procedure for the Monte Carlo simulation is set out as follows:

1. Determine random parameters and the characteristics of these parameters for the input data. In this study, nine parameters were chosen as the random parameters because they were expected to have the most uncertainty in the model.

2. Determine a number of simulations to assure that enough events were simulated to determine representative outputs of the model.

3. Repeat the determined number of the model simulations using the random parameters in order to obtain a set of the model output. The set of the model output is used to estimate the response statistics.

The varied parameters in Table I were used as the random parameters. The same value of the coefficients of variation, 0.0333, and mean values in Table I were used in this study of the Monte Carlo simulation. The normal random numbers with the above properties were generated using available programs developed by Press et al. (1986). The uniform random number generator, FUNCTION RAN2(IDUM) installed in SUBROUTINE INITIVA, generates a uniform random value between 0.0 and 1.0. The normal random number generator, FUNCTION GASDEV(IDUM) using RAN2(IDUM) was also

installed in SUBROUTINE INITIVA, and produces a normally distributed value with an ensemble mean of 0.0 and an ensemble standard deviation of 1.0. Then, normal random numbers are obtained as follows:

$$X(i) = X + sZ(i) \tag{43}$$

Where:

$X(i)$ = value of a normal random variable at some
point in the sequence of random number

X = deterministic variable

s = the desired standard deviation of $X(i)$

$Z(i)$ = normal random number generated by the random
number generator

Using the needed random values generated for the model inputs, the program performs repetitive execution until a desired number of results are obtained.

The fraction of the number of particles remaining, (N/No), was selected to observe the model responses. The number of particles remaining allows for prediction of the flocculation performance. Model outputs were prepared at compartments 1, 2,and 3 and shown in Figure 28. A determination of the number of simulations that can assure representative output and avoid numerous unwarranted simulations was conducted by running simulations 20, 40, 60, 80, 100, 120, 140, 160, 180, and 200 times. The number of simulations was increased until the average, upper and lower 95% confidence intervals reached a constant value. Results of this procedure are presented in Figure 29. The
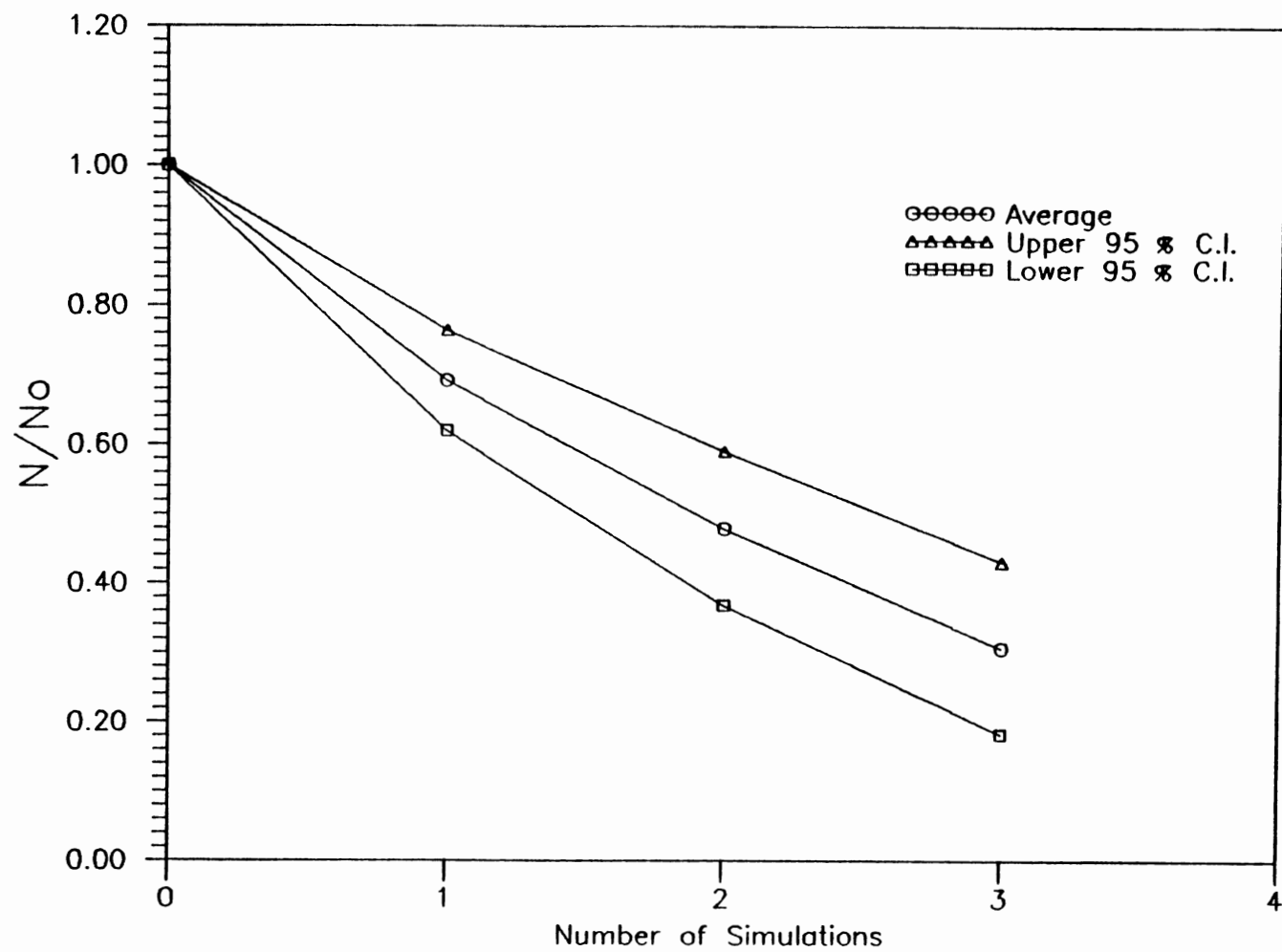
Figure 28 Frequency distribution of modified model predictions
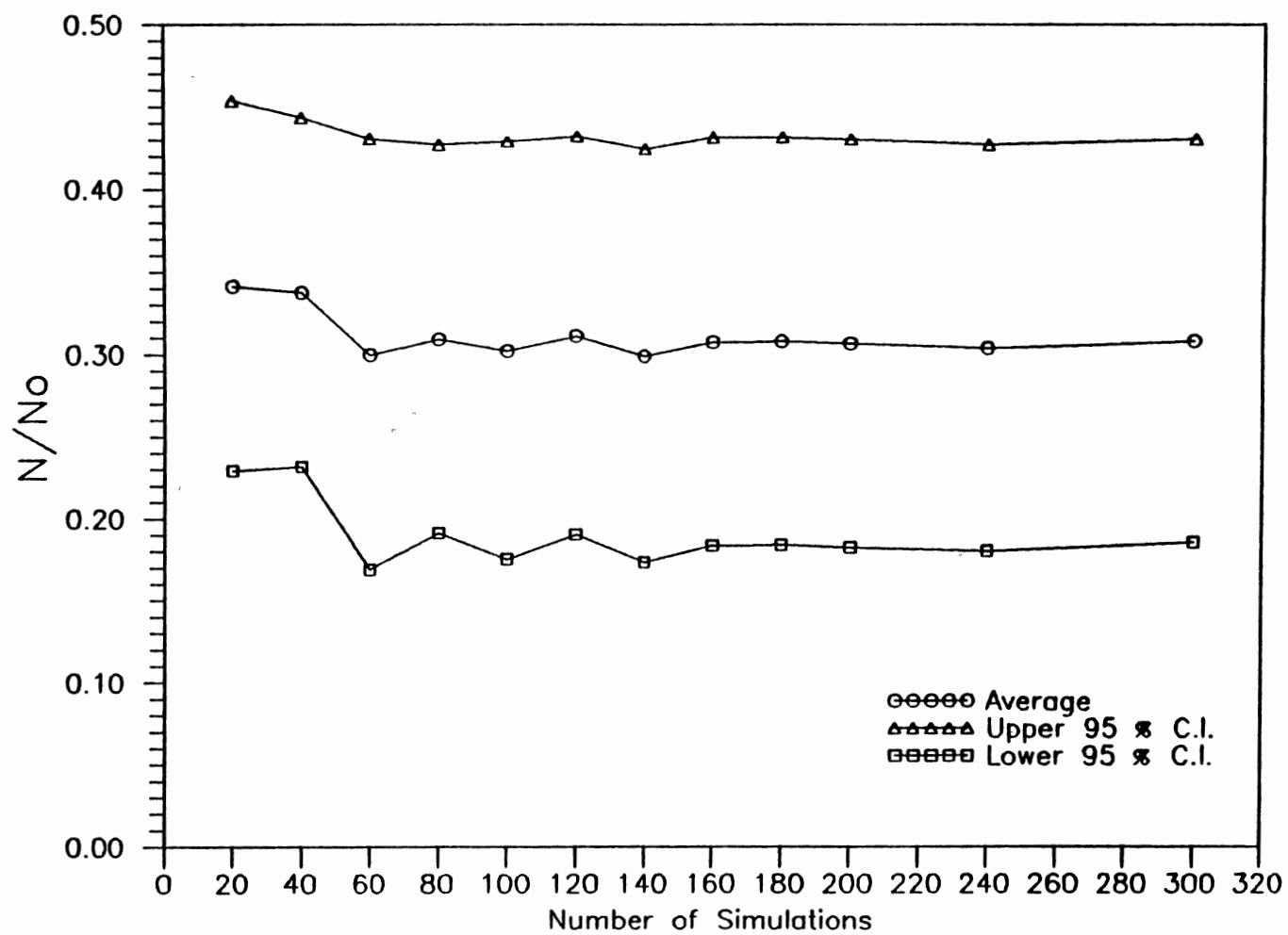
Figure 29. Covergence characteristics of Monte Carlo Simulation with modified model (third compartment)

95% confidence interval was computed with an assumption of normal distribution for each set and then plotted as (N/No) versus the number of simulations performed. The results show that about 200 simulations are enough to obtain sufficient precision in the model output. Simulations were conducted 240 and 300 times to ensure that the choice of 200 simulations was enough.

The probability distribution of the third compartment was determined by plotting of the 200 run simulation results and is shown in Figure 30. As seen in Figure 30, the simulation results (particle number remaining) are distributed linearly so that the results could be expressed as a normal distribution. This figure indicates the previous assumption of normal distribution is valid. The probability figure can be used in the explanation of how safety factors for the flocculation process might be calculated (Berryman and Himmelblau, 1971; Cockerham and Himmelblau, 1974). When a design is conducted, a safety factor should be added to or multiplied into a design which is based on the model prediction in order to allow for uncertainty in the model and the operating process. The mean value of N/No at a third compartment is 0.31. The upper confidence interval for the model response is 0.43. The safety factor, f, in this case could be the ratio of the upper 95 % confidence value to the mean value i.e., f = 0.43/0.31 = 1.39. Cockerham and Himmelblau (1974) used Argaman and Kaufman's flocculation model and performed a
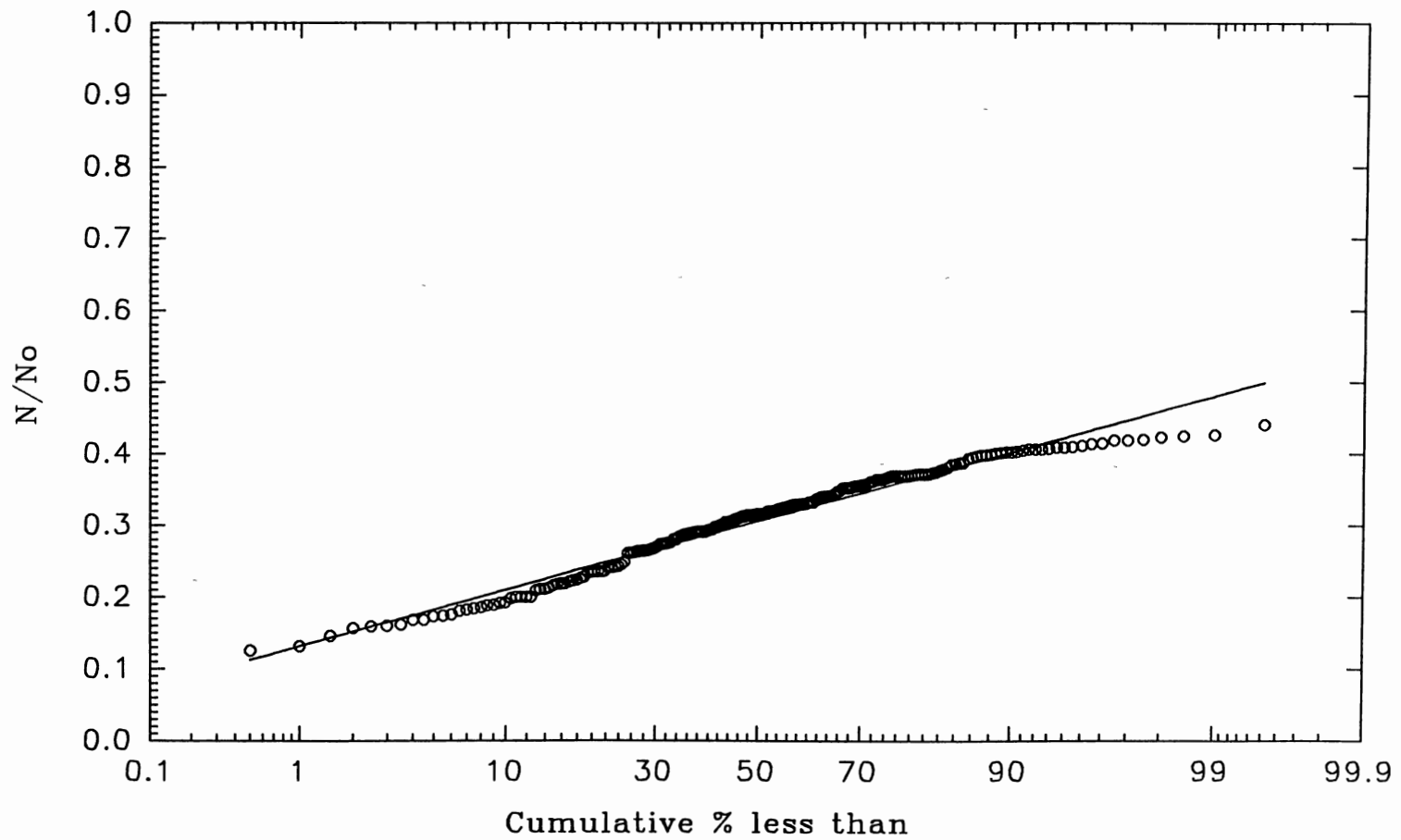
Figure 30. Probability distribution of N/No at third compartment

Monte Carlo simulation. They found that the safety factor was approximately 1.4 for variations of the flow rates. If they considered all the input parameters as random, the value of the safety factor was higher than for variations of flow rates.

CHAPTER V

DISCUSSION

A Coulter counter was used at the Davis Water
Treatment Plant, Austin, Texas, to measure the particle
size distribution. Lawler's model prediction more closely
fit the measured results for the intermediate concentration
(820 mg/L). The predictions of the modified model and
Lawler's model overestimate the measured results for the
small particle concentration (417 mg/L). But better
agreement between the modified model predictions and the
measured results occurred at the larger concentration (912
mg/L). However, Lawler's model (1984) required a value for
the collision efficiency factor (α = 0.1 or 0.2) in order
to fit the model prediction to the experimental results.
The value of α, which is less than 1, is required to
compensate for an overprediction of the frequency of
particle collisions by the model. The modified model sets
the value of α to 1.0. Setting α equal to 1 removed the
need to use a correction factor for overprediction by the
model. The removing of α, which was used for calibrating,
would be an indication of model improvement. This value has
to be determined by calibrating the model to a set of
experimental results. It is very likely that the value
varies with the nature of the model used and the nature of

the coagulant types. Because α, the collision efficiency factor, could not be measurable independently, its value had to be found via application of the old model. The approach was to take α as a correction factor to fit the model predicted PSD and the experimental PSD. In order to obtain knowledge about the range of α, the literature was reviewed. According to Gregory's literature review (1989), α is typically in the range 0.1 to 0.5. Lawler et al. (1983) reported values between 0.16 and 0.20 for α in batch flocculation; their model was formulated with equations 1, 2 and 3. Their model considered the particle removal from the suspension by sedimentation. Lawler and Wilkes (1984) used values of 0.1 and 0.2 for α in a full scale operating flocculation basin. The later model did not consider particle removal by sedimentation. Tambo and Watanabe (1979) reported the value of 0.33 for the optimum coagulation condition of clay-aluminum flocs. Lu and Spielman (1984) also reported a similar range from 0.32 to 0.35 at optimum dosage of clay-polymer flocs. Under different conditions and in different models, different values of α have to be used to fit the measured results.

The 280 μm aperture was the largest diameter used to measured the particle size distribution of the Davis Water Treatment Plant by Lawler and Wilkes (1984). According to Treweek and Morgan (1977), a Coulter counter measured particle size was reliable from 10 to 40 percent of the aperture diameter. Thus a 280 μm aperture can reliably

measure a particle size from 28 to 112 μm. The modified
model selected 100 μm as the maximum particle diameter and
compared the predicted particle size distribution to the
particle size distribution data measured by the Coulter
counter. The 100 μm maximum particle diameter (close to 112
μm) is fairly small compared to the reported experimental
maximum particle size at G = 22 sec^{-1}. According to the data
collected by Glasgow and Kim (1989), approximately 200 μm
maximum particles were found at the operating velocity
gradient (22 sec^{-1}). The relatively small size of the
maximum particle measured by the Coulter counter implies
that the Coulter counter causes particle breakup.

The Southern Nevada Water System uses a HIAC to
measure the particle size distribution. The reported
particle numbers were in five discrete particle size
ranges. The discrete particle size ranges were larger than
the preset particle size ranges in the model, therefore
data manipulation was required. A power law relationship
found by linear regression was used to obtain the number of
particles less than 5 μm in size. For more accurate
comparison, a more detailed particle size distribution in
the range of the predetermined particle size ranges is
required. The model prediction with the particle size
distribution based on the power law relationship was
compared to the measured results. Even if there was the
possibility of the loss of particle number caused by
sedimentation, the model prediction seemed to underestimate

the flocculation performance of the small number concentration seen in this case as well as the second data set from the Davis Water Treatment Plant.

The modified model predictions fit well the measured results from the AIA used at ISU (Hanson, 1989). However, the volume distribution plots demonstrated that the model predictions deviated in the region of the large particle size. This was due to limits in the accuracy of the particle size measuring capability of the AIA. According to Hanson (1989), the AIA was not able to provide a crisp image if the floc was in excess of 50 μm. The out of focus image was possibly measured as a larger particle size than the actual particle size. Hanson mentioned that the unfocused image was due to the microscope's limited depth of focus, called the focal depth. This limitation occurs when performing quantitative measurements on irregular objects whose vertical dimension is larger than the depth of focus. A 20x objective (system magnification of 474.6x) installed in the AIA is not appropriate to measured the particle sizes larger than 50 μm.

The comparison between the model prediction and the measured results in the three cases showed that the model underestimated the flocculation rates mostly in the intermediate size region (3 to 15 μm). The modified collision frequency function, $\beta'(i,j)$, employed in the modified model is a function of particle size and density. As mentioned earlier, floc size increases as the density

decreases so that the collision frequency increases. However, the experimental data (Tambo and Watanabe, 1979) used in this study were obtained from the density of large particles because the experimental data for the density of small particles were scarce. The values of 0.0013 and 0.9 for a and k were used to describe the relationship between floc density and size. These values gave 3.5 μm as transition floc diameter (floc density = 2.65 g/cm^3) so that the density of particles below 3.5 μm was set to 2.65 g/cm^3. The selected values of 0.0013 and 0.9 for a and k can be obtained from equations 13 and 14 when the ALT ratio approaches zero. The 3.5 μm particle size was the primary particle used in the experiment conducted by Tambo and Watanabe (1979). When the ALT ratio is zero, the transition floc diameter is equal to the primary particle. In this research the primary particle size is 0.89 μm so that other values of a and k need to be used in the model. The effects of the ALT ratio on the model predictions were not determined because equations 13 and 14 did not represent the floc density decreasing as the ALT ratio increases. Figure 31 shows the floc density and size relationships. As the ALT ratio increases, the transition floc diameter increase. To incorporate the ALT ratio into the model, the relationship between the floc size and density especially in the small range is required. Assuming constant density below the transition diameter causes an underestimating of the collision frequency. But the small
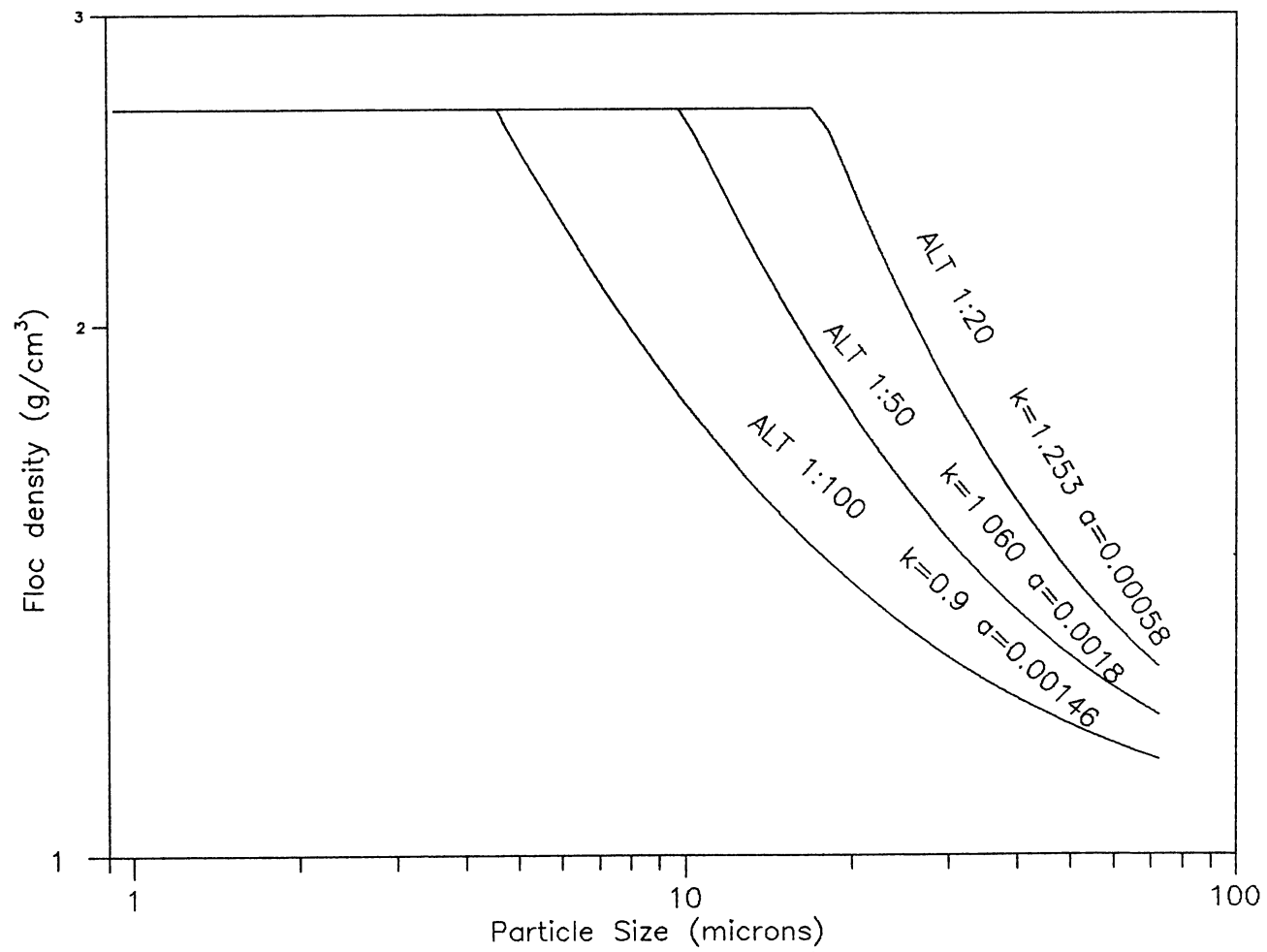
Figure 31. Relationship between floc density and size

value of 0.9 reduces the collision frequency in the large floc size range. As the value of k increases, more collision frequency will be predicted. When setting the fractal dimension D = 3-k, the collision frequency increases as the fractal dimension, D, decreases (k increases). Selecting the appropriate values of k and a are very important factors for model prediction. Recently, several researchers (Jiang and Logan, 1991; Wiesner 1992) derived the floc diameter expressions containing the fractal dimension assuming a primary particle size. This was used in the collision frequency function to calculate collision frequency. Both expressions fix a transition floc diameter as the primary particle size so the transition floc diameter size is not changed. Both results showed more collision frequency than the original collision frequency. But none of these results was verified with experimental data.

The uncertainties of the nine input parameters were handled by completing a sensitivity analysis and a Monte Carlo Simulation. Sensitivity analysis indicated that the power law constant, B, and the effective density constant, k, had the greatest effects on flocculation. This implies that particle size distribution is the most important information to describe the flocculation process. A reliable particle counter has to be employed to get good prediction. In the previous paragraph, the requirement for more work on the effective density constant was discussed.

Interestingly, the effect shear rate constant, s, and velocity gradient, G, had a small effect on flocculation. The model response due to changes in maximum particle size is closely related the parameters G and s. The sensitivity of s, G, and D_{max} on model response should be considered together. However, the comparison between the model predictions and the ISU experimental data showed that the modified model response was little affected by velocity gradient. The comparison also illustrated that G had more effect on flocculation performance than the model prediction. Potentially, a more appropriate parameter for G in the model may be required. The significance of correlation among the input parameters on errors in the model response has to examined also. Song and Brown (1990) reported that correlation among the input parameters was important in output uncertainty from the Streeter-Phelps water-quality model. However, we do not know how the input parameters are correlated so we were unable to develop meaningful bounds for the random input parameters. Reliable quantitative information on the variances and correlation coefficients among the input parameters have to be used. The safety factor for the modified model obtained by Monte Carlo simulation was smaller than the safety factor estimated by Cockerham and Himmelblau (1974). The smaller safety factor to accommodate the reality of uncertainty is a recognition of the advancement of the flocculation model. Approximately 2 minutes, including compile time, was needed

for one model simulation using a 486 IBM compatible microcomputer with 4 Mb RAM.

The predictions of the flocculation model using particle size distribution proposed herein indicate what happens during the flocculation process and point out possibilities that warrant further development. The present water industry concern over two protozoal organisms, cysts of <u>Giardia lamblia</u> in the 8-12 μm size range and <u>Cryptosporidium</u> in the 3-5 μm size range, impacts on finished water quality (Amirtharajah, 1988). The existence of these organisms can be quantified in particle size distribution. These size could be controlled in the flocculation process in order to optimize water treatment process and improve water quality. However, the model applications for operation of an existing flocculation plant and design of new or modified flocculation plant is limited. A better understanding and improved expressions for some physical and chemical phenomena which occur during the flocculation process are necessary.

CHAPTER VI

SUMMARY AND CONCLUSIONS

In this research, the flocculation model was modified and its predictions tested using data from two operating water treatment plants and a lab scale data set. Each data set was measured using different measuring equipment. In order to assess the contribution of various input parameters to uncertainty in the model prediction and obtain a safety factor, sensitivity analysis and a Monte Carlo simulation were conducted. The following conclusions are drawn from the research. With a realization of the problems encountered, a number of recommendations are also made.

Conclusions

1. Improvements in a flocculation model were made by incorporating terms for interparticle forces, floc break-up phenomena, floc density, shape effects, and effective velocity gradient.

2. The modified model prediction without the collision efficiency factor (α) matched the measured results at the high concentration but underestimated the flocculation rate at low concentration. The modified

model predictions do not show the sudden peak point at the largest particle size which was noticed in Lawler's model prediction.

3. In SNWS, the modified model underestimated flocculation rate for low particle concentration and the loss of particle number in measured results was observed.

4. The modified model predicted well the ISU particle size distribution, measured by an automatic image analyzer, results obtained while operating at $G = 22 \text{ sec}^{-1}$. However, the modified model prediction overestimated the particle size distribution conducted at $G = 60 \text{ sec}^{-1}$.

5. The sensitivity analysis indicated that the power law constant, B, which describes the particle size distribution, and the effective density constant, k, which relates the particle density and size, were the major contributors to uncertainty in the flocculation model.

6. The Monte Carlo simulation was applied to the modified model. The model output could be represented by a normal distribution. A safety factor was calculated from the model output mean and confidence interval.

Recommendations

1. More work on the relationship between the floc density and size is needed especially in small particle

size range.

2. Sensitivity analysis and Monte Carlo simulation have been shown to be useful tools in assessing the uncertainty in the model prediction. Reliable information on the variances and correlation coefficients among model parameters is important for these techniques to be used with confidence. Methods for determining input parameter correlation coefficients require further study.

3. With more sensitive and reliable particle counters, the improvement of flocculation model could be made.

4. Individual processes of water treatment, rapid mixing, flocculation, sedimentation and filtration, are combined in series to perform solid-liquid separation. More study to improve the present sedimentation and filtration model and linkage of each model is required to determine and predict the effect of one treatment process on those that follow.

REFERENCES

Adler, P. M. (1981). Streamlines in and around porous particles. Journal of Colloid and Interface Science, 81(2), 531-535.

Adler, P. M. (1981). Heterocoagulation in shear flow. Journal of Colloid and Interface Science, 83(1), 106-115.

Akers, R. J., Rushton, A. G., and Stenhouse, J. I. T. (1987). Floc breakage : the dynamic respond of the particle size distribution in a flocculated suspension to a step change in turbulent energy dissipation. Chemical Engineering Science, 42(4), 787-798.

Amirtharajah, A (1988). Some theoretical and conceptual views of filtration. Journal AWWA, December, 36-46.

APHA (1985). Standard method for the examination of water and wastewater. American Public Health Association, Washington, DC..

Baba, K., Yoda, M., Ichika, H. and Osumi, A. (1988). A floc monitoring system with image processing for water purification plants. Water Supply, 6, 323-327.

Berryman, J. E. and Himmelblau, D. M. (1971). Effect of stochastic inputs and parameters on process analysis and design. Ind. Eng. Chem. Process Des. Develop., 10(4), 441-449.

Brown, L. C. and Barnwell, T. O. (1987). The enhanced stream water quality model QUAL2E and QUAL2E-UNCAS: Documentation and user model. EPA/600/3-87/007, U.S. Envir. Protection Agency, Envir. Res. Lab., Athens, Ga., May.

Brown, D. L. and Glatz, C. E. (1987). Aggregate breakage in protein precipitation. Chemical Engineering Science, 42(7), 1831-1839.

Cockerham, P. W. and Himmelblau, D. M. (1974). Stochastic analysis of orthokinetic flocculation. Journal of Environmental Engineering, 100, 279-293.

Dentel, S. K., Boder, T. A. and Ivans, P. D. (1985). A physical - chemical model of coagulation. American Water Works Association. Conference., 659-680.

François, R. J. (1987). Strength of aluminum hydroxide flocs. Water Research, 21(9), 1023-1030.

Gibbs, R. J. (1982). Floc breakage during HIAC light-blocking analysis. Enviro. Sci. Technol., 16(5), 298-299.

Glasgow, L. A. and Kim, Y. H. (1989). A review of the role of the physicochemical environment in the production of certain floc properties. Water, Air, and Soil Pollution, 47, 153-174.

Gregory, J. (1989). Fundamentals of flocculation. CRC Critical Reviews in Environ. Control, 19(3), 185-230.

Hanson, A. T. (1989). The effects of temperature and reactor geometry on turbulent flocculation. Unpublished Ph.D Dissertation, Iowa State University.

Hanson, A. T. and Cleasby, J. L. (1990). The effects of temperature on Turbulent flocculation: Fluid dynamics and chemistry. Journal AWWA, November, 56-73.

Higashitani, K. and Mastsuno, Y. (1982). Kinetic theory of shear coagulation for particles in a viscous fluid. Journal of chemical Engineering of Japan, 15(4), 299-304.

Hudson, H. E. Jr.(1981). Water clarification processes: Practical design and evaluation. Van Nostrand Reinhold Co., New York.

Hutchinson, C. W. (1985). On-Line particle counting for filtration control. ISA Transaction, 24(3), 75-82.

Jiang, Q. and Logan, B. E. (1991). Fractal dimensions of aggregates determined from steady-state size distributions. Environ. Sci. Technol., 25(12), 2031-2038.

Koh, P. T. L., Abdrews, J. R. G. and Uhlherr, P. H. T. (1984). Flocculation in stirred tanks. Chemical Engineering Science, 39(6), 975-985.

Koh, P. T. L. (1984). Compartmental modeling of stirred tank for flocculation requiring a minimum critical shear rate. Chemical Engineering Science, 39(12), 1759-1764.

Koh, P. T. L., Andrews, J. R. G. and Uhlherr, P. H. T. (1987). Modeling shear-flocculation by population balances. Chemical Engineering Science, 42(2), 353-362

Koglin, B. (1977). Assessment to the degree of agglomeration in suspensions. Powder Technology, 17, 219-227.

Kuo, C., Amy, G. L. and Bryant, C. W. (1988). Factors affecting coagulation with aluminum sulfate - I. Particle formation and growth. Water Research, 22(7), 853-862.

Lawler, D. F., O'Melia, C. R and Tobiason, J. E. (1980). Integral water treatment plant design from particle size to plant performance. Adv. Chem. Ser., 189, 353-388.

Lawler, D. F. and Wilkes, D. R. (1984). Flocculation model testing:Particle sizes in a softening plant. Journal AWWA, 76, 90-97.

Lawler, D. F. (1987). Particle size distributions: Measurements in flocculation. pp. 19-30. In AWWA Seminar Proceedings: Influence of Coagulation on the Selection, Operation, and Performance of Water treatment Facilities. AWWA, Denver, June.

Letterman, R. D. and Iyer, D. R. (1985). Modeling the effects of hydrolyzed aluminum and solution chemistry on flocculation kinetics. Environ. Sci. Technol., 19(8), 673-681.

Li, D. and Ganczarczyk, J. J. (1986). Physical characteristics of activated sludge flocs. CRC Critical Reviews in Environ. Control, 17(1), 53-87.

Li, D. and Ganczarczyk, J. J. (1987). Stroboscopic determination of settling velocity, size and porosity of activated sludge flocs. Water Research, 21(3), 257-262.

Li, D. and Ganczarczyk, J. J. (1989). Fractal geometry of particle aggregates generated in water and wastewater treatment processes. Environ. Sci. Technol., 23(11), 1385-1389.

Logsdon, G. S. (1987). Evaluating treatment plants for particulate contaminant removal. Journal AWWA, September, 82-92.

Lu, C. F. and Spielman, L. A. (1985). Kinetics of floc breakage and aggregation in agitated liquid suspensions. <u>Journal of Colloid and Interface Science</u>, 103(1), 95-105.

Melik, D. H. and Fogler, H. S. (1984). Gravity induced flocculation. <u>Journal of Colloid & Interface Sci.</u>, 101(1), 72-83.

Metcalf and Eddy, Inc. (1979). <u>Wastewater engineering</u>. McGraw-Hill, Inc..

Monscvitz, J. T. and Rexing, D. J. (1983). Direct filtration control by particle counting. <u>Proceedings AWWA 1983 Annual Conference</u>, Las Vegas, Nevada, June, 1983.

Montgomery, J. M. (1985). <u>Water Treatment Principles and Design</u>, John Wiley & Sons, Inc.

O'Melia, C. R. (1978). Coagulation in wastewater treatment, in <u>The Scientific Basis of Flocculation</u>, Ives, K. J., Ed., Sijthoff and Noordhoff Int., Alphen aan den Rijn, The Netherlands.

Peavy, H. S., Rowe, D. R. and Tchobanoglous, G. (1985). <u>Environmental Engineering</u>, McGraw-Hill, Inc..

Press, W. H., Flannery, B. P., Teukolsky, S. A., and Vetterling, W. T. (1986). <u>Numerical Recipes: The Art of Scientific Computing</u>, Cambridge University Press.

Pandya, J. D. and Spielman, L. A. (1982). Floc breakage in agitated suspensions: theory and data processing strategy. <u>Journal of Colloid and Interface Science</u>, 90(2), 517-531.

Reed, G. D. and Mery, P. C. (1986). Influence of floc size distribution on clarification. <u>Journal AWWA</u>, August, 75-80

Rexing, D. J. (1991). Personal Communication. Unpublished flocculation performance data from Southern Nevada Water System, Boulder City, Nevada. These data were provide by Rexing, D. J..

Reynolds, T. D. (1982). <u>Unit operations and processes in environmental engineering</u>, Monterey, Ca.: Brooks/Cole Engineering Division.

Sawyer, C. N. and McCarty, P. L. (1978). <u>Chemistry for environmental engineering</u>, McGraw-Hill.

Smoluchowski, M. (1917). Versuch einer mathematischen theorie der koagulations kinetik kolloider losungen. <u>Zeitschrift fur PhysikalischeChemie</u>, 92(2).

Song, Q. and Brown, L. C. (1990). DO model uncertainty with correlated inputs. <u>Journal of Environmental Engineering</u>, 116(6), 1164-1180.

Srivastave, R. M. (1988). Impact of rapid mixing and temperature on flocculation of clay suspensions in water. unpublished M. S. thesis, Iowa State University.

Stumm, W. and Morgan, J. J. (1981). <u>Aquatic Chemistry</u>. John Wiley & Sons. Inc.

Tambo, N. and Hozumi, H. (1979). Physical characteristics of flocs-II.Strength of floc. <u>Water Research</u>, 13, 421-423.

Tambo, N. and Watanabe, Y. (1979). Physical characteristics of flocs-I.The floc density function and aluminum floc. <u>Water Research</u>, 13, 409-419.

Tate, C. H. and Trussell, R. R. (1978). The use of particle counting in developing plant design criteria. <u>Journal AWWA</u>, December. 691-698.

Treweek, G. P. and Morgan J. J. (1977). Size distribution of flocculated particles: Application of electronic particle counters. <u>Environ. Sci. Technol.</u>, 11(7), 707-714

Valioulis, I. A. and List, E. J. (1984). Numerical simulation of a sedimentation basin. 1. Model development. 2. Design application. <u>Environ. Sci. Technol.</u>, 18(4), 242-253.

van de Ven, T. G. M. and Mason, S. G. (1976). The microrheology of colloid dispersions. IV. pairs of interacting spheres in shear flow. <u>Journal of Colloid and Interface Science</u>, 57(3),505-516.

Visser, J. (1972). On Hamaker constants: a comparison between Hamaker constants and Lifshitz - van der Waals constants. <u>Advan. Colloid Interface Sci.</u>, 3, 331-363.

Water Engineering and Management (1990). Low health risk in use of water tracing agent. <u>Water Engineering and Management</u>, October, 18.

Wiesner, M. R. and Mazounie, P. (1989). Raw water
    characteristics and the selection of treatment
    configurations for particle removal. <u>Journal AWWA</u>,
    May, 80-89.

Wiesner, M. R. (1992). Kinetics of aggregate formation in
    rapid mix. <u>Water Research</u>, 26(3), 379-387.

Wolff, A. (1990). Sensitivity analysis of catalytic
    conversion of n-C . <u>Chem. Eng. Technol.</u>, 13, 277-288.

APPENDIXES

COMPUTER PROGRAM FOR FLOCCULATION MODEL

```
C       IMPLICIT REAL*8(A-H, O-Z)
C  ALPHA : STICKIMESS FACTOR, FRACTION OF SUCCESSFUL COLL.
C  AVNUDI :  NUMBER AVERAGE DIAMETER
C  AVSUDI : SURFACE AREA AVERAGE DIAMETER
C  AVVODI : VOLUME AVERAGE DIAMETER
C  BETA : SUM OF COLLISION EFFICIENCY, CM**3/SEC
C  BETABR : BROWNIAN COLLISION EFFICIENCY
C  BETASE : SEDIMENTATION COLLISION EFFICIENCY
C  BETASH : SHEAR COLLISION EFFICIENCY
C  BOLTZ : BOLTZMANS CONSTANT, GM-CM**2/(SEC**2*DEG.KELVIN)
C  CALCTI : THE CALCULATED TIME FROM FLOW EFFECT IN EACH COMPARTMENT
C  CONBET :  CALCULATED CONSTANT FOR BETASE
C  CON3 : CALCULATED CONSTANT, (6/PI)**(1/3)
C  CON4 : CALCULATED CONSTANT, 2.3*PI/6
C  DCON : CONSTANT(A) IN PARTICEL SIZE-DENSITY RELATIONSHIP
C  DELTAD : PARTICLE DIAMETER INTERVAL
C  DKP : CONSTANT(K) IN PARTICLE SIZE-DENSITY RELATIONSHIP
C  DT : DETENTION TIME OF FLOCCULATION BASIN, MINUTES
C  DY : NUMERICAL VALUE OF DIFFERENTIAL EQUATION
C  EDEN : EFFECTIVE DENSITY
C  ERROR : ALLOWABLE % DIFFERENCE IN SETTLING VEL. TEST
C  FASTL : THE VALUE OF THE FASTEST CHANGING DERIVATIVE
C  FDEN : FLOC DENSITY
C  FRAC : FRACTION OF NEW PARTICLE ASSIGNED TO V(RESULT)
C  FRAREN : NUMBER FRACTION REMAINING, N/NO
C  GRAVCO : GRAVITATIONAL CONSTANT, 980 CM/SEC**2
C  H : STEP SIZE (TIME) WHEN INTEGRATING
C  HMIN : MINIMUM STEP SIZE
C  HMAX : MAXIMUM STEP SIZE
C  HMKCON : HAMAKER CONSTANT, JOULES
C  NJ : NUMBER OF PARTICLE SIZE IN EXPERIMENTAL DATA
C  NPEAK : PARTICLE SIZE OF PEAK IN THE NUMBER DISTRIBUTION
C  NTI : NUMBER OF OUTPUT CALL
C  OUTTIM : TIMES THAT OUTPUTS ARE DESIRED, MINUTES
C  PEAKND : THE PEAK IN NUMBER DISTRIBUTION
C  PEAKVD : THE PEAK IN VOLUME DISTRIBUTION
C  PI : 3.1415926535
C  PLAW1 : POWER LAW CONSTANT
C  PLAW2 : PLAW2*PSIZE(I)**(-PLAW2)
C  PND : NUMBER DISTRIBUTION
C  PSIZE : PARTICLE DIAMETER, MICRONS
C  PSD : SURFACE DISTRIBUTION
C  PSZLOG : LOG OF PARTICLE DIAMETER
C  PVD : VOLUME DISTRIBUTION
C  RHO : DENSITY OF PARTICLES, GRAMS/CM**3
C  RHOWAT : DINSITY OF WATER, GRAMS/CM**3
C  T : TIME, SEC
C  TEMP : TEMPERATURE, KELVIN
C  TMAX : MAXIMUM TIME, SECONDS
C  TOTDIA : TOTAL DIAMETER OF PARTICLES
C  TOTMAS : TOTAL MASS OF PARTICLES
C  TOTNUM : TOTAL NUMBER OF PARTICLES
C  TOTSUM : TOTAL SURFACE OF PARTICLES
C  TOTVUM : TOTAL VOLUME OF PARTICLES
C  TOTYIN : TOTAL NUMBER OF INPUT PARTICLES
C  TT : TIME FOR HYDROLOGICAL CALCULATION
```

```
C  V : VOLUME OF PARTICLES
C  VCON : VOLUME AVERAGE SHEAR RATE
C  VELGRA : VELOCITY GRADIENT
C  VISCOS : VISCOSITY, GM/CM-SEC
C  VPEAK : PARTICLE SIZE OF PEAK IN VOLUME DISTRIBUTION
C  VSTLOG : LOG OF VOLUME STEPS
C  Y : NUMBER OF PARTICLES PER ML
C
C
      INTEGER PEAKND,PEAKVD
      LOGICAL FAIL
      EXTERNAL DIFFUN
      DIMENSION BETA(100,100),TOTN(4,400),CALCTI(10,10),DELTAD(100),
     *       PSIZE(100),PND(100),PVD(100),FRAC(100,100),PSZLOG(100),
     *       PSD(100),OUTTIM(50),FDEN(100),VF(100),V(100),DY(100),
     *       Y(100),PNAVG(10,10,100),YY(100)
      COMMON/B/ BETA
      COMMON/F/ FRAC
      COMMON FAIL
      FAIL =.FALSE.
      OPEN(UNIT=6,FILE='FLOC.OUT',STATUS='NEW')
      LFLAG = 1
      NINI = 0
C
      DO 11 III=1, 300
      CALL INITVA(N,NC,NT,MFLAG,KFLAG,H,HMIN,HMAX,ALPHA,RHO,
     *      RHOWAT,BOLTZ,PI,TEMP,VISCOS,T,TMAX,GRAVCO,VSTLOG,DELTAD,
     *      PSIZE,PSZLOG,PSD,V,Y,DY,TOTYIN,NDCALL,NTI,OUTTIM,CON3,
     *      CON4,VELGRA,CALCTI,HMKCON,DCON,DKP,
     *      VCON,DMAX,IFLOC,NINI,IMON,NOUT)
      CALL BETACA(N,GRAVCO,VISCOS,RHO,RHOWAT,BOLTZ,TEMP,PI,
     *      VELGRA ,ALPHA,PSIZE,V,HMKCON,DCON,DKP,
     *      VCON,DMAX,FDEN)
      CALL FRACCA(N,V,VSTLOG)
      CALL MASSSU(N,Y,V,DELTAD,PSIZE,PSD,PVD,PND,TOTNUM,TOTVOL,
     *      TOTSUR,TOTDIA,TOTMAS,TOTYIN,AVVODI,AVSUDI,AVNUDI,
     *      PEAKVD,PEAKND,FRAREN,CON3,CON4,RHO,FDEN,VF,IFLOC)
      IF (IMON.EQ.0) THEN
         WRITE(6,68)
68       FORMAT(//,2X,'INITIAL PARTICLE SIZE DISTRIBUTION DATA')
      CALL OUTPUT(N,NDCALL,KFLAG,MFLAG,NTI,TOTNUM,TOTMAS,FRAREN,
     *      AVVODI,AVSUDI,AVNUDI,PSD,PVD,PND,PEAKVD,PEAKND,
     *      PSZLOG,PSIZE,DY,T,Y,VF,IFLOC,TOTVOL,FDEN)
      ENDIF
      DO 100 J=1,500
         IF (T.LT.TMAX.OR..NOT.FAIL) THEN
         CALL STIFDI(N,H,HMIN,HMAX,KFLAG,Y,DY,T,LFLAG
     *                ,NDCALL,DIFFUN)
         IF (MFLAG.EQ.1) THEN
            DO 20 IM=1, NC
            DO 25 JM=1, NT
              IF (T.GE.CALCTI(IM,JM)) THEN
                CALCTI(IM,JM)=TMAX+HMAX+50000.
                DO 30 I=1,N
                  PNAVG(IM,JM,I)=Y(I)
30              CONTINUE
              ENDIF
25          CONTINUE
20          CONTINUE
         ENDIF
       IF (KFLAG.EQ.1) THEN
         IF (T.GE.OUTTIM(NTI)) THEN
         OUTTIM(NTI) = TMAX+HMAX+1
         IF (NTI.LE.NOUT) THEN
         CALL MASSSU(N,Y,V,DELTAD,PSIZE,PSD,PVD,PND,TOTNUM,TOTVOL,
     *         TOTSUR,TOTDIA,TOTMAS,TOTYIN,AVVODI,AVSUDI,AVNUDI,
     *         PEAKVD,PEAKND,FRAREN,CON3,CON4,RHO,FDEN,VF,IFLOC)
         IF (IMON.EQ.0) THEN
         CALL OUTPUT(N,NDCALL,KFLAG,MFLAG,NTI,TOTNUM,TOTMAS,FRAREN,
     *         AVVODI,AVSUDI,AVNUDI,PSD,PVD,PND,PEAKVD,PEAKND,
     *         PSZLOG,PSIZE,DY,T,Y,VF,IFLOC,TOTVOL,FDEN)
         ENDIF
         ENDIF
```

```fortran
            ENDIF
          ENDIF
        ELSE
          GOTO 110
        ENDIF
  100 CONTINUE
  110 CONTINUE
C     AFTER THE MODEL HAS RUN FOR ALL OF THE DESIGNATED BY
C     TMAX, THE DISTRIBUTIONS FOR EACH COMPARTMENT CAN BE
C     CALCULATED AND PRINTED WHEN THE NON-IDEAL CASE IS USED
        IF (MFLAG.EQ.1) THEN
          DO 50 IM=1, NC
            DO 51 I=1,N
              YY(I) = 0.0
   51       CONTINUE
            IF (IMON.EQ.0) THEN
              WRITE(6,60) IM
   60       FORMAT(//'THE MODEL PREDICTION AT COMPAREMENT NUMBER',I10)
            ENDIF
            DO 65 JM=1,NT
            DO 65 I=1,N
              YY(I) = YY(I) +PNAVG(IM,JM,I)
   65       CONTINUE
            DO 66 I=1,N
              Y(I) = YY(I)/5.0
   66       CONTINUE
            CALL MASSSU(N,Y,V,DELTAD,PSIZE,PSD,PVD,PND,TOTNUM,TOTVOL,
     *          TOTSUR,TOTDIA,TOTMAS,TOTYIN,AVVODI,AVSUDI,AVNUDI,
     *          PEAKVD,PEAKND,FRAREN,CON3,CON4,RHO,FDEN,VF,IFLOC)
            IF (IMON.EQ.0) THEN
            CALL OUTPUT(N,NDCALL,KFALG,MFLAG,NTI,TOTNUM,TOTMAS,FRAREN,
     *          AVVODI,AVSUDI,AVNUDI,PSD,PVD,PND,PEAKVD,PEAKND,
     *          PSZLOG,PSIZE,DY,T,Y,VF,IFLOC,TOTVOL,FDEN)
            ENDIF
            TOTN(IM,III) = FRAREN
   50     CONTINUE
        ENDIF
        IF (IMON.EQ.1) THEN
        WRITE(6,16) III,TOTN(1,III),TOTN(2,III),TOTN(3,III)
   16   FORMAT(5X,I4,2X,3F15.5)
        ENDIF
        IF (IMON.EQ.0) STOP
   11 CONTINUE
        STOP
        END
C
C
      SUBROUTINE INITVA(N,NC,NT,MFLAG,KFLAG,H,HMIN,HMAX,ALPHA,RHO,
     *      RHOWAT,BOLTZ,PI,TEMP,VISCOS,T,TMAX,GRAVCO,VSTLOG,DELTAD,
     *      PSIZE,PSZLOG,PSD,V,Y,DY,TOTYIN,NDCALL,NTI,OUTTIM,CON3,
     *      CON4,VELGRA,CALCTI,HMKCON,DCON,DKP,
     *      VCON,DMAX,IFLOC,NINI,IMON,NOUT)
C     IMPLICIT REAL*8(A-H, O-Z)
      DIMENSION CALCTI(10,10), DELTAD(100),PSIZE(100), V(100),
     *      PSZLOG(100),PSD(100),PVLOG(100),OUTTIM(20),Y(100),DY(100),
     *      CY(100),DI(100),YI(100),XHMKCO(300),XVCON(300),
     *      XVELGR(300),XDMAX(300),XDKP(300),XDCON(300),XDT(300),
     *      XPLAW1(300),XPLAW2(300)
      OPEN(UNIT=5,FILE='ISU4530.IN',STATUS='UNKNOWN')
C     INPUT DATA
C     IF MFLAG=1; THE OUTPUT WILL PRINTED BASED ON
C                 THE NON-IDEAL FLOW CASE
C     IF MFLAG=0; THE IDEAL(PLUG FLOW) CASE
      MFLAG = 1
C     IF KFLAG=1; THE OUTPUT WILL PRINTED DESIGNATED TIME (MIN.) BY USER
      KFLAG = 0
C     IMON = 1;  DO MONTE CARLO SIMULATION
      IMON = 0
C     IFLOC = 0 ; CONSTANT DENSITY WILL BE USED
C     IFLOC = 1 ; VARIABLE DENSITY WILL BE USED FOR
C                 CALCULATION FLOC VOLUME
      IFLOC = 1
C     IFLOW = 1 ; CACULATE F CURVE FOR EQUAL VOLUME OF
```

```
C                    FLOCCULATOR SERIES
C        IFLOW = 2 ; USE EXPERIMENTAL F CURVE DATA
         IFLOW = 1
C        NUMERICAL PARAMETERS
         H = 10.0
         HMIN = 1.0
         HMAX = 100
         PVLOG(1) = -0.462
         T = 0.0
         TOTYIN = 0.0
         TMAX = 8000.0
         VSTLOG = 0.09
C
         RHO = 2.65
         RHOWAT = 1.0
         VISCOS = 0.01
         TEMP = 293.0
         GRAVCO = 980.
         PI = 3.1415926535
         BOLTZ = 1.38E-16
         HMKCON = 2.0E-19
C
         ALPHA = 1.
         VELGRA = 25.0
         VCON = 0.39
         DMAX = 200.0
         DT = 15.
         DCON = 0.0013
         DKP  = 0.9
C         ALT = 1./20.
C         DCON = - 0.00126 * ALOG10(ALT) - 0.00106
C         DKP = 0.4854 * ALOG10(ALT) + 1.885
C
C        INPUT MFLAG
C             N=NUMBER OF DIFFERENT PARTICLE VOLUMES
C             NC=NUMBER OF COMPARTMENTS OR BASINS
C             NT=NUMBER OF AVERAGING TIMES
         IF (MFLAG.EQ.1) THEN
                 N= 64
                 NC=3
                 NT=5
C        INPUT MATRIX OF TIMES USED TO AVERAGE THE Y VALUES
C        FOR USE IN THE FINAL OUTPUT FOR NON-IDEAL FLOW
C        CASE. TIMES ARE DETERMINED FROM EITHER MEASURED OR
C        THEORETICAL FLOW CURVES
C        IFLOW =1 : EQUAL VOLUME OF FLOCCULATOR SERIES
C        IFLOW =2 : DIFFERENT VOLUME OF FLOCCULATIOR SERIES
C        IFLOW =3 : EXPERIMENTAL DATA FOR FLOW
C
         IF (IFLOW.EQ.1) THEN
           CALL EFLOW(NC,DT, CALCTI)
C         ELSEIF (IFLOW.EQ.2) THEN
C           CALL DFLOW(NC, CALCTI)
         ELSEIF (IFLOW.EQ.2) THEN
           CALCTI(1,1) = 5.
           CALCTI(1,2) = 7.2
           CALCTI(1,3) = 11.2
           CALCTI(1,4) = 19.2
           CALCTI(1,5) = 47.2
           CALCTI(2,1) = 14.4
           CALCTI(2,2) = 20.
           CALCTI(2,3) = 30.4
           CALCTI(2,4) = 44.
           CALCTI(2,5) = 90.4
           CALCTI(3,1) = 28.
           CALCTI(3,2) = 41.6
           CALCTI(3,3) = 58.6
           CALCTI(3,4) = 80.0
           CALCTI(3,5) = 130.0
         ENDIF
         DO 322 I=1,NC
         DO 323 J=1,NT
           CALCTI(I,J) = CALCTI(I,J)*60.
```

```
      323   CONTINUE
      322     CONTINUE
          ELSE
                  N=72
          ENDIF
C         NDCALL : NUMBER OF OUTPUT AT EACH SPECIFIED TIME (MIN)
          NOUT = 6
            OUTTIM(1) = 300.
            OUTTIM(2) = 600.
            OUTTIM(3) = 900.
            OUTTIM(4) = 1200
            OUTTIM(5) = 1500.
            OUTTIM(6) = 1800.
C
          GRAVCO=980.
          PI=3.1415926535
          NDCALL=0
          NTI = 0
          TOTYIN = 0.0
          DO 30 I=1,N
            DY(I)=0.
            Y(I)=0.
       30 CONTINUE
          ERROR=0.
          CON1=1.
          CONBET=PI/4.*(6./PI)**(5./6.)*(4.*GRAVCO/3.*((RHO-RHOWAT)/
        * RHOWAT))**(1./2.)*(1.0E-04)**(5./2.)
          CON3=(6./PI)**(1./3)
          CON4=2.3*PI/6.
          DO 200 I=2, N
              PVLOG(I)=PVLOG(I-1)+VSTLOG
      200 CONTINUE
          DO 210 I=1, N
              V(I)=10.**PVLOG(I)
              PSIZE(I)=(6./PI*10**(PVLOG(I)))**(1./3.)
              PSZLOG(I)=ALOG10(PSIZE(I))
              DELTAD(I)=(6./PI*10**(PVLOG(I)+0.5*VSTLOG))**(1./3.)
        *               -(6./PI*10.**(PVLOG(I)-0.5*VSTLOG))**(1./3.)
      210 CONTINUE
C     INMODE ; INPUT MODE FOR PARTICLE SIZE DISTRIBUTION
C     INMODE = 1 ; READ Y(I) NUMBER OF PARTICLE PER ML
C     INMODE = 2 ; READ PARTICLE SIZE DISTRIBUTION
C     INMODE = 3 ; READ PSD FUNCTION AND CALCULATE Y(I)
C     INMODE = 4 ; READ YI(I), NUMBER OF PARTICLE PER ML WITH WITH
C                  PARTICLE DIAMETER DI(I)  UM
          INMODE = 3
          IF (INMODE.EQ.1) THEN
            TY = 0.0
            DO 230 I=1, N
              IF (PSIZE(I).LE.10.0) THEN
                Y(I) = 58.208*PSIZE(I) - 200.187 - TY
              ELSEIF (PSIZE(I).GT.10.0.AND.PSIZE(I).LE.20.0) THEN
                Y(I) = 9.1505*PSIZE(I) + 290.388 - TY
              ELSEIF (PSIZE(I).GT.20.0.AND.PSIZE(I).LE.40.0) THEN
                Y(I) = 0.363562*PSIZE(I) + 466.126 - TY
              ELSE
                Y(I) = 0.0
              ENDIF
              TY = TY + Y(I)
              IF (Y(I).LE.0.5) GO TO 230
              PSD(I)=ALOG10(Y(I)/DELTAD(I))
              TOTYIN=TOTYIN+Y(I)
      230   CONTINUE
          ELSEIF (INMODE.EQ.2) THEN
            DO 250 I=1, N
C             READ(5,270) PSD(I)
C 270         FORMAT(F10.5)
              IF (PSD(I).EQ.0.0) THEN
                Y(I)=0.
              ELSEIF (PSD(I).EQ.999.0) THEN
                Y(I)=0.
                GOTO 250
              ELSE
```

```
                     Y(I)=DELTAD(I)*10**PSD(I)
                     TOTYIN=TOTYIN+Y(I)
                  ENDIF
     250    CONTINUE
          ELSEIF (INMODE.EQ.3) THEN
C         INPUT FOR POWER LAW CONSTANT
          PLAW1 = 2.0E7
          PLAW2 = 4.0
          DO 252 I=1,N
C            YOU NEED TO PUT PSD FUNCTION IN HERE
             IF (PSIZE(I).LE.30) THEN
             PSD(I) = PLAW1*PSIZE(I)**(-PLAW2)
             Y(I) = DELTAD(I)*PSD(I)
             ELSE
             Y(I) = 0.0
             ENDIF
             IF (Y(I).LE.0.5) Y(I)=0.0
             TOTYIN=TOTYIN+Y(I)
     252    CONTINUE
          ELSEIF (INMODE.EQ.4) THEN
            TOTYIN = 0.0
            NJ = 15
            DO 253 I=1,NJ
              READ(5,254) DI(I),YI(I)
     254      FORMAT(F7.2,E10.3)
     257      FORMAT(2X,F7.2,2X,E10.3,2X,E12.5)
              IF (DI(I).EQ.999.00) THEN
              NI=I
              GO TO 255
              ENDIF
               TOT = TOT + YI(I)
                CY(I) = TOT
             WRITE(6,257) DI(I),YI(I),CY(I)
     253    CONTINUE
     255    CONTINUE
            TY = 0.0
            J=2
            DO 260 I=1,N
C             NJ IS THE NUMBER OF PARTICLE SIZE
              NJ = 17
     262       CONTINUE
             IF (PSIZE(I).LE.DI(J)) THEN
                JJ=J-1
                SLOPE = (CY(J)-CY(JJ))/(DI(J)-DI(JJ))
                TRCPT = CY(J)-SLOPE*DI(J)
                YY = SLOPE*PSIZE(I)+TRCPT
                Y(I) = YY-TOTYIN
                TOTYIN = TOTYIN+Y(I)
             ELSEIF (PSIZE(I).GE.DI(NJ)) THEN
                Y(I) = 0.0
             ELSE
                J = J+1
                GO TO 262
             ENDIF
     260    CONTINUE
          ENDIF
C
          NINI = NINI + 1
          IF (IMON.EQ.1) THEN
C         MONTE CARLO SIMULATION
C         CALL GAUSSIAN RANDOM NUMBER GENERATOR
C         NEED TO SET IDUM IT ANY NEGATIVEL VALUE
C         CVAR ; COEFFICIENT OF VARIATION
          IF (NINI.GE.2) GOTO 347
          IDUM = -1
          DO 342 I=1,300
            CVAR = 0.0333
            XHMKCO(I) = HMKCON + CVAR*HMKCON*GASDEV(IDUM)
            XVCON(I)  = VCON + CVAR*VCON*GASDEV(IDUM)
            XVELGR(I) = VELGRA + CVAR*VELGRA*GASDEV(IDUM)
            XDMAX(I)  = DMAX + CVAR*DMAX*GASDEV(IDUM)
            XDCON(I)  = DCON + CVAR*DCON*GASDEV(IDUM)
            XDKP(I)   = DKP + CVAR*DKP*GASDEV(IDUM)
```

```
          XDT(I)    = DT + CVAR*DT*GASDEV(IDUM)
          XPLAW1(I) = PLAW1 + CVAR*PLAW1*GASDEV(IDUM)
          XPLAW2(I) = PLAW2 + CVAR*PLAW2*GASDEV(IDUM)
  342 CONTINUE
  347 CONTINUE
      VCON = XVCON(NINI)
      DMAX = XDMAX(NINI)
      DCON = XDCON(NINI)
      DKP  = XDKP(NINI)
      DT   = XDT(NINI)
      PLAW1= XPLAW1(NINI)
      PLAW2= XPLAW2(NINI)
C      WRITE(6,349) VCON,DMAX,DCON,DKP,DT,PLAW1,PLAW2
C  349 FORMAT(2X,7E10.4)
      ENDIF
C
      IF (IMON.EQ.0) THEN
      WRITE(6,330)
  330 FORMAT(//,2X,'**********MODEL INPUT**********')
      WRITE(6,340)
  340 FORMAT(/2X,5HALPHA,7X,7HHAMAKER,8X,4HTEMP,7X,9HVISCOSITY,7X,
     *          7HDENSITY)
      WRITE(6,350)
  350 FORMAT(2X,15X,3H(J),7X,8H(KELBIN),2X,11H(GM/CM-SEC),5X,
     *          10H(GM/CM**3))
      WRITE(6,360) ALPHA,HMKCON,TEMP,VISCOS,RHO
  360 FORMAT(2X,F5.3,7X,E9.2,6X,F5.1,8X, F6.4, 10X, F4.2)
      WRITE(6,362)
  362 FORMAT(/,2X,4HDMAX,10X,4HVCON,9X,2HDT,10X,4HDCON,12X,3HDKP)
      WRITE(6,364) DMAX,VCON,DT,DCON,DKP
  364 FORMAT(F6.1,8X,F6.1,7X,F5.1,8X,F6.5,7X,F6.2)
      WRITE(6,370)
  370 FORMAT(/,2X,1HH,13X,4HHMIN,8X,4HHMAX,8X,4HTMAX)
      WRITE(6,380) H, HMIN, HMAX,TMAX
  380 FORMAT(1X,F5.1, 8X, F5.1, 8X, F5.1,5X,F7.1)
      ENDIF
      RETURN
      END
C
C
C
      SUBROUTINE EFLOW(NC, DT, CALCTI)
      DIMENSION CALCTI(10,10), F(10)
C     THIS SUBROUTINE CALCULATE F(I) CURVES FOR EQUAL VOLUME OF
C     COMPLETELY-MIXED REACTORS
      DO 10 J=1,150
        TT = J
        F(1) = 1. - EXP(-TT/DT)
        IF (F(1).LE.0.2) THEN
          CALCTI(1,1) = TT
        ELSEIF (F(1).LE.0.4) THEN
          CALCTI(1,2) = TT
        ELSEIF (F(1).LE.0.6) THEN
          CALCTI(1,3) = TT
        ELSEIF (F(1).LE.0.8) THEN
          CALCTI(1,4) = TT
        ELSEIF (F(1).LE.0.975) THEN
          CALCTI(1,5) = TT
        ENDIF
   10 CONTINUE
      FSUM = 0.
      ISUM = 1
      TSUM = 1.
      DO 15 J =1, 150
        TT = J
        II = NC -1
        FSUM = 0.
        ISUM = 1
        DO 20 I=1,II
          ISUM = ISUM*I
          SSUM = (TT/DT)**I/ISUM
          FSUM = FSUM + SSUM
          IJ = I+1
```

```
                   F(IJ) = 1. - (FSUM+1.)*EXP(-TT/DT)
                   IF (F(IJ).LE.0.2) THEN
                     CALCTI(IJ,1) = TT
                   ELSEIF (F(IJ).LE.0.4) THEN
                     CALCTI(IJ,2) = TT
                   ELSEIF (F(IJ).LE.0.6) THEN
                     CALCTI(IJ,3) = TT
                   ELSEIF (F(IJ).LE.0.8) THEN
                     CALCTI(IJ,4) = TT
                   ELSEIF (F(IJ).LE.0.975) THEN
                     CALCTI(IJ,5) = TT
                   ENDIF
    20 CONTINUE
    15 CONTINUE
       RETURN
       END
C
C
C
       SUBROUTINE BETACA(N,GRAVCO,VISCOS,RHO,RHOWAT,BOLTZ,TEMP,PI,
      *              VELGRA,ALPHA,PSIZE,V,HMKCON,DCON,
      *              DKP,VCON,DMAX,FDEN)
C      IMPLICIT REAL*8(A-H, O-Z)
       DIMENSION BETA(100,100),BETASH(100,100),BETABR(100,100),
      *  BETASE(100,100),PSIZE(100),PSCM(100),DRAGCO(100),
      *  STOKSV(100),REYNNO(100),SVEL(100),V(100),
      *  GBETA(100,100),GBBR(100,100),GBSH(100,100),GBSE(100,100),
      *  EDEN(100),FDEN(100),FSIZE(100),FSCM(100),FV(100),
      *  A1(7),B1(7),C1(7),D1(7),A2(4),B2(4),C2(4),D2(4),
      *  A3(3),B3(3),C3(3)
       COMMON/B/ BETA
       DATA A1/0.21811,0.25878,0.31151,0.37254,0.44285,0.53814,0.7048/
       DATA B1/2.9593E-2,3.0338E-2,3.0339E-2,2.9251E-2,2.6954E-2,
      *        2.2834E-2,1.3481E-2/
       DATA C1/-4.9962E-4,-5.3031E-4,-5.4760E-4,-5.4055E-4,-5.0576E-4,
      *        -4.331E-4,-2.4753E-4/
       DATA D1/2.6953E-6,2.9043E-6,3.0409E-6,3.0318E-6,2.855E-6,
      *        2.4569E-6,1.3845E-6/
       DATA A2/-1.189,0.766,0.145,0.017/
       DATA B2/0.118,0.007,-0.0006,-0.001/
       DATA C2/-3.431,-0.006,-1.137,-1.442/
       DATA D2/0.331,1.547,0.775,0.557/
       DATA A3/-0.031061,-0.12386,-0.31818/
       DATA B3/0.027924,0.11031,0.26333/
       DATA C3/0.0027,0.0328167,0.412667/
C
C      IN THIS PROCEDURE, THE DRAG COEFFICIENT IS CALCULATED AND
C      USE IN THE CALCULATION OF THE DIFFERENCE IN SETTLING VELOCITIES
C      FOR BETA-SED. THIS METHOD IS USED TO ACCOUNT FOR DIVERGENCE
C      FROM STOKES SETTLLING BY LATGE PARTICLES
C
C      WRITE(6,1330) VCON,DCON,DKP
C 1330 FORMAT(2X,'VCON=',F10.4,2F15.5)
       AK=(RHO-RHOWAT)/DCON
       DO 155 I=1,N
          PSCM(I) = PSIZE(I)*0.0001
          FSCM(I)=(AK*PSCM(I)**3)**(1./(3-DKP))
          FSIZE(I)=FSCM(I)*10000.0
          FV(I)=1./6.*PI*FSIZE(I)**3
          EDEN(I)=DCON/(FSCM(I)**DKP)
          FDEN(I)=EDEN(I)+RHOWAT
          IF (FDEN(I).GT.RHO) THEN
            FDEN(I) = RHO
            FSCM(I) = PSCM(I)
            FSIZE(I) = PSIZE(I)
            FV(I) = V(I)
          ENDIF
C         WRITE(6,144) I,FSCM(I),EDEN(I),FDEN(I)
C  144    FORMAT(2X,I5,2X,3F10.5)
   155 CONTINUE
       DO 300 I=1, N
          STOKSV(I)=GRAVCO/(18*VISCOS)*(FDEN(I)-RHOWAT)*PSCM(I)**2
          REYNNO(I)=STOKSV(I)*RHOWAT*PSCM(I)/VISCOS
```

```
  300 CONTINUE
      CON=2.*BOLTZ*TEMP/(3.*VISCOS)
      CON2=3./(4.*PI)
      DO 10 I=1, N
      DO 20 J=1, N
        BETABR(I,J)=0.
        BETASH(I,J)=0.
        BETASE(I,J)=0.
   20 CONTINUE
   10 CONTINUE
C
      DO 320 I=1, N
        IF (REYNNO(I).LE.1.) THEN
          DRAGCO(I)=24./REYNNO(I)
          SVEL(I)=STOKSV(I)
        ELSE
          VEL1=SVEL(I-1)
          VEL2=STOKSV(I)
  330     CONTINUE
          IF (ERROR.GE.0.01) THEN
            TRIVEL=(VEL2+VEL1)/2.
            RE=TRIVEL*RHOWAT*PSCM(I)/VISCOS
            CD=24./RE+3./RE**(1./2.)+0.34
            VELNEW=(4.*GRAVCO/(3.*CD)*((FDEN(I)-RHOWAT)/RHOWAT)
     *             *PSCM(I))**(1./2.)
            ERROR=ABS((VELNEW-TRIVEL)/TRIVEL)
            IF (VELNEW.GT.TRIVEL) THEN
              VEL1=TRIVEL
            ELSE
                  VEL2=TRIVEL
            ENDIF
            GO TO 330
          ENDIF
          SVEL(I)=VELNEW
          REYNNO(I)=SVEL(I)*PSCM(I)*RHOWAT/VISCOS
          DRAGCO(I)=24./REYNNO(I)+3./REYNNO(I)**(1./2.)+0.34
        ENDIF
        ERROR=1.0
  320 CONTINUE
C     I = 1
      DO 350 I=1,N
      DO 360 J=1,N
        IF (PSIZE(I).GE.PSIZE(J)) THEN
          DRATIO = PSIZE(I)/PSIZE(J)
          BPSIZE = PSIZE(I)
          SPSIZE = PSIZE(J)
        ELSE
          DRATIO = PSIZE(J)/PSIZE(I)
          BPSIZE = PSIZE(J)
          SPSIZE = PSIZE(I)
        ENDIF
C
C     BROWIAN MODIFICATION
      AKT = HMKCON*1.0E7/(BOLTZ*TEMP)
      IF (AKT.LT.0.0001) THEN
        GAMABR=A1(1)+B1(1)*DRATIO+C1(1)*DRATIO**2+D1(1)*DRATIO**3
      ELSEIF (AKT.LT.0.001.AND.AKT.GE.0.0001) THEN
        BR1=A1(1)+B1(1)*DRATIO+C1(1)*DRATIO**2+D1(1)*DRATIO**3
        BR2=A1(2)+B1(2)*DRATIO+C1(2)*DRATIO**2+D1(2)*DRATIO**3
        GAMABR=BR1+(BR2-BR1)/0.0009*(AKT-0.0001)
      ELSEIF (AKT.LT.0.01.AND.AKT.GE.0.001) THEN
        BR1=A1(2)+B1(2)*DRATIO+C1(2)*DRATIO**2+D1(2)*DRATIO**3
        BR2=A1(3)+B1(3)*DRATIO+C1(3)*DRATIO**2+D1(3)*DRATIO**3
        GAMABR=BR1+(BR2-BR1)/0.009*(AKT-0.001)
      ELSEIF (AKT.LT.0.1.AND.AKT.GE.0.01) THEN
        BR1=A1(3)+B1(3)*DRATIO+C1(3)*DRATIO**2+D1(3)*DRATIO**3
        BR2=A1(4)+B1(4)*DRATIO+C1(4)*DRATIO**2+D1(4)*DRATIO**3
        GAMABR=BR1+(BR2-BR1)/0.09*(AKT-0.01)
      ELSEIF (AKT.LT.1.AND.AKT.GE.0.1) THEN
        BR1=A1(4)+B1(4)*DRATIO+C1(4)*DRATIO**2+D1(4)*DRATIO**3
        BR2=A1(5)+B1(5)*DRATIO+C1(5)*DRATIO**2+D1(5)*DRATIO**3
        GAMABR=BR1+(BR2-BR1)/0.9*(AKT-0.1)
      ELSEIF (AKT.LT.10.AND.AKT.GE.1.0) THEN
```

```
      BR1=A1(5)+B1(5)*DRATIO+C1(5)*DRATIO**2+D1(5)*DRATIO**3
      BR2=A1(6)+B1(6)*DRATIO+C1(6)*DRATIO**2+D1(6)*DRATIO**3
      GAMABR=BR1+(BR2-BR1)/9.*(AKT-9)
    ELSEIF (AKT.LT.100.AND.AKT.GE.10) THEN
      BR1=A1(6)+B1(6)*DRATIO+C1(6)*DRATIO**2+D1(6)*DRATIO**3
      BR2=A1(7)+B1(7)*DRATIO+C1(7)*DRATIO**2+D1(7)*DRATIO**3
      GAMABR=BR1+(BR2-BR1)/90.*(AKT-9)
    ELSE
      GAMABR=A1(7)+B1(7)*DRATIO+C1(7)*DRATIO**2+D1(7)*DRATIO**3
    ENDIF
    IF (GAMABR.LT.0.2) GAMABR=0.2
    IF (GAMABR.GE.1.0) GAMABR=1.0
      BETABR(I,J)=CON*((1./FV(I)**(1./3.))+(1./FV(J)**(1./3.)))
   *              *((FV(I)**(1./3.))+(FV(J)**(1./3.)))
      GBBR(I,J) = GAMABR*BETABR(I,J)
C
C     SHEAR MODIFICATION
      EVELGRA = VCON*VELGRA
      AKINEMA = 0.009403
      SCALEK = (AKINEMA/EVELGRA)**(1/2.)
      TU = (FSIZE(I) + FSIZE(J))/2.
      IF (TU.LE.SCALEK) THEN
        UVELGRA = 0.306*EVELGRA
      ELSE
        UVELGRA = 2.56*(AKINEMA*EVELGRA**2)**(1./3.)
   *              *(FSIZE(I)+FSIZE(J))**(1./3.)
      ENDIF
      IF (I.GE.J) THEN
        II = I
      ELSE
        II = J
      ENDIF
      PORO = (RHO-FDEN(II))/(RHO-RHOWAT)
      HA=HMKCON*1.E19/(18.0*PI*VISCOS*BPSIZE**3*EVELGRA)
      IF (HA.GE.1.0E-2) THEN
      GAMASH = (A2(1)+B2(1)*DRATIO)
   *      /(1.+C2(1)*DRATIO+D2(1)*DRATIO**2)*8./(1.+1./DRATIO)**3
      ELSEIF (HA.LT.1.0E-2.AND.HA.GE.1.0E-3) THEN
      G1 = (A2(1)+B2(1)*DRATIO)
   *      /(1.+C2(1)*DRATIO+D2(1)*DRATIO**2)*8./(1.+1./DRATIO)**3
      G2 = (A2(2)+B2(2)*DRATIO)
   *      /(1.+C2(2)*DRATIO+D2(2)*DRATIO**2)*8./(1.+1./DRATIO)**3
      G3 = G2+(G1-G2)*(HA-1.0E-3)/(1.0E-2-1.0E-3)
      GAMASH = G3
      ELSEIF (HA.LT.1.0E-3.AND.HA.GE.1.0E-4) THEN
      G1 = (A2(2)+B2(2)*DRATIO)
   *      /(1.+C2(2)*DRATIO+D2(2)*DRATIO**2)*8./(1.+1./DRATIO)**3
      G2 = (A2(3)+B2(3)*DRATIO)
   *      /(1.+C2(3)*DRATIO+D2(3)*DRATIO**2)*8./(1.+1./DRATIO)**3
      G3 = G2+(G1-G2)*(HA-1.0E-4)/(1.0E-3-1.0E-4)
      GAMASH = G3
      ELSEIF (HA.LT.1.0E-4.AND.HA.GT.1.05E-5) THEN
      G1 = (A2(3)+B2(3)*DRATIO)
   *      /(1.+C2(3)*DRATIO+D2(3)*DRATIO**2)*8./(1.+1./DRATIO)**3
      G2 = (A2(4)+B2(4)*DRATIO)
   *      /(1.+C2(4)*DRATIO+D2(4)*DRATIO**2)*8./(1.+1./DRATIO)**3
      G3 = G2+(G1-G2)*(HA-1.0E-5)/(1.0E-4-1.0E-5)
      GAMASH = G3
      ELSE
      G3 = (A2(4)+B2(4)*DRATIO)
   *      /(1.+C2(4)*DRATIO+D2(4)*DRATIO**2)*8./(1.+1./DRATIO)**3
      GAMASH = G3
      ENDIF
      IF (GAMASH.LE.1.0E-5) THEN
        GAMASH = 1.0E-5
      ENDIF
      IF (PORO.GE.1.) THEN
        WRITE(6,11)
   11   FORMAT(//,4X,'POROSITY IS GREATER THAN 1')
        STOP
      ELSEIF (PORO.LT.0.0) THEN
        WRITE(6,112) FDEN(II), RHO, RHOWAT
  112   FORMAT(//,4X,3E15.7,2X,'POROSITY IS LESS THAN 0')
```

```
      STOP
    ENDIF
    IF (PORO.LE.0.5) THEN
      ESH = 0.0
    ELSE
      P = (FSIZE(II)/10)**2/18.*(3.+4./(1-PORO)-3.*(8./(1-PORO)-3)
    *      **0.5)
      ZETA = FSIZE(II)/(2.*P**0.5)
      ESH = 1.6185*EXP(-0.4902*ZETA)
    ENDIF
    IF (ESH.LE.0.0) THEN
      ESH = 0.0
    ELSEIF (ESH.GE.1.0) THEN
      ESH = 0.9999
    ENDIF
    SHEFF = GAMASH +ESH
    BETASH(I,J)=(((CON2*FV(I))**(1./3.))+((CON2*FV(J))**(1./3)))
    *            **3*4.*EVELGRA/3.*1.E-12
    GBSH(I,J) = SHEFF*BETASH(I,J)
    IF (GBSH(I,J).LE.0.0) THEN
      WRITE (6,12)
12    FORMAT(//,5X,'ESH IS LESS THAN ZERO')
      STOP
    ELSEIF (GBSH(I,J).GE.1.0) THEN
      WRITE (6,13)
13    FORMAT(//,5X,'ESH IS GREATER THAN 1')
      STOP
    ENDIF
C
C   DIFFERENTIAL SEDIMENTATION
    IF (I.EQ.J) THEN
      BETASE(I,J)=0.0
    ELSE
      GN = ABS(SVEL(I)-SVEL(J))*3.0*VISCOS*PI*PSIZE(I)*PSIZE(J)
    *        *(1.+1/DRATIO)/(2.*HMKCON*DRATIO*1.0E15)
      IF (GN.GE.1.0E6) THEN
        GAMASE=A3(1)/DRATIO**2+B3(1)/DRATIO+C3(1)
      ELSEIF (GN.GE.100.0.AND. GN.LT.1.0E6) THEN
        SE1=A3(1)/DRATIO**2+B3(1)/DRATIO+C3(1)
        SE2=A3(2)/DRATIO**2+B3(2)/DRATIO+C3(2)
        GAMASE=SE1+(SE2-SE1)/999900.0*(1.E6-GN)
      ELSEIF (GN.GE.0.1.AND.GN.LT.100.0) THEN
        SE1=A3(2)/DRATIO**2+B3(2)/DRATIO+C3(2)
        SE2=A3(3)/DRATIO**2+B3(3)/DRATIO+C3(3)
        GAMASE=SE1+(SE2-SE1)/99.9*(100.0-GN)
      ELSE
        GAMASE=A3(3)/DRATIO**2+B3(3)/DRATIO+C3(3)
      ENDIF
      IF (GAMASE.LE.1.E-18) THEN
        WRITE(6,15)
15      FORMAT(//,'GAMASE IS LESS THAN E-18')
        STOP
      ELSEIF (GAMASE.GE.1.) THEN
        WRITE(6,16)
16      FORMAT(//,'GAMASE IS LARGER THAN 1.')
        STOP
      ENDIF
      IF (GAMASE.LE.1.0E-5) THEN
        GAMASE=1.0E-5
      ELSEIF (GAMASE.GE.1.0) THEN
        GAMASE=1.0
      ENDIF
      IF (PORO.LE.0.5) THEN
        EDS=0.0
      ELSE
        ETA = 2.*ZETA**2+3.-3.*TANH(ZETA)/ZETA
        AA = -1./ETA*(ZETA**5+6*ZETA**3-TANH(ZETA)/ZETA
    *          *(3.*ZETA**5+6*ZETA**3))
        BB = 1/ETA*3.*ZETA**3*(1.-TANH(ZETA)/ZETA)
        EDS = 1.-BB/ZETA-AA/ZETA**3
      ENDIF
      IF (EDS.GE.1.) THEN
        EDS = 0.9999
```

```fortran
          ELSEIF (EDS.LT.0.) THEN
            EDS = 1.0E-5
          ENDIF
          BETASE(I,J)=PI/4.*(FSCM(I)+FSCM(J))**2
     *               *ABS(SVEL(I)-SVEL(J))
          SDEFF = GAMASE + EDS
          GBSE(I,J) = SDEFF*BETASE(I,J)
        ENDIF
C       FLOC BREAK-UP FACTOR (ZERO COLLISION EFFICIENCY)
        PSUM = PSIZE(I)+PSIZE(J)
        IF (PSUM.LT.DMAX) THEN
          ZBETA = (1.-PSUM/DMAX)**3
        ELSE
          ZBETA = 0.0
        ENDIF
C
C       CALCULATION OF BETA AND MODIFIED GBETA
C         BETA(I,J)=ALPHA*(BETABR(I,J)+BETASH(I,J)+BETASE(I,J))
          GBETA(I,J)=ALPHA*ZBETA*(GBBR(I,J)+GBSH(I,J)+GBSE(I,J))
          BETA(I,J) = GBETA(I,J)
        MOON = 0
        IF (MOON.EQ.1) THEN
          WRITE(6,1122) J,PSIZE(J),FSIZE(J),P,ZETA,ESH
 1122     FORMAT(2X,I5,2X,5F10.3)
          IF (J.EQ.99) STOP
        ENDIF
  360 CONTINUE
  350 CONTINUE
      RETURN
      END
C
C
C
      SUBROUTINE FRACCA(N,V,VSTLOG)
C      IMPLICIT REAL*8(A-H, O-Z)
      INTEGER RESULT
      DIMENSION FRAC(100,100), V(100)
      COMMON/F/ FRAC
C
C     FRAC(K,1) IS THE FRACTION OF THE NEW PARTICLE FORMED FROM
C     PARTICLE I AND PARTICLE J THAT IS ASSIGNED TO V(RESULT)
C     RESULT IS THE NUMBER OF THE SMALLER OF THE TWO STANDARD
C     VOLUMES THAT THE SUM OF V(I) FALLS BETWEEN.
C     FRAC(K,1) IS TO BE USED WHEN RESULT < N
C     K=J-I+1, SO FOR EXAMPLE WHEN CONBINING A '6' PARTICLE
C     WITH A '9' PARTICLE, USE K=9-6+1=4
C
      DO 10 I=1, N
        DO 20 J=1, N
          FRAC(I,J)=0.
   20   CONTINUE
   10 CONTINUE
      I=1
      IJ=N-1
      DO 400 J=1, IJ
        K=J-I+1
        IF (K.GT.20) THEN
          RESULT=K
        ELSE
          RESULT=I+ INT(ALOG10(1.+10.**((J-I)*VSTLOG))/VSTLOG)
        ENDIF
        VOLIJ=V(I)+V(J)
        FRAC(K,1)=(V(RESULT+1)-VOLIJ)/(V(RESULT+1)-V(RESULT))
  400 CONTINUE
C
C     FRAC(K,2) IS TO BE USED WHEN COMBINING A 'K' PATTICLE
C     WITH 'N' PARTICLE
C     ITS CALCULATION FOLLOWS
C
      I=N
      DO 410 J=1, N
        K=J
        VOLIJ=V(I)+V(J)
```

```
         FRAC(K,2)=VOLIJ/V(N)
  410    CONTINUE
C
C    FRAC(K,3) IS TO BE USED WHEN COMBINING TWO PARTICLES BOTH OF
C    LESS THAN SIZE 'N' THAT YIELD ONE LARGER THAN SIZE 'N'
C    KEY TO USING FRAC(K,3)
C       I      J      K
C      N-3    N-3     1
C      N-2    N-5     2
C      N-2    N-4     3
C      N-2    N-3     4
C      N-2    N-2     5
C      N-1    N-8     6
C      N-1    N-7     7
C      N-1    N-6     8
C      N-1    N-5     9
C      N-1    N-4    10
C      N-1    N-3    11
C      N-1    N-2    12
C      N-1    N-1    13
C
C    THE CALCULATION OF FRAC(K,3) FOLLOWS
C
         I=N-3
         K=0
         J=N-3
         K=K+1
         VOLIJ=V(I)+V(J)
         FRAC(K,3)=VOLIJ/V(N)
           I=N-2
           II=N-5
           DO 420 J=II,I
             K=K+1
             VOLIJ=V(I)+V(J)
             FRAC(K,3)=VOLIJ/V(N)
  420    CONTINUE
           I=N-1
           II=N-8
           DO 430 J=II, I
             K=K+1
             VOLIJ=V(I)+V(J)
             FRAC(K,3)=VOLIJ/V(N)
  430    CONTINUE
C
         f=1
         if (f.eq.0) then
         WRITE(6,440)
  440 FORMAT(//,5X,11HFRAC VALUES)
         DO 450 J=1,N
           WRITE(6,470) J,(FRAC(J,I),I=1,3)
  470    FORMAT(2X,I4,2X,3F12.4)
  450 CONTINUE
         endif
         RETURN
         END
C
C
C
         SUBROUTINE STIFDI(N,H,HMIN,HMAX,KFLAG,Y,DY,T,
      *                   LFLAG,NDCALL,DIFFUN)
C      IMPLICIT REAL*8(A-H, O-Z)
         LOGICAL FAIL
         DIMENSION Y(100),DY(100),PNNEXT(100),BETA(100,100),FRAC(100,100)
      *          ,YO(100),XK1(100),XK2(100),XK3(100),XK4(100),
      *           XX1(100),XX2(100),XX3(100)
         COMMON/B/ BETA
         COMMON/F/ FRAC
         COMMON FAIL
C
         CALL DIFFUN(N,Y,DY,NDCALL,TOTNUM)
         FASTLO=0.
         IQUICK=1
         LFLAG =1
```

```
      DO 35 J=1,N
        I=J
        IF (.NOT.FAIL) GO TO 35
        IF (NDCALL.GT.4000) THEN
          WRITE (6,300)
300       FORMAT(//,5X,'TOO MANY DIFFUN CALL')
          STOP
        ENDIF
        IF (DY(I).LT.FASTLO) THEN
            FASTLO=DY(I)
            IQUICK=I
        ENDIF
        IF (LFLAG.EQ.0) STOP
        PNNEXT(I)=Y(I)+H*DY(I)
        IF (PNNEXT(I).LT.0.) THEN
          WRITE(6,20) T, I
20        FORMAT(/'PREDICTED NEG. PARTICLE CONC. AT T=',
     *              F10.5, 2X, 'FOR PARTICLE SIZE',I3)
          IF (H.EQ.HMIN) THEN
            WRITE(6,30)
30          FORMAT(/'NO GO AT HMIN')
            KFLAG=-4
            LFLAG=0
            FAIL=.TRUE.
          ENDIF
          H=0.99999*ABS(Y(I)/DY(I))
          IF (H.LT.HMIN) THEN
              H=HMIN
          ENDIF
          IF (H.GT.HMAX) THEN
              H=HMAX
          ENDIF
          I=I-1
        ENDIF
35 CONTINUE
38 CONTINUE
      T=T+H
      DO 41 I=1,N
41    YO(I)=Y(I)
      DO 42 I=1,N
        XK1(I)=H*DY(I)
42    XX1(I)=YO(I)+XK1(I)/2.0
      CALL DIFFUN(N,XX1,DY,NDCALL,TOTNUM)
      DO 44 I=1,N
        XK2(I)=H*DY(I)
44    XX2(I)=YO(I)+XK2(I)/2.0
      CALL DIFFUN(N,XX2,DY,NDCALL,TOTNUM)
      DO 46 I=1,N
        XK3(I)=H*DY(I)
46    XX3(I)=YO(I)+XK3(I)
      CALL DIFFUN(N,XX3,DY,NDCALL,TOTNUM)
      DO 48 I=1,N
48    XK4(I)=H*DY(I)
      DO 50 I=1,N
50    Y(I)=YO(I)+(XK1(I)+2.0*XK2(I)+2.0*XK3(I)+XK4(I))/6.0
      IF (ABS(FASTLO).GT.1.0D-30) THEN
      H=ABS(0.75*Y(IQUICK)/FASTLO)
      ENDIF
      IF (H.LT.HMIN) THEN
          H=HMIN
      ENDIF
      IF (H.GT.HMAX) THEN
          H=HMAX
      ENDIF
      RETURN
      END
C
C
C
      SUBROUTINE DIFFUN(N,Y,DY,NDCALL,TOTNUM)
C      IMPLICIT REAL*8(A-H, O-Z)
      DIMENSION BETA(100,100),FRAC(100,100),Y(100),DY(100)
      COMMON/B/ BETA
```

```
        COMMON/F/ FRAC
C
C     THE CALCULATION OF THE DIFFERENTIAL EQUATIONS FOLLOWS
C     K IS THE NUMBER OF THE DIFFERENTIAL EQUATION, I.E., IT IS THE
C     PARTICLE SIZE NUMBER BEGIN FORMED OR LOST.
C
        NDCALL=NDCALL+1
        DO 10 J=1,N
          TN=1.0E-10*TOTNUM
          IF (Y(J).LE.TN) THEN
             Y(J)=0.
          ENDIF
     10 CONTINUE
        GAINP1=0.
        DO 20 K=1, N
          GAIN=GAINP1
          GAINP1=0.
          IF (K.EQ.N) GO TO 200
C
C     COMBINATIONS WITH 'K' PARTICLES
          IJ=K-8
          IF (IJ.GT.0) THEN
            DO 30 J=1, IJ
               GAIN=GAIN+BETA(J,K)*FRAC(K-J+1,1)*Y(K)*Y(J)
               GAINP1=GAINP1+BETA(J,K)*(1.-FRAC(K-J+1,1))*Y(K)*Y(J)
     30     CONTINUE
          ENDIF
C
C    COMBINATIONS WITH 'K-1' PARTICLES
        II=K-8
        IJ=K-5
C     IF (II.GT.0) THEN
          DO 40 J=II, IJ
             IF (J.LT.1) GO TO 40
             GAIN=GAIN+BETA(J,K-1)*FRAC(K-J,1)*Y(K-1)*Y(J)
             GAINP1=GAINP1+BETA(J,K-1)*(1-FRAC(K-J,1))*Y(K-1)*Y(J)
     40   CONTINUE
C
C        COMBINATIONS WITH 'K-2' PARTICLES
        II=K-5
        IJ=K-3
          DO 50 J=II, IJ
             IF (J.GT.0) THEN
             GAIN=GAIN+BETA(J,K-2)*FRAC(K-J-1,1)*Y(K-2)*Y(J)
             GAINP1=GAINP1+BETA(J,K-2)*(1-FRAC(K-J-1,1))*Y(K-2)*Y(J)
             ENDIF
     50   CONTINUE
        J=K-3
        IF(J.GT.0) THEN
             GAIN=GAIN+0.5*BETA(J,K-3)*FRAC(K-J-2,1)*Y(K-3)*Y(J)
             GAINP1=GAINP1+0.5*BETA(J,K-3)*(1-FRAC(K-J-2,1))*Y(K-3)*Y(J)
        ENDIF
        GO TO 210
C
C     THE CALCULATION FOR THE CREATION OF SIZE N PARTICLES FOLLOWS
C     COMBINATIONS WITH 'N' PARTICLES
    200 CONTINUE
        DO 60 J=1, N-1
          GAIN=GAIN+BETA(J,K)*FRAC(J,2)*Y(K)*Y(J)
     60 CONTINUE
        J=N
        GAIN=GAIN+0.5*BETA(J,K)*FRAC(J,2)*Y(K)*Y(J)
C
C    COMBINATIONS WITH 'N-1' PARTICLES
        II=K-8
        IJ=K-2
        DO 65 J=II, IJ
          GAIN=GAIN+BETA(J,K-1)*FRAC(J-(N-14),3)*Y(K-1)*Y(J)
     65 CONTINUE
        J=N-1
        GAIN=GAIN+0.5*BETA(J,K-1)*FRAC(J-(N-14),3)*Y(K-1)*Y(J)
C
C    COMBINATIONS WITH 'N-2' PARTICLES
```

```
      II=K-5
      IJ=K-3
      DO 70 J=II, IJ
          GAIN=GAIN+BETA(J,K-2)*FRAC(J-(N-7),3)*Y(K-2)*Y(J)
   70 CONTINUE
      J=K-2
      GAIN=GAIN+0.5*BETA(J,K-2)*FRAC(J-(N-7),3)*Y(K-2)*Y(J)
C
C     COMBINATIONS WITH 'N-3' PARTICLES
      J=K-3
      GAIN=GAIN+0.5*BETA(J,K-3)*FRAC(J-(N-4),3)*Y(K-3)*Y(J)
C     END OF CACULATION OF GAIN
C
C
C     LOSS CALCULATION FOLLOWS
  210 CONTINUE
      ALOSS=0
      DO 80 I=1, N
          ALOSS=ALOSS+BETA(I,K)*Y(I)*Y(K)
   80 CONTINUE
C     END OF LOSS CALCULATION
C
      DY(K)=GAIN-ALOSS
   20 CONTINUE
      RETURN
      END
C
C
C
      SUBROUTINE MASSSU(N,Y,V,DELTAD,PSIZE,PSD,PVD,PND,TOTNUM,TOTVOL,
     *            TOTSUR,TOTDIA,TOTMAS,TOTYIN,AVVODI,AVSUDI,AVNUDI,
     *            PEAKVD,PEAKND,FRAREN,CON3,CON4,RHO,
     *            FDEN,VF,IFLOC)
C       IMPLICIT REAL*8(A-H, O-Z)
      REAL NPEAK,VPEAK
      INTEGER PEAKND,PEAKVD
      DIMENSION PSD(100),PND(100),PVD(100),PSIZE(100),V(100),
     *            Y(100),DELTAD(100),FDEN(100),VF(100),YMASS(100)
      DO 10 I=1,N
       PSD(I)=0.
   10 CONTINUE
      TOTDIA=0.
      TOTMAS=0.
      TOTNUM=0.
      TOTSUR=0.
      TOTVOL=0.
      VPEAK=0.
      NPEAK=0.
        DO 20 I=1,N
          PND(I)=0.
          PVD(I)=0.
   20   CONTINUE
        DO 30 I=1,N
          IF (Y(I).GT.0.) THEN
            PSD(I)=ALOG10(Y(I)/DELTAD(I))
            TOTNUM=TOTNUM+Y(I)
            YMASS(I)=RHO*V(I)*1.0E-12
            VF(I)=YMASS(I)/FDEN(I)*1.0E12
            IF (IFLOC.EQ.0) THEN
               TOTVOL=TOTVOL+Y(I)*V(I)
               TOTSUR=TOTSUR+Y(I)*V(I)**(2./3.)
               TOTDIA=TOTDIA+Y(I)*V(I)**(1./3.)
               TOTMAS=TOTMAS+Y(I)*V(I)*RHO*1.0E-6
            ELSE
               TOTVOL=TOTVOL+Y(I)*RHO*V(I)/FDEN(I)
               TOTSUR=TOTSUR+Y(I)*VF(I)**(2./3.)
               TOTDIA=TOTDIA+Y(I)*VF(I)**(1./3.)
               TOTMAS=TOTMAS+Y(I)*V(I)*RHO*1.0E-6
            ENDIF
            PVD(I)=CON4*PSIZE(I)**4*Y(I)/DELTAD(I)
            PND(I)=2.3*PSIZE(I)*Y(I)/DELTAD(I)
            IF(PVD(I).GT.VPEAK) THEN
               VPEAK =PVD(I)
```

```fortran
                PEAKVD=I
             ENDIF
             IF (PND(I).GT.NPEAK) THEN
               NPEAK=PND(I)
               PEAKND=I
             ENDIF
           ENDIF
  30    CONTINUE
        FRAREN=TOTNUM/TOTYIN
        AVVODI=CON3*(TOTVOL/TOTNUM)**(1./3.)
        AVSUDI=CON3*(TOTSUR/TOTNUM)**(1./3.)
        AVNUDI=CON3*(TOTDIA/TOTNUM)
        RETURN
        END
C
C
C
      SUBROUTINE OUTPUT(N,NDCALL,KFLAG,MFLAG,NTI,TOTNUM,TOTMAS,FRAREN,
     *                  AVVODI,AVSUDI,AVNUDI,PSD,PVD,PND,PEAKVD,
     *                  PEAKND,PSZLOG,PSIZE,DY,T,Y,VF,IFLOC,
     *                  TOTVOL,FDEN)
C     IMPLICIT REAL*8(A-H, O-Z)
      INTEGER PEAKND, PEAKVD
      DIMENSION PSD(100),PVD(100),PND(100),PSZLOG(100),PSIZE(100),
     *          DY(100),Y(100),VF(100),FDEN(100),FLSIZE(100)
C
      NTI=NTI+1.
      TMINUT=T/60.
      WRITE(6,10) TMINUT, KFLAG,MFLAG, NDCALL
  10 FORMAT(/,2X,'TIME (MINUTES)=', F5.1,2X, 'KFLAG=', I2,
     *       2X, 'MFLAG=', I2, 2X, 'NUMBER OF CALLS TO DIFFUN=',
     *       I4)
      WRITE(6,20) TOTNUM
  20 FORMAT(2X, 'TOTAL NUM CONC (#/cc)     =', E11.4)
      WRITE(6,22) TOTVOL
  22 FORMAT(2X, 'TOTAL VOLUME (UM**3/cc)  =', E11.4)
      WRITE(6,23) TOTMAS
  23 FORMAT(2X, 'TOTAL MASS (MG/L)         =', E11.4)
      WRITE(6,24) FRAREN
  24 FORMAT(2X, 'NUM. FRAC. REMAIN  =',F7.4)
      WRITE(6,30) AVVODI
  30 FORMAT(2X, 'VOLUME AVE. PSIZE  =',F7.4)
      WRITE(6,32) AVSUDI
  32 FORMAT(2X, 'SURFACE AVE. PSIZE =',F7.4)
      WRITE(6,34) AVNUDI
  34 FORMAT(2X, 'NUMBER AVE. PSIZE  =',F7.4)
      WRITE(6,40)
  40 FORMAT(/,20X, 'PARTICLE SIZE DISTRIBUTION ')
      IF (IFLOC.EQ.0) THEN
      WRITE(6,45)
  45 FORMAT(/,6X,'I',3X,'PSIZE(I)',4X,'Y(I)',6X,'PSD(I)',
     *       5X,'PVD(I)',8X,'PND(I)')
      DO 500 I=1,N
      WRITE(6,50) I,ALOG10(PSIZE(I)),Y(I),PSD(I), PVD(I), PND(I)
  50 FORMAT(5X,I2,2X,F5.2,F15.2,F7.2,2F15.2)
 500 CONTINUE
      ELSE
        WRITE(6,55)
  55    FORMAT(6X,'I',3X,'FSIZE(I)',1X,'FDEN(I)',7X,'Y(I)',6X,'PSD(I)'
     *         5X,'PVD(I)',8X,'PND(I)')
        DO 502 I=1,N
          IF (VF(I).GT.0) THEN
          FLSIZE(I) = ALOG10((VF(I)*6.0/3.141592)**(1./3.))
          WRITE(6,57) I,FLSIZE(I),FDEN(I),Y(I),PSD(I),PVD(I),PND(I)
  57      FORMAT(5X,I2,2X,F5.2,4X,F7.4,F15.2,f7.2,2F15.2)
          ENDIF
 502    CONTINUE
      ENDIF
      WRITE(6,60) PEAKVD, PSZLOG(PEAKVD)
  60 FORMAT(/,2X, 'VOLUME PEAK IS IN SIZE',
     *       I3, 2X, 'WITH LOG DIAMETER=', F5.2)
      WRITE(6,80) PEAKND, PSZLOG(PEAKND)
  80 FORMAT(/,2X, 'NUMBER PEAK IS IN SIZE',
```

```
     *          I3, 2X, 'WITH LOG DIAMETER=', F5.2)
       RETURN
       END
C
C
       FUNCTION RAN2(IDUM)
       PARAMETER (M=714025,IA=1366,IC=150889,RM=1./M)
       DIMENSION IR(97)
       DATA IFF /0/
       IF (IDUM.LT.0.OR.IFF.EQ.0) THEN
            IFF=1
            IDUM=MOD(IC-IDUM,M)
            DO 11 J=1,97
               IDUM=MOD(IA*IDUM+IC,M)
               IR(J)=IDUM
11          CONTINUE
            IDUM=MOD(IA*IDUM+IC,M)
            IY=IDUM
       ENDIF
       J=1+(97*IY)/M
       IF(J.GT.97.OR.J.LT.1)PAUSE
       IY=IR(J)
       RAN2=IY*RM
       IDUM=MOD(IA*IDUM+IC,M)
       IR(J)=IDUM
       RETURN
       END
C
       FUNCTION GASDEV(IDUM)
       DATA ISET/0/
       IF (ISET.EQ.0) THEN
1          V1=2.*RAN2(IDUM)-1.
           V2=2.*RAN2(IDUM)-1.
           R=V1**2+V2**2
           IF(R.GE.1.) GOTO 1
           FAC=SQRT(-2.*LOG(R)/R)
           GSET=V1*FAC
           GASDEV=V2*FAC
           ISET=1
       ELSE
           GASDEV=GSET
           ISET=0
       ENDIF
       RETURN
       END
```

APPENDIX B

COMPUTER PROGRAM OUTPUT

**********MODEL INPUT**********

ALPHA	HAMAKER (J)	TEMP (KELBIN)	VISCOSITY (GM/CM-SEC)	DENSITY (GM/CM**3)
1.000	.20E-18	293.0	.0100	2.65

DMAX	VCON	DT	DCON	DKP
200.0	.4	15.0	.00130	.90

H	HMIN	HMAX	TMAX
10.0	1.0	100.0	8000.0

INITIAL PARTICLE SIZE DISTRIBUTION DATA

TIME (MINUTES)=   .0 KFLAG= 0 MFLAG= 1 NUMBER OF CALLS TO DIFFUN=   0
TOTAL NUM CONC (#/cc)   = .1120E+08
TOTAL VOLUME (UM**3/cc) = .5585E+08
TOTAL MASS (MG/L)   = .9970E+02
NUM. FRAC. REMAIN = 1.0000
VOLUME AVE. PSIZE = 2.1197
SURFACE AVE. PSIZE = 1.4006
NUMBER AVE. PSIZE = 1.2689

PARTICLE SIZE DISTRIBUTION

I	FSIZE(I)	FDEN(I)	Y(I)	PSD(I)	PVD(I)	PND(I)
1	-.06	2.6500	2096293.00	7.54	24085540.00	69784100.00
2	-.03	2.6500	1703931.00	7.42	24085540.00	56722650.00
3	.00	2.6500	1385007.00	7.30	24085540.00	46105900.00
4	.03	2.6500	1125776.00	7.18	24085540.00	37476270.00
5	.06	2.6500	915065.10	7.06	24085540.00	30461860.00
6	.09	2.6500	743792.80	6.94	24085540.00	24760330.00
7	.12	2.6500	604577.50	6.82	24085540.00	20125950.00
8	.15	2.6500	491419.00	6.70	24085540.00	16358990.00
9	.18	2.6500	399440.40	6.58	24085540.00	13297090.00
10	.21	2.6500	324677.30	6.46	24085540.00	10808280.00
11	.24	2.6500	263907.60	6.34	24085540.00	8785297.00
12	.27	2.6500	214512.20	6.22	24085540.00	7140958.00
13	.30	2.6500	174362.00	6.10	24085540.00	5804388.00
14	.33	2.6500	141726.80	5.98	24085540.00	4717983.00
15	.36	2.6500	115199.80	5.86	24085540.00	3834921.00
16	.39	2.6500	93637.93	5.74	24085540.00	3117140.00
17	.42	2.6500	76111.75	5.62	24085540.00	2533706.00
18	.45	2.6500	61865.95	5.50	24085540.00	2059473.00
19	.48	2.6500	50286.54	5.38	24085540.00	1674003.00
20	.51	2.6500	40874.42	5.26	24085540.00	1360680.00
21	.54	2.6500	33223.97	5.14	24085540.00	1106003.00
22	.57	2.5642	27005.46	5.02	24085540.00	898992.60
23	.61	2.4312	21950.86	4.90	24085540.00	730728.40
24	.65	2.3096	17842.33	4.78	24085540.00	593958.30
25	.69	2.1983	14502.79	4.66	24085540.00	482787.50
26	.72	2.0965	11788.31	4.54	24085540.00	392424.30
27	.76	2.0033	9581.90	4.42	24085540.00	318974.50
28	.80	1.9180	7788.46	4.30	24085540.00	259272.10
29	.83	1.8400	6330.69	4.18	24085540.00	210744.30
30	.87	1.7686	5145.78	4.06	24085540.00	171299.40

31	.90	1.7033	4182.65	3.94	24085540.00	139237.40
32	.94	1.6435	3399.79	3.82	24085540.00	113176.40
33	.97	1.5888	2763.45	3.70	24085540.00	91993.29
34	1.01	1.5388	2246.22	3.58	24085540.00	74774.95
35	1.04	1.4930	1825.79	3.46	24085540.00	60779.38
36	1.08	1.4511	1484.06	3.34	24085540.00	49403.36
37	1.11	1.4128	1206.29	3.22	24085540.00	40156.55
38	1.14	1.3777	980.51	3.10	24085540.00	32640.48
39	1.18	1.3456	796.99	2.98	24085540.00	26531.19
40	1.21	1.3162	647.82	2.86	24085540.00	21565.36
41	1.24	1.2894	526.57	2.74	24085540.00	17528.99
42	1.28	1.2648	428.01	2.62	24085540.00	14248.10
43	1.31	1.2423	347.90	2.50	24085540.00	11581.29
44	1.34	1.2217	282.78	2.38	24085540.00	9413.63
45	1.37	1.2028	229.85	2.26	24085540.00	7651.69
46	1.41	1.1856	186.83	2.14	24085540.00	6219.52
47	1.44	1.1698	151.86	2.02	24085540.00	5055.42
48	1.47	1.1554	123.44	1.90	24085540.00	4109.20
49	1.50	1.1422	100.34	1.78	24085540.00	3340.08
50	1.53	1.1301	81.56	1.66	24085540.00	2714.92
51	1.56	1.1190	66.29	1.54	24085540.00	2206.77
52	1.60	1.1089	53.88	1.42	24085540.00	1793.73

VOLUME PEAK IS IN SIZE   2 WITH LOG DIAMETER= -.03

NUMBER PEAK IS IN SIZE   1 WITH LOG DIAMETER= -.06

THE MODEL PREDICTION AT COMPAREMENT NUMBER   1

TIME (MINUTES)= 83.3 KFLAG= 0 MFLAG= 1 NUMBER OF CALLS TO DIFFUN=2000
TOTAL NUM CONC (#/cc)   = .7832E+07
TOTAL VOLUME (UM**3/cc) = .6464E+08
TOTAL MASS (MG/L)   = .9970E+02
NUM. FRAC. REMAIN = .6993
VOLUME AVE. PSIZE = 2.5073
SURFACE AVE. PSIZE = 1.4471
NUMBER AVE. PSIZE = 1.2993

PARTICLE SIZE DISTRIBUTION

I	FSIZE(I)	FDEN(I)	Y(I)	PSD(I)	PVD(I)	PND(I)
1	-.06	2.6500	1418651.00	7.37	16299710.00	47225870.00
2	-.03	2.6500	1147170.00	7.25	16215570.00	38188470.00
3	.00	2.6500	926745.30	7.13	16116280.00	30850690.00
4	.03	2.6500	756858.90	7.01	16192710.00	25195300.00
5	.06	2.6500	634782.90	6.90	16708200.00	21131470.00
6	.09	2.6500	528551.60	6.79	17115590.00	17595110.00
7	.12	2.6500	436021.70	6.68	17370510.00	14514850.00
8	.15	2.6500	358422.20	6.57	17567070.00	11931620.00
9	.18	2.6500	295391.40	6.45	17811580.00	9833371.00
10	.21	2.6500	241994.20	6.33	17951860.00	8055814.00
11	.24	2.6500	198001.00	6.22	18070570.00	6591311.00
12	.27	2.6500	161919.70	6.10	18180440.00	5390193.00
13	.30	2.6500	132392.10	5.98	18288010.00	4407238.00
14	.33	2.6500	108246.10	5.87	18395730.00	3603437.00
15	.36	2.6500	88514.30	5.75	18506230.00	2946578.00
16	.39	2.6500	72399.61	5.63	18622620.00	2410132.00
17	.42	2.6500	59244.18	5.51	18747800.00	1972197.00
18	.45	2.6500	48504.50	5.40	18883690.00	1614680.00
19	.48	2.6500	39737.20	5.28	19032770.00	1322823.00
20	.51	2.6500	32579.23	5.16	19197540.00	1084539.00
21	.54	2.6500	26990.69	5.05	19566760.00	898500.80
22	.57	2.5642	22216.72	4.94	19814580.00	739578.80
23	.61	2.4312	18120.18	4.82	19882340.00	603207.90
24	.65	2.3096	14718.90	4.70	19869200.00	489981.80
25	.69	2.1983	11933.44	4.58	19818490.00	397255.70
26	.72	2.0965	9673.39	4.46	19764410.00	322020.30
27	.76	2.0033	7846.81	4.34	19724150.00	261214.80
28	.80	1.9180	6370.26	4.22	19699830.00	212061.50
29	..83	1.8400	5175.52	4.09	19690590.00	172289.20
30	.87	1.7686	4205.10	3.97	19682540.00	139984.70
31	.90	1.7033	3422.91	3.86	19710620.00	113946.20
32	.94	1.6435	2796.17	3.74	19809250.00	93082.44

33	.97	1.5888	2284.59	3.62	19911880.00	76052.23
34	1.01	1.5388	1861.08	3.50	19955860.00	61954.11
35	1.04	1.4930	1513.68	3.38	19968230.00	50389.42
36	1.08	1.4511	1229.80	3.26	19959060.00	40939.27
37	1.11	1.4128	998.22	3.14	19931160.00	33230.18
38	1.14	1.3777	809.31	3.02	19880080.00	26941.28
39	1.18	1.3456	655.29	2.90	19803440.00	21814.28
40	1.21	1.3162	530.01	2.78	19705470.00	17643.60
41	1.24	1.2894	428.44	2.65	19597400.00	14262.61
42	1.28	1.2648	346.43	2.53	19494690.00	11532.32
43	1.31	1.2423	281.33	2.41	19476570.00	9365.11
44	1.34	1.2217	228.86	2.29	19493150.00	7618.73
45	1.37	1.2028	185.83	2.17	19471950.00	6186.00
46	1.41	1.1856	151.34	2.05	19510350.00	5038.09
47	1.44	1.1698	123.70	1.93	19618960.00	4117.91
48	1.47	1.1554	101.60	1.82	19824650.00	3382.26
49	1.50	1.1422	83.88	1.70	20136660.00	2792.47
50	1.53	1.1301	69.60	1.59	20555290.00	2316.99
51	1.56	1.1190	58.11	1.49	21114050.00	1934.52
52	1.60	1.1089	48.85	1.38	21835340.00	1626.15
53	1.63	1.0997	32.47	1.17	17856780.00	1080.95
54	1.66	1.0912	21.75	.97	14715950.00	724.08
55	1.69	1.0834	15.04	.78	12516730.00	500.60
56	1.72	1.0764	10.62	.60	10872330.00	353.45
57	1.75	1.0699	7.64	.42	9619761.00	254.19
58	1.78	1.0639	5.59	.26	8664281.00	186.09
59	1.81	1.0585	4.17	.10	7947769.00	138.75
60	1.84	1.0535	3.18	-.05	7453130.00	105.76
61	1.87	1.0490	2.49	-.18	7187915.00	82.91
62	1.90	1.0448	2.02	-.30	7165737.00	67.18
63	1.93	1.0410	1.70	-.41	7408391.00	56.46
64	1.97	1.0375	27.81	.78	149441300.00	925.70

VOLUME PEAK IS IN SIZE 64 WITH LOG DIAMETER= 1.83

NUMBER PEAK IS IN SIZE 1 WITH LOG DIAMETER= -.06

THE MODEL PREDICTION AT COMPAREMENT NUMBER   2

TIME (MINUTES)= 83.3 KFLAG= 0 MFLAG= 1 NUMBER OF CALLS TO DIFFUN=2000
TOTAL NUM CONC (#/cc)   = .5492E+07
TOTAL VOLUME (UM**3/cc) = .7221E+08
TOTAL MASS (MG/L)   = .9969E+02
NUM. FRAC. REMAIN   = .4904
VOLUME AVE. PSIZE   = 2.9283
SURFACE AVE. PSIZE = 1.4903
NUMBER AVE. PSIZE   = 1.3229

PARTICLE SIZE DISTRIBUTION

I	FSIZE(I)	FDEN(I)	Y(I)	PSD(I)	PVD(I)	PND(I)
1	-.06	2.6500	971588.30	7.21	11163150.00	32343480.00
2	-.03	2.6500	782612.60	7.08	11062450.00	26052610.00
3	.00	2.6500	629324.40	6.96	10944080.00	20949760.00
4	.03	2.6500	515681.60	6.84	11032810.00	17166670.00
5	.06	2.6500	442063.70	6.75	11635610.00	14715990.00
6	.09	2.6500	373927.90	6.64	12108560.00	12447800.00
7	.12	2.6500	311536.20	6.53	12411180.00	10370820.00
8	.15	2.6500	258145.50	6.42	12652290.00	8593479.00
9	.18	2.6500	214794.80	6.31	12951740.00	7150366.00
10	.21	2.6500	176995.90	6.20	13130090.00	5892067.00
11	.24	2.6500	145536.90	6.08	13282430.00	4844819.00
12	.27	2.6500	119553.00	5.97	13423470.00	3979834.00
13	.30	2.6500	98178.46	5.85	13561910.00	3268291.00
14	.33	2.6500	80618.48	5.74	13700590.00	2683732.00
15	.36	2.6500	66209.61	5.62	13842850.00	2204071.00
16	.39	2.6500	54400.39	5.51	13992870.00	1810950.00
17	.42	2.6500	44729.25	5.39	14154560.00	1489005.00
18	.45	2.6500	36809.13	5.28	14330470.00	1225350.00
19	.48	2.6500	30323.64	5.16	14523990.00	1009452.00
20	.51	2.6500	25012.15	5.05	14738590.00	832636.80
21	.54	2.6500	20970.77	4.94	15202650.00	698102.00
22	.57	2.5642	17416.05	4.83	15532970.00	579767.80

23	.61	2.4312	14253.79	4.71	15639950.00	474498.60
24	.65	2.3096	11583.98	4.59	15637340.00	385622.50
25	.69	2.1983	9382.24	4.47	15581590.00	312328.20
26	.72	2.0965	7594.94	4.35	15517760.00	252830.00
27	.76	2.0033	6154.24	4.23	15469610.00	204870.30
28	.80	1.9180	4993.18	4.11	15441240.00	166219.30
29	.83	1.8400	4056.24	3.99	15432230.00	135029.30
30	.87	1.7686	3295.68	3.87	15425910.00	109711.00
31	.90	1.7033	2685.33	3.75	15463320.00	89392.75
32	.94	1.6435	2200.29	3.63	15587830.00	73246.22
33	.97	1.5888	1803.73	3.52	15720880.00	60044.98
34	1.01	1.5388	1471.97	3.40	15783500.00	49000.79
35	1.04	1.4930	1197.91	3.28	15802640.00	39877.63
36	1.08	1.4511	972.99	3.16	15791060.00	32390.03
37	1.11	1.4128	788.96	3.04	15752880.00	26263.95
38	1.14	1.3777	638.46	2.92	15683270.00	21253.81
39	1.18	1.3456	515.52	2.79	15579450.00	17161.38
40	1.21	1.3162	415.45	2.67	15446160.00	13829.95
41	1.24	1.2894	334.42	2.55	15296470.00	11132.47
42	1.28	1.2648	269.19	2.42	15148460.00	8961.26
43	1.31	1.2423	218.00	2.30	15092620.00	7257.14
44	1.34	1.2217	177.03	2.18	15078230.00	5893.20
45	1.37	1.2028	143.34	2.06	15020350.00	4771.78
46	1.41	1.1856	116.48	1.94	15016090.00	3877.55
47	1.44	1.1698	95.09	1.82	15081590.00	3165.54
48	1.47	1.1554	78.14	1.70	15247350.00	2601.33
49	1.50	1.1422	64.69	1.59	15528980.00	2153.50
50	1.53	1.1301	53.95	1.48	15933890.00	1796.07
51	1.56	1.1190	45.42	1.38	16503340.00	1512.07
52	1.60	1.1089	38.63	1.28	17269550.00	1286.12
53	1.63	1.0997	31.76	1.16	17468190.00	1057.42
54	1.66	1.0912	25.26	1.03	17091100.00	840.95
55	1.69	1.0834	19.74	.90	16429280.00	657.08
56	1.72	1.0764	15.33	.76	15700790.00	510.41
57	1.75	1.0699	11.91	.62	14999180.00	396.34
58	1.78	1.0639	9.28	.48	14377490.00	308.80
59	1.81	1.0585	7.28	.34	13881690.00	242.35
60	1.84	1.0535	5.78	.21	13558120.00	192.40
61	1.87	1.0490	4.66	.09	13441150.00	155.04
62	1.90	1.0448	3.81	-.03	13538100.00	126.93
63	1.93	1.0410	3.17	-.14	13836350.00	105.44
64	1.97	1.0375	61.71	1.12	331641600.00	2054.32

VOLUME PEAK IS IN SIZE 64 WITH LOG DIAMETER= 1.83

NUMBER PEAK IS IN SIZE 1 WITH LOG DIAMETER= -.06

THE MODEL PREDICTION AT COMPAREMENT NUMBER   3

TIME (MINUTES)= 83.3 KFLAG= 0 MFLAG= 1 NUMBER OF CALLS TO DIFFUN=2000
TOTAL NUM CONC (#/cc)   = .3555E+07
TOTAL VOLUME (UM**3/cc)   = .6037E+08
TOTAL MASS (MG/L)   = .7976E+02
NUM. FRAC. REMAIN   = .3174
VOLUME AVE. PSIZE   = 3.1892
SURFACE AVE. PSIZE = 1.5247
NUMBER AVE. PSIZE = 1.3429

PARTICLE SIZE DISTRIBUTION

I	FSIZE(I)	FDEN(I)	Y(I)	PSD(I)	PVD(I)	PND(I)
1	-.06	2.6500	617166.40	7.01	7090988.00	20545030.00
2	-.03	2.6500	495624.70	6.89	7005795.00	16498990.00
3	.00	2.6500	397121.00	6.76	6906012.00	13219880.00
4	.03	2.6500	326228.00	6.64	6979525.00	10859900.00
5	.06	2.6500	284188.70	6.55	7480167.00	9460440.00
6	.09	2.6500	243041.40	6.46	7870181.00	8090676.00
7	.12	2.6500	203961.90	6.35	8125562.00	6789745.00
8	.15	2.6500	170069.50	6.24	8335485.00	5661492.00
9	.18	2.6500	142560.70	6.13	8596154.00	4745743.00
10	.21	2.6500	118053.20	6.02	8757542.00	3929906.00
11	.24	2.6500	97487.89	5.91	8897238.00	3245303.00
12	.27	2.6500	80399.02	5.80	9027245.00	2676426.00

13	.30	2.6500	66279.80	5.68	9155576.00	2206407.00
14	.33	2.6500	54633.46	5.57	9284602.00	1818709.00
15	.36	2.6500	45042.73	5.45	9417361.00	1499440.00
16	.39	2.6500	37158.13	5.34	9557812.00	1236968.00
17	.42	2.6500	30683.51	5.23	9709790.00	1021432.00
18	.45	2.6500	25366.82	5.12	9875768.00	844443.50
19	.48	2.6500	21001.80	5.00	10059150.00	699134.90
20	.51	2.6500	17417.56	4.89	10263420.00	579818.10
21	.54	2.6500	14740.94	4.79	10686370.00	490715.40
22	.57	2.5642	12339.20	4.68	11005050.00	410763.30
23	.61	2.4312	10140.58	4.57	11126730.00	337572.60
24	.65	2.3096	8255.02	4.45	11143540.00	274803.80
25	.69	2.1983	6687.76	4.33	11106710.00	222630.60
26	.72	2.0965	5412.44	4.20	11058540.00	180176.20
27	.76	2.0033	4385.06	4.08	11022520.00	145975.60
28	.80	1.9180	3558.29	3.96	11003900.00	118452.90
29	.83	1.8400	2892.10	3.84	11003180.00	96275.92
30	.87	1.7686	2351.43	3.72	11006170.00	78277.27
31	.90	1.7033	1918.50	3.60	11047560.00	63865.43
32	.94	1.6435	1576.05	3.49	11165400.00	52465.49
33	.97	1.5888	1295.59	3.37	11292060.00	43129.33
34	1.01	1.5388	1059.19	3.26	11357380.00	35259.65
35	1.04	1.4930	862.65	3.14	11379920.00	28717.00
36	1.08	1.4511	700.63	3.02	11370860.00	23323.47
37	1.11	1.4128	567.68	2.90	11334570.00	18897.52
38	1.14	1.3777	458.69	2.77	11267500.00	15269.61
39	1.18	1.3456	369.53	2.65	11167380.00	12301.31
40	1.21	1.3162	296.89	2.52	11038100.00	9883.13
41	1.24	1.2894	238.10	2.40	10890710.00	7926.04
42	1.28	1.2648	190.86	2.27	10740520.00	6353.69
43	1.31	1.2423	154.00	2.15	10661980.00	5126.71
44	1.34	1.2217	124.66	2.03	10617380.00	4149.71
45	1.37	1.2028	100.55	1.90	10536230.00	3347.23
46	1.41	1.1856	81.36	1.78	10488710.00	2708.46
47	1.44	1.1698	66.13	1.66	10487650.00	2201.30
48	1.47	1.1554	54.10	1.54	10556310.00	1801.00
49	1.50	1.1422	44.61	1.43	10707650.00	1484.89
50	1.53	1.1301	37.08	1.32	10949810.00	1234.26
51	1.56	1.1190	31.15	1.21	11316280.00	1036.82
52	1.60	1.1089	26.48	1.11	11835400.00	881.42
53	1.63	1.0997	22.58	1.01	12419940.00	751.83
54	1.66	1.0912	19.17	.91	12967250.00	638.04
55	1.69	1.0834	16.14	.81	13434770.00	537.32
56	1.72	1.0764	13.51	.70	13837530.00	449.84
57	1.75	1.0699	11.27	.59	14195010.00	375.09
58	1.78	1.0639	9.38	.48	14537960.00	312.25
59	1.81	1.0585	7.82	.37	14911850.00	260.33
60	1.84	1.0535	6.56	.27	15388670.00	218.37
61	1.87	1.0490	5.56	.17	16043600.00	185.06
62	1.90	1.0448	4.77	.07	16919790.00	158.63
63	1.93	1.0410	4.13	-.02	18036850.00	137.45
64	1.97	1.0375	58.51	1.10	314438400.00	1947.76

VOLUME PEAK IS IN SIZE 64   WITH LOG DIAMETER= 1.83

NUMBER PEAK IS IN SIZE 1   WITH LOG DIAMETER= -.06

VITA $\sqrt[n]{\nu}$

Byung-Hyun Moon

Candidate for the Degree of

Doctor of Philosophy

Thesis: MODELING OF FLOCCULATION SYSTEMS USING PARTICLE SIZE
        DISTRIBUTION

Major Field: Civil Engineering

Biographical:

    Personal Date: Born in Sooncheon, Korea, May 17, 1960,
        the son of Kwang-Hee Moon and Hok Lee.

    Education: Graduated from Po-Sung High School, Seoul,
        Korea, in January, 1978; received the Bachelor of
        Science Degree in Chemical Engineering from Sung
        Kyun Kwan University in August, 1984; received the
        Master of Science degree in Chemical Engineering
        from Oklahoma State University in May, 1988;
        completed the requirements for the Doctor of
        Philosophy degree at Oklahoma State University in
        May, 1992.

    Professional Experience: Teaching Assistant, School of
        Civil Engineering, Oklahoma State University,
        August, 1989, to May, 1992.